ZKZ 64717
7-06

Bodo´s Power Systems

Systems Design Motion and Conversion

September 2006

Thermal and Mechanical Analysis

Power Modules
PFC Correction
PWM Controller
Signal Isolator

Bodo´s Power Systems

Viewpoint
Engineers for Power and Peace 2

Events 2

News 4

Product of the Month
ePhysics v2 Dynamic-Link Co-Simulation of Thermal and Stress Analysis 8

Guest Editorial
The Third edition of IEC60601-1 seems to indicate potential cost saving in power supplies for medical devices but at what price?;
By Steve Elliott, Industry Director - Medical for XP Power 10

Market
The Lennox Report; *By Robert Lennox* 12

Market
Power Factor Correction Market Driven by Regulations; *By Linnea Brush, Senior Research Analyst, Darnell Group* 14

Cover Story
The Help of Thermal and Mechanical Analysis; *By Fabio Brucchi, Semikron Italia* 18

Power Modules
Innovative Cooling Concept for Power Modules; *By Klaus Olesen, Danfoss Silicon Power GmbH* 22

Rectifier
The SmartRectifier in Practical Design; *By Mario Battello, International Rectifier* 26

Power Quality
Interleaving Enhances Power Factor Corrector Performance; *By Marcus Zimnik, Texas Instruments* 30

Power Management
PWM Controller Simplifies High Power LED Designs; *By Tony Armstrong, Product Marketing Manager, Linear Technology Corporation* 52

Signal Isolator
Analog Transmission Across Digital Barriers; *By Keith Coffey, Silicon Laboratories Inc.* 34

Sensors
New Applications for Hall-Effect Current Sensors; *By Andreas Friedrich, Allegro MicroSystems Europe* 38

Capacitors
Ultracapacitors - Powering the Shift to Hybrid Electric Vehicles; *By Jürgen Auer, Maxwell Technologies* 40

Transformers
How to Select an Off-The-Shelf Current Transformer; *By Ariel General, Senior Design Applications Engineer, Datatronics, Inc.* 42

Oscillator Design
Crystal Oscillator Design and Negative Resistance; *By Anthony M. Scalpi, Applications Engineer Senior Staff, Cypress Semiconductor* 44

Communication Power
The Next BIG Thing Part 2; *By Mark E. Hazen, Senior Technical Writer, Intellon Corporation* 50

New Products 53

Bodo´s Power Systems

A Media
Katzbek 17a
D-24235 Laboe, Germany
Phone: +49 4343 42 17 90
Fax: +49 4343 42 17 89
editor@bodospower.com
www.bodospower.com

Publishing Editor
Bodo Arlt, *Dipl.-Ing.*
editor@bodospower.com

Creative Direction & Production
Repro Studio Peschke
Repro.Peschke@t-online.de

Free Subscrition to qualified readers

Bodo´s Power Systems magazine is available for the following subscription charges:
Annual charge (12 issues) is 150 € world wide
Single issue is 18 €
subscription@bodospower.com

Printing by:
Central-Druck Trost GmbH & Co
Heusenstamm, Germany

EVENTS

Digital Power Forum (DPF '06)
September 18-20,
Richardson, Texas
www:darnell.com

H2Expo,
October 25-26, Hamburg,
www.h2expo

ELECTRONICA 2006,
Nov. 14 – 17, Munich,
www.electronica.de

SPS/IPC/DRIVES 2006,
Nov. 28 – 30, Nuremberg,
www.mesago.de

Engineers for Power and Peace

It is once again September and in the world we are faced with confrontation, war and terrorism.

It is a slow process for people to feel more satisfaction from constructive planning and compromise than from aggression. Education is one major factor we can provide to our children to help in this process. With better education, an entry into professional employment begins.

To work for life is one thing - but to enjoy the work is more important. At a certain point we need to help young people with the choice of a profession that will be a stimulating one for them.

Engineering is a continuous process of learning and of improving technology. The Engineer in power electronics is challenged to find applications and develop products that continue performance improvement. Those working with energy consuming products must include the goal of conserving our natural resources. Clean air and water are necessities to a good life – examples where pollution has impacted health and made life quite difficult are all too common. Power electronics can lead to the right solutions. Ignition IGBTs, together with engine control circuits, lower fuel consumption and reduce pollution. Hybrid vehicles further improve this goal and also recoup regenerative energy. Wind and solar power are green resources. But without modern MOSFETs and IGBT switch technology, we would not to be able to economically harvest these sources. Engineers develop all these exciting technologies.

So we need to find ways to guide and motivate young people to see satisfaction in becoming Engineers. We need to overcome the highly publicised negative example of a few industry executives exploiting their company for personal gain - while engineers are hired and fired to balance accounts. We are not talking about small companies - the daily press puts before us cases such as Koslowskie.

So what do we do to encourage a young person to become an Engineer ? My contribution will be to offer young Engineers an opportunity to write an article in their preferred area of expertise and have it published in my magazine. The three best articles will get the authors an invitation to visit htc-network for a full assessment, through the high-tech consulting network company's full qualification process. The candidates

will receive professional feedback to make the best decision is selecting a career position. To reach University students and engineers, I have included European Institutes of Power Electronics and of Electrical Drives in my circulation.

Even younger children can have technical toys for birthday and Christmas, instead of the arthritis developing computer games. Building blocks and trains can challenge the imagination and develop a handiness to build and modify structures - a whole system can result from an extensive effort to complete a project. The satisfaction of having a running train set usually involves teamwork: support with finances, hands-on help and advice, wiring reviews for functionality even up to a digitised level of control – a perfect platform for kids on the way to becoming engineers. No question about it - Engineers of all ages have trains running in their basement !

And - satisfied Engineers contribute to world stability and peace.

Best regards

Danfoss ISO/TS 16949 Automotive Certified

Danfoss Silicon Power GmbH received ISO/TS 16949 certification from the Deutsche Gesellschaft zur Zertifizierung von Managementsystemen. Claus Petersen, President of Danfoss Silicon Power, received the certificate from Jörg Göllner and Harald Scheerer during a celebration at the home office in Schleswig, Germany. Jørgen M. Clausen, President and CEO of The Danfoss Group, attended the presentation.

Jörg Göllner, VDE and Claus A. Petersen, Danfoss

Automotive customers demand products that conform to the highest levels of quality and reliability, creating the primary motivation to attain ISO/TS 16949 Certification. Danfoss Silicon Power has delivered customer-specified power modules to leading European automakers for many years. Danfoss modules are already in use in the European high-end luxury car segment. Future automotive market growth is expected in both Drive-by-Wire and Hybrid Electric Vehicle applications. ISO/TS 16949 Certification is an investment in the future.

Danfoss Silicon Power began operations in 2000 in Schleswig, Germany with 25 employees. Before the end of 2006, at least 125 very talented people will make their marks in the industry at Danfoss Silicon Power. The Danfoss Group is a family-owned, global company with approximately 19,300 employees in 21 countries. The Danfoss Group was founded 75 years ago by Danish engineer Mads Clausen.

http://siliconpower.danfoss.com

htc-network 5th anniversary

Klaus Nolte

Founded during the hype of the high-tech market, at the beginning of the decade, htc-network became one of the most professional recruitment consultancy in the technology sector. In close cooperation with key customers, an intense qualification process has been developed, suited to the needs of the high-tech industry.

"However, even the most thorough assessment by a third-party recruiter is no match for the subjective appraisal by the person, who will become the new employee's direct supervisor," states Klaus Nolte, Founder and Managing Director of htc-network. "To address this fact, we developed a unique assessment documentation tool, the htc-network Candidate Video-CD. The htc-CD contains video files of all interviews with the candidate. This CD enables all people, who are involved in the decision-making process to make an individual assessment of candidates, suitability for the position. To my knowledge, no other recruitment consultancy offers this transparency for the pre selection of candidates, before inviting them to a personal interview."

"Of course all candidates will also receive their own personal Candidate Video-CD after our interviews" adds Klaus Nolte. "This will give them an excellent opportunity to review their performance during htc's assessment and learn from it."

www.htc-network.com

Bob Mahoney Executive VP

ON Semiconductor, a leading industry supplier of power solutions, has named Bob Mahoney Executive Vice President of Global Sales and Marketing. Mr. Mahoney takes on his new responsibilities after successfully directing the company's Sales for the Americas as Vice President. During his tenure with ON Semiconductor, Mr. Mahoney has been instrumental to the company's growth of market share and bottom line profitability. Since joining the company in 2003, he has held executive responsibilities throughout the sales organization - including Vice President of Global Distribution and the Electronic Manufacturing Services Industry (EMSI), and Vice President of North America Sales, Computing Segment Sales and Sales Operations.

Mr. Mahoney brings more than 20 years of semiconductor industry experience in sales and sales management to his new role as Executive Vice President of Global Sales and Marketing for ON Semiconductor. Just prior to joining the company, he was Vice President of World Wide Sales for Xicor Semiconductor. Previously, at Altera, he was Vice President of Strategic Accounts. During his career, he has also held sales management roles at Analog Devices and National Semiconductor.

www.onsemi.com

Bob Mahoney

The Best-Selling 2-Channel IGBT Driver Core

The 2SD315AI is a 2-channel driver for IGBTs up to 1700V (optionally up to 3300V). Its gate current capability of ±15A is optimized for IGBTs from 200A to 1200A.

The 2SD315AI has been established on the market as an industrial standard for the last four years. The driver has been tried and tested within hundreds of thousands of industrial and traction applications. The calculated MTBF to MIL Hdbk 217F is 10 million hours at 40°C. According to field data, the actual reliability is even higher. The operating temperature is -40°C...+85°C.

The driver is equipped with the award-winning CONCEPT SCALE driver chipset, consisting of the gate driver ASIC IGD001 and the logic-to-driver interface ASIC LDI001.

Chipset Features

- Short-circuit protection
- Supply undervoltage lockout
- Direct or half-bridge mode
- Dead-time generation
- High dv/dt immunity up to 100kV/us
- Transformer interface
- Isolated status feedback
- 5V...15V logic signals
- Schmitt-trigger inputs
- Switching frequency DC to >100kHz
- Duty cycle 0...100%
- Delay time typ. 325ns

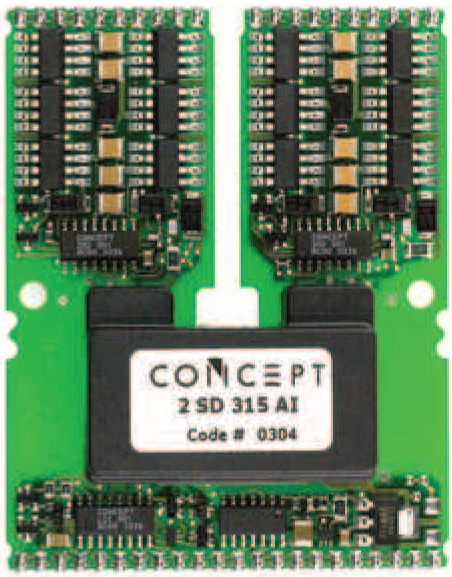

Driver stage for a gate current up to ±15A per channel, stabilized by large ceramic capacitors

Specially designed transformers for creepage distances of 21mm between inputs and outputs or between the two channels. Insulating materials to UL V-0. Partial discharge test according IEC270.

Isolated DC/DC power supply with 3W per channel

More information: www.IGBT-Driver.com/go/2SD315AI

Automotive Focus at electronica 2006

Munich Trade Fairs International (MMI), the organiser behind the World's largest and most successful trade fair for the global electronics industry, continues to develop the event's focus on key applications areas with the news that electronica 2006 will headline the rapidly growing automotive electronics sector. electronica automotive presents an Automotive Conference organised to begin the day before electronica opens its doors as well as a focused exhibition area and a Forum which will be the platform for information exchange.

Europe's automotive market is the second largest in the World playing an important part in driving the financial health of the region's economy and many of the cars and trucks designed and manufactured in Europe enjoy significant sales success throughout the World. But it is through the influence that Europe's automotive design community has on the World's car and truck industry that gives it its global technology applications leadership. Manufacturers like Daimler-Chrysler, Volvo, BMW, Audi and Renault lead the industry in the use of technology to make their vehicles safer, more reliable and more enjoyable to drive. As well as the car and truck manufacturers themselves, Europe boasts large numbers of design houses working alongside the Global automotive industry to develop the vehicles of tomorrow. electronica 2006 will be the venue to see and discuss how electronic products and systems will influence future car and truck design.

www.electronica.de

ICOS Vision Systems and IMEC Collaborate

ICOS Vision Systems Corporation NV, a leading supplier of inspection solutions for the semiconductor industry and IMEC, a world-leading independent research center in nanoelectronics and nanotechnology, have agreed to work together under a two-year Joint Exploration and Development Program (JEDP), in the field of inspection and metrology for three dimensional (3D) packaging. According to market analysts, the market for 3D packaging will grow rapidly over the next years, driven by the quest for smaller and higher performance Integrated Circuits (IC's).

Research will be performed at the IMEC laboratories and ICOS will provide technology and equipment for inspection and metrology. The joint research program will concentrate on the development and optimization of several 3D packaging processes for IC's, including Wafer Level Packaging (WLP), flip chip, systems-in-a-package (SiP) and micro-electromechanical systems (MEMS) and on the optimization of the 3D metrology methods for these applications. The program will be closely connected to IMEC's industrial affiliation program (IIAP) on 3D stacked IC's. The IIAP program brings together the researchers of IMEC and of world-leading suppliers of IC's, to jointly develop the technologies of future generation products. "Packaging is becoming an increasingly important part of semiconductor manufacturing and we are expanding our research efforts in the packaging field, including a large research program on 3D packaging," said Gilbert Declerck, CEO of IMEC. "We are delighted to work with ICOS on the advancements of the 3D packaging processes and the metrology tools that are needed."

Gilbert Declerck

www.icos.be

www.imec.be

Andy Gales

Andy Gales VP Sales

Vicor, a leading power supply company, announces the promotion of Andy Gales to the newly-created position of Vice President, International Sales. In this role Gales is responsible for all commercial activities throughout Europe, the Middle East, Africa and the near and Far East, excluding Japan. Based in Vicor's UK office, Gales will continue to drive the growth in Vicor's international business, working closely with the company's network of design-in distributors. He reports directly to the president of Vicor's Brick division, Barry Kelleher.

Gales has worked as a senior member of Vicor's international team for 13 years, expanding his territorial responsibilities over this time. He has extensive experience in the international electronics industry, with knowledge and expertise built up over 30 years. Trained as an electronics engineer, prior to joining Vicor Gales worked for UK distributor, Acal.

www.vicoreurope.com

Hydrogen Powered Buses

6th International Conference and Trade Fair on Hydrogen and Fuel Cell Technologies, in Hamburg from 25 to 26 October 2006.
It is now a proven fact – hydrogen, the "fuel of the future" is specially suitable for public transport. Fuel cell buses have been tested in the framework of the EU project CUTE (Clean Urban Transport for Europe) in European urban traffic in the last two years, proving their viability in everyday operation. Further experience is now to be gathered in the follow-up project HyFleet:Cute. There will be new additions to the fleet, i.e. buses with hydrogen internal combustion engines. The H2Expo, 6th International Conference and Trade Fair on Hydrogen and Fuel Cell Technologies, to be held at the CCH-Congress Center Hamburg from 25 to 26 October, will give scientists from all over the world a platform to present their research results, and enable highly reputed manufacturers to present their projects and new developments. This will also be a good opportunity to get an overview of the current use of hydrogen and fuel cells in buses, for sustainable urban mobility.
Emission-free, sustainable mobility based on hydrogen is more and more coming into reach. The H2Expo is a major industry meeting point, reporting on the current status of technological development and projects. The H2Expo, International Conference and Trade Fair on Hydrogen and Fuel Cell Technologies, takes place at the CCH-Congress Center Hamburg from 25 to 26 October, from 9am to 5pm daily.

www.h2expo.de

www.global-electronics.net

Primarion at Darnell Digital Power Forum

Primarion, a mixed-signal semiconductor company that provides digital controllers for power solutions, will be exhibiting and speaking at Darnell Group's third annual Digital Power Forum (DPF) on September 18-20. Primarion is one of the platinum sponsors of the event this year and would be available to discuss any trends regarding digital power solutions at the conference.
Primarion to speak three times at DPF:
Monday, September 18th at 9:30 a.m. – 12:15 p.m. – Ron Van Dell, CEO & President,
"**Digital Power Management: Changing the Value Ecosystem**"
Monday, September 18th at 2:00 p.m. – 3:30 p.m. – Deepak Savadatti, VP Marketing,
"**Roundtable Discussion: When Will the Switchover to Digital Take Place?**"
Wednesday, September 20th at 8:30 a.m. – 10:00 a.m. – Stephen Pullen, VP Systems and
Applications, "**Digital Today – Providing Power Management Solutions**"
Primarion will also have a booth at the event. They will be located in booth # 29.

www.primarion.com

Tyco Grants Technology to Astec

Tyco Electronics Power Systems announced that they have entered into a royalty-based technology licensing agreement with Astec Power that will allow Astec Power and its affiliates to use patented Tyco Power Systems technology in their current designs for their isolated converter eighth-brick and sixteenth-brick families of power modules.
This agreement, which currently extends for the life of the patents, will benefit customers by allowing them to receive Astec's power modules supported by patented technology from Tyco Power Systems.
This valuable technology (U.S. Pat. Re. 36571 and a number of related patents) is designed to increase the effectiveness and efficiency of self-synchronized rectifiers for application to clamped-mode power converters. Previously, efficiency had been limited because of the nature of switching boost converters and the variability of the transformer reset voltages in the forward type converters. By introducing a hybrid rectifier with a MOSFET rectifying device, Tyco Power Systems enhanced the efficiency of the rectifier, thereby increasing the efficiency and effectiveness of the manufactured power converters.

www.tycoelectronics.com

Schaffner sells EMC Test Systems

Management buyout ensures continuity for employees and customers.
Luterbach location to become a center of competence for EMC test systems development.
The Schaffner Group is selling the EMC test systems business line through an MBO to a group of investors led by Johannes Schmid, the Head of the Test Systems Division. The parties have agreed not to disclose details of the price. The sale of the EMC test systems business line, which contributed some CHF 30 million to Group sales in fiscal 2004/2005, represents a decisive step in Schaffner's strategy to refocus the Group on the dynamic market for components and modules to ensure the proper functioning of electrical and electronic devices. Following the sales of the Power Electronics and EMC test systems business lines, discussions with potential buyers for the remaining Cable & ElectroEmulation business line are continuing as a matter of priority. "Just as with the previous two, we will only consider selling the last business line at a price that reflects its realistic value," stressed Fritz Gantert, President & Chief Executive Officer of the Schaffner Group.

www.schaffner.com

ePhysics v2 Dynamic-Link Co-Simulation of Thermal and Stress Analysis

Ansoft Corporation announced the immediate availability of ePhysics v2. ePhysics v2 provides dynamic-link co-simulation of thermal and stress analysis with HFSS and Maxwell 3D.

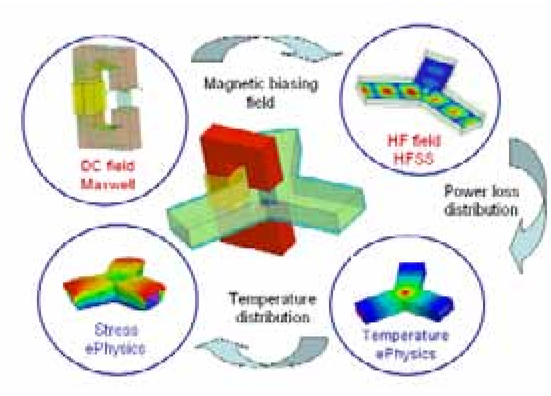

This latest version enhances ePhysics' 3D steady-state thermal, transient thermal and linear stress analyses coupling to HFSS and Maxwell 3D with dynamic-link co-simulation. The new capability allows engineers to simulate heating, stress and deformation consequences of high- and low-frequency electromagnetic fields.

ePhysics v2 responds to the market demand to have an integrated, multi-disciplinary approach to electrical component design, essential for devices operating under high power, faster data rates and reduced physical size, where thermal and mechanical effects need to be evaluated due to their influence on the overall performance.

The ePhysics user interface, including design management front-end, 3D modeler, parametric control, simulation set-up and post-processing interfaces, have been migrated to the Ansoft desktop concept shared by HFSS and Maxwell 3D. Engineers can easily account for the thermal and mechanical quantities that significantly contribute to a design's overall performance directly within the familiar, easy-to-use, Ansoft environment.

Coupling ePhysics with Maxwell 3D provides the cross-disciplinary analysis required in the design of electromechanical devices. Typical applications include the analysis of electric machines, power-generation systems, transformers, microelectromechanical systems (MEMS) and solenoids.

"Now that ePhysics v2 can be coupled directly to Maxwell, we are able to assess the thermal and stress behavior of magnetic components very conveniently," said Richard Osman, PE, principal product engineer, Siemens Energy & Automation Inc. "This advanced capability from Ansoft has greatly improved our ability to validate and optimize our designs before building hardware."

HFSS with ePhysics is vital for applications such as high-speed packages, antennas, monolithic microwave integrated circuits (MMICs), high-power microwave devices, military and broadcast communications and biological heating with radio frequency (RF) sources. These analyses include high-power, temperature-induced stress and size changes of design components.

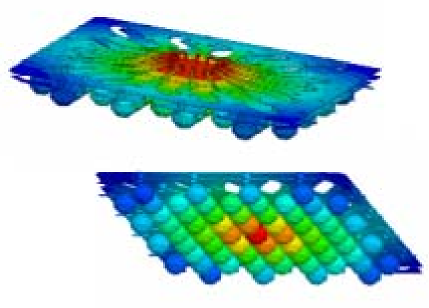

Figure 2: The thermal and stress behavior of components

New features include:

- New Ansoft desktop interface
- Dynamic-link coupling with Maxwell 3D and HFSS, which includes automatic mapping of power loss and force densities integrated with adaptive meshing technology
- Multiple design couplings that may be "daisy chained" in the process of creating complex applications
- Maxwell Transient - Thermal Transient
- HFSS Transient Sequence - Thermal Transient
- Nonlinear thermal properties (conductivity vs. Temp)
- Anisotropic stress solution
- 64-bit solvers available

ePhysics is available immediately for PC and UNIX(R) platforms. To learn more, visit www.ansoft.com/ephysics.

Ansoft is a leading developer of high-performance electronic design automation (EDA) software. Engineers use Ansoft software to design state-of-the-art electronic products, such as cellular phones, Internet-access devices, broadband networking components and systems, integrated circuits (ICs), printed circuit boards (PCBs), automotive electronic systems and power electronics. Ansoft markets its products worldwide through its own direct sales force and has comprehensive customer-support and training offices throughout North America, Asia and Europe.

www.ansoft.com

Your Quality Partner *for* Power Solutions

New DualPACKs

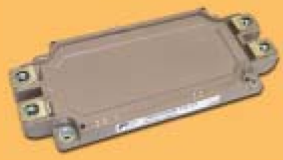

with Soldering Pins
1200V : 225A - 450A

with Spring Contacts
1200V : 225A - 450A

New High Power IGBT

1-Pack
1200V : 1200A - 3600A
1700V : 1200A - 3600A

2-Pack
1200V : 800A & 1200A
1700V : 600A & 1200A

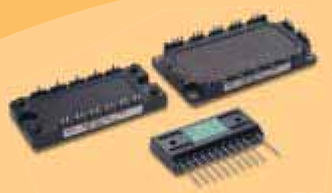

6-Pack IGBT
600V : 15A - 150A
1200V : 10A - 150A
1700V : 100A & 150A

PIM IGBT
600V : 30A - 100A
1200V : 10A - 75A

High Power 6-Pack
1200V : 225A - 450A
1700V : 225A - 450A

Special version available for rough environments

2-Pack IGBT
600V : 50A - 600A
1200V : 50A - 450A
1700V : 150A - 400A

1-Pack IGBT
600V : 600A
1200V : 200A - 800A

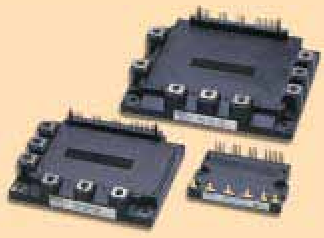

IPM-IGBT
600V : 15A - 300A
1200V : 15A - 150A

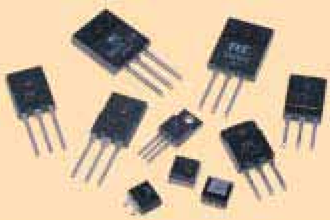

Discrete IGBT
600V : 5A - 75A
1200V : 3A - 25A

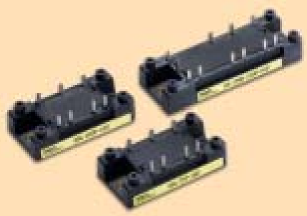

Rectifier Modules
800V : 30A - 250A
1600V : 30A - 125A

FUJI ELECTRIC
DEVICE TECHNOLOGY
e-Front runners

Fuji Electric Device Technology Europe GmbH
Goethering 58 · 63067 Offenbach am Main · Germany
Fon +49 (0)69 - 66 90 29 0 · Fax +49 (0)69 - 66 90 29 56
semi-info@fujielectric.de

www.fujielectric.de

The third edition of IEC60601-1 seems to indicate potential cost savings in power supplies for medical devices, but at what price?

By Steve Elliott, Industry Director – Medical, XP Power.

The third edition of IEC60601-1 was published in December 2005 and medical device manufacturers can now use it when designing new devices. There will be a period of 3 to 5 years when companies can produce devices to the specifications detailed in either the third or second editions, after which the second edition will be withdrawn.

IEC60601-1 third edition includes specifications for both 'basic safety' and 'essential performance' of medical devices. The second edition was only concerned with the basic safety of devices. It did not define a requirement for devices to remain functional; fail-safe was adequate, and compliance to each clause was on a pass/fail test criteria without taking in to consideration the essential performance of the medical device.

With respect to power supplies, the most important consideration is electrical safety. For the first time, the third edition now makes a distinction between the operator of a medical device and the patient to whom its operation applies. Different levels of isolation are applied to operator and patient circuits and defined as Means Of Operator Protection (MOOP) or Means Of Patient Protection (MOPP). The difference between the two is that MOOP falls in line with IEC60950 requirements - an information technology equipment (ITE) standard - and MOPP falls in line with IEC60601-1 second edition requirements, with IEC60950 being the less stringent of the two.

Clearly, a power supply that meets IEC60950 could be used for some applications and appears to offer potential cost savings to the medical equipment OEM. However, if the power unit drives any part of a circuit needing to provide a MOPP, secondary isolation will be needed to meet both isolation and patient leakage requirements.

Furthermore, a MOOP power supply still has to meet the earth leakage current requirements for a medical device used within the patient vicinity – so it probably needs to be modified to do this and additional filters, either within the power supply or in the form of external modules, could then be needed. The whole equipment may then need to go through the expensive and time-consuming process of being re-approved with respect to safety and/or EMC performance.

It's also important to remember that the use of an IEC60950 unit may limit the use of the medical device in some applications or markets. Already, some manufactures choose to design their products to IEC60601-1 even though it may not be technically necessary in order to satisfy end customer concerns. For example, where the equipment maybe physically located within a health facility.

Once a risk assessment has been carried out, medical device OEMs can choose to save a few dollars by buying an IEC60950 approved unit, rather than a power supply approved to IEC60601-1 or look for cost-effective power supplies that meet IEC60601-1. Five years ago, the latter were rare but in recent times new component technologies and design techniques have led power supply makers to produce units that simultaneously meet industrial, ITE and medical specifications. The higher volume manufacturing that this approach permits has brought down the cost of medical power.

A typical power supply in the 60W to 100W region costs around $50 US in quantities of a few hundred pieces. Moving to an ITE-only approved device is unlikely to produce cost savings of more than $5 and this approach is likely to limit application flexibility, lead to costly modifications to meet leakage current requirements, have a negative impact on the device manufacturers' brand, and, in extreme circumstances, put patients at risk. With only a small cost saving available is it worth it to risk patient safety and company reputation?

www.xppower.com

THE LENNOX REPORT

ELECTRONIC COMPONENTS INDUSTRY

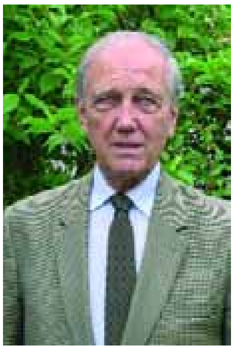

SEMICONDUCTORS

A recent study commissioned by **SEMI** concluded that makers of chip equipment and materials will need to spend $ 16 B to $ 20 B annually on research by 2010 to keep up the pace of innovation. But given the slower semiconductor industry growth rate they can only afford about $ 10.4 B pointing to a possible slowdown in the pace of Moore's law. This does not mean that nanotechnology research is being neglected. Recent examples of efforts in this area are France's Minatec, a new R&D center in Grenoble, and a UK consortium to use e-science and grid technology to tackle nano-CMOS design challenges.

iSuppli recently examined the world power management semiconductor market put last year at $ 22 B, or about 9.3% of total, but European-based firms supplied about $ 4.5 B, or 20.7% of total though only an 11.5% part of the overall semiconductor world market.

ON Semiconductor has completed the acquisition agreed upon in April of LSI Logic's Oregon 8" fab, is continuing research with Nantero (which the latter began with LSI Logic) on processes to integrate nano tubes into chip production while **Texas Instruments** and Conexant settled a long-standing legal dispute involving the latter's acquisition of Globespan Virata which allegedly infringed TI's ADSL patents. Meanwhile TI has seen its focus on ICs for mobile devices pay off where it holds a 58% share of the $ 8 B market and effectively helped force Intel out of this segment. The firm will run its 45 nm process in its Dallas 300 mm fab with a low-power ASIC design package available by year-end followed by first SoC samples early in 2007.

National Semiconductor's Willi Müller claims important sales gains by some of his distributors and is confident about Europe's role in design for some key industries such as automotive, industrial, automation and medical technologies backed by competitive Eastern European production.

Mitsubishi's last year sales of semiconductors amounted to $ 1.5 B including $ 825 M power semiconductors and the remainder RF and optoelectronic components. Japan made up 40%, in-house 23% and Europe 13% of first quarter 2006 $ 456 M revenue. Power semiconductors, a priority product line, will soon be produced on 8" wafers at an existing Renesas fab.

Intersil, formerly a key factor in wireless LAN, has become N° 6 in the high performance analog industry, so its CEO Rich Beyer, is expected to hit sales of $ 770 M this year. The firm has 110 design engineers considered key to its success as gross margin was 57% in the first quarter following revenue growth of 12% in 2005. Targets include high speed converters and automotive which has been made a division under VP Susan Hardman with a European design center a possibility. Peter Oaklander, ex-Analog Devices, has recently been named Sr. VP for worldwide sales in replacement of retiring Alden Chauvin.

Bosch plans to invest € 550 M in a new fab for automotive semiconductors located near Stuttgart and a daily capacity of 1000 200 mm wafers while **ABB Switzerland** has converted its Lenzburg BiMos line from 5" to 6" wafers so as to meet demand for IGBT dies for ABB's own Modules and foundry customers.

AUTOMATION COMPONENTS

According to **IMS** the European AC/DC and DC/DC drive systems market grew 15% in the first quarter, a growth topped only by China and fueled by demand of more efficient systems.

Carlo Gavazzi celebrated its 75 th anniversary, saw its automation division grow 8.4% to CHF 171 M in fiscal year ended March 31, 2006 driven in part by own production and sales in China and increased coverage in North America.

Rockwell Automation will sell two units, Dodge mechanical and Reliance electric motors, as it exits gears and motors to concentrate on factory automation systems.

PRINTED CIRCUIT BOARDS

According to the VdL/ZVEI the **world PCB market** grew 5.7% last year to $ 38 B with Japan and South East Asia accounting for 58% and Europe 14.8%, up 1.8% with an 3.5% increase expected this year. There were 379 PCB makers in Europe in 2005, down from 426 in 2004, employment declined 9.4% to 25 700. Germany made up 36% of European PCB production with automotive major customer segment at 34% followed by industrial 24% and communication 18%.

Invotec is the UK's largest PCB maker and expanding capacity with nearest rivals Prestwick and Ciratex having closed last year.

OTHER COMPONENTS

Schneider Electric has created seven product divisions to focus on markets and accelerate decision making.

editor@bodospower.com

Power Factor Correction Market Driven by Regulations

PFC can help meeting North American energy efficiency standards

PFC got a boost in power supplies in 2001, when the International Electrotechnical Commission (IEC) standard 61000-3-2 went into effect in Europe. This specification required new electronic equipment consuming more than 75W to meet certain standards for harmonic content, which basically required the use of PFC.

By Linnea Brush, Senior Research Analyst, Darnell Group

Although power factor correction (PFC) has been used for a number of years, the actual market for PFC products is still governed by regulations and standards that vary from region to region. PFC got a boost in power supplies in 2001, when the International Electrotechnical Commission (IEC) standard 61000-3-2 went into effect in Europe. This specification required new electronic equipment consuming more than 75W to meet certain standards for harmonic content, which basically required the use of PFC. In the United Kingdom, the standard goes by the designation of BSEN 61000-3-2; and in Japan, JIC-C-61000-3-2. The China Compulsory Certificate (CCC) mark is a compulsory safety and quality mark for many products sold on the Chinese market and includes similar requirements to the IEC 1000-3-2 standard.

No similar requirements have gone into effect for North America, although PFC can help power supply manufacturers meet current North American energy efficiency standards. PFC can often add cost and does not necessarily benefit the end user. So its advantage to suppliers can be a way of differentiating themselves by providing an energy efficiency benefit to society. The Electric Power Research Institute says that some manufacturers have claimed energy savings up to 10% through the application of power factor correction equipment in industrial facilities. It is also a way that larger original equipment manufacturers can "meet the spec" in Europe and Asia, while selling "added value" in other regions.
Any PFC forecasts are, therefore, considered "potential," since PFC is only required in certain products, at certain wattage levels, and in certain regions. Even then, compliance is sometimes an issue, and certain industries are lobbying for exemptions from the regulations. Forecasts are based on applications that have adopted PFC already and those likely to adopt it in the future, along with the wattage ranges identified in the IEC standard.

Europe, Japan and China currently have harmonic regulations that basically require the use of PFC, so these regions have a higher share of the worldwide PFC market. The European and Asian regulations typically require PFC between 75W (26W for lighting devices) and 600W, but only for certain classes of devices. Class D harmonic limits are the most restrictive and apply to personal computers, computer monitors and television receivers. Application and wattage parameters, therefore, determine what applications and power levels were the "best" opportunities for PFC.

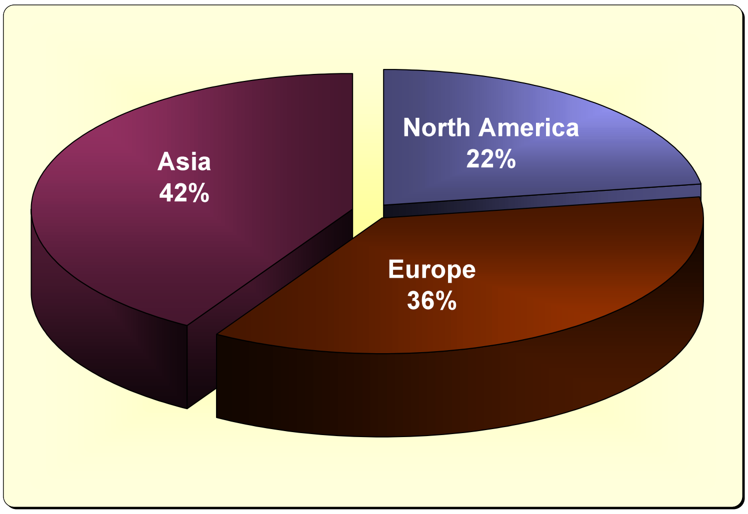

Figure 1: Worldwide Active PFC Market by Region (unit market share)

The waters get murkier when forecasting active versus passive PFC. Cost is the biggest issue determining when active or passive is used, and volume production and price declines are starting to drive the adoption of active over passive PFC. Space constraints can also make a passive solution impractical in lighter-weight devices. It is unlikely that original equipment manufacturers will stop using passive PFC if they are not required to by regulation, especially if there is no cost benefit to doing so.

The total Worldwide market for PFC (both active and passive) is expected to be approximately 1.3 billion units in 2006, increasing to 2.2 billion units in 2011, a compound annual growth rate (CAGR) of 11.4%.

The potential Worldwide Active PFC market is expected to grow from approximately 1.2 billion units in 2006 to 2.1 billion units in 2011, a CAGR of 12.3%. Although the European standard is the most encompassing, the Europe Active PFC market is smaller than the Asia Active PFC market. Europe's share is expected to be about 36.2% of the

Worldwide total, whereas Asia represents about 41.4% of the Active PFC market. North America, with no compulsory regulations to meet, will have the lowest share from 2006 to 2011, at 22.4%.

Power factor correction can be important at higher power levels. If maximum power is needed, PFC is required. It has been most commonly used in motor drives and pumps greater than 75W, such as refrigeration and heating. EN61000-3-2 has evolved since its introduction in 2001, with Amendment A14 reclassifying nearly 90% of the electronic devices in Class D (which basically required PFC) to the less stringent Class A. Under Class A requirements, a 180W power supply can get by with just a simple passive filter. In the future, notebook power supplies <50W, as well as devices that have active front ends, could be excluded from future PFC requirements, but this is still a “contentious” issue, according to individuals working with these standards. Some high-volume applications that could be subjected to new regulations include notebook computers, LCD desktop monitors and LCD televisions.

Lighting ballasts also often use PFC, in part because of the Class C requirements of EN61000-3-2. PFC implementation is likely in distributed power architectures, including embedded ac-dc power supplies. Active PFC is a requirement for Server System Infrastructure (SSI) compliance. Flat panel displays are also potential applications for PFC.

White Goods, including Air Conditioners, are the largest worldwide Consumer market. The White Goods segment has a larger impact on the wattage forecasts in Europe than other application segments. Due to new environmental regulations and designs, demand for dishwashers, microwave ovens, air conditioners and other household goods is growing throughout Europe, and many of these designs are smaller than appliances sold in other parts of the world. In addition, the saturation levels for many major appliances are only half what they are in the U.S. Dishwashers have the least penetration, for example, because they take up space in the kitchen required by other appliances.

The combined Europe White Goods and Air Conditioner market is expected to be 59.2 million units in 2006, growing at 7.6% to 85.2 million units in 2011. Germany is the largest market for European appliance manufacturers, followed closely by France, England and Italy. European washing machines are, in general, smaller than U.S. versions and most have horizontally mounted drums. Air conditioning is still a relative rarity in Europe. Companies are also looking at full digital power factor correction, and new designs could potentially reduce costs. PFC greatly benefits from non-linear programming. Digital implementation allows two separate functions to be integrated into a single unit and allows the power converter to be changed to accommodate different loads. This improves efficiency, which will help drive customer demand for digital control of power supplies.

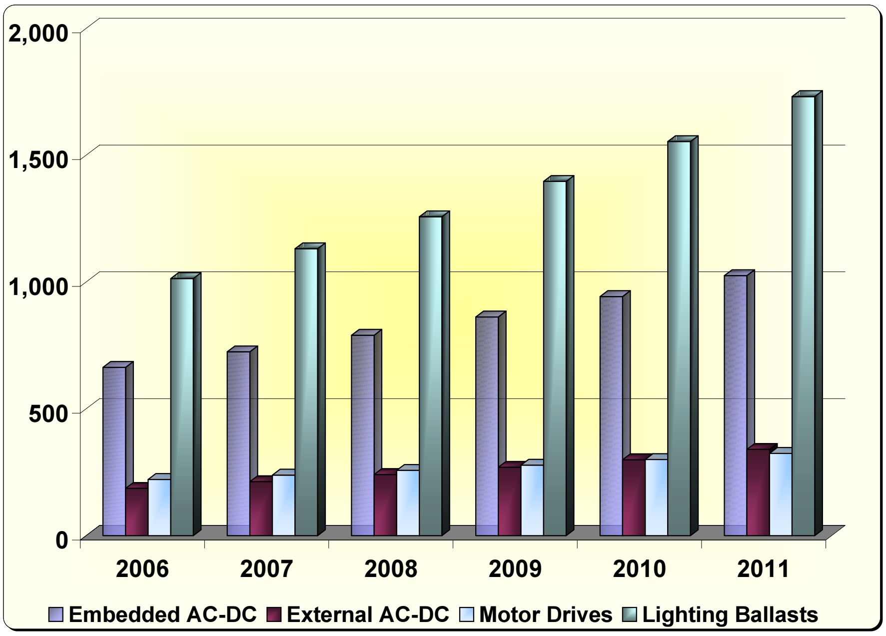

Figure 2: Worldwide Power Supply Market by Product (millions of units)

Driven by regulations, the development and production of PFC components is expected to continue to expand at a steady pace over the next several years. The industry should remain extremely competitive, with large, multinational companies like STMicroelectronics, Fairchild, Texas Instruments and International Rectifier competing for market share with dozens of smaller regional companies worldwide.

A number of new products have been announced that are designed for PFC applications in switch-mode power supplies. Infineon Technologies introduced its second-generation Schottky diodes based on silicon carbide (SiC) technology. The thinQ 2G family have at least double the surge-current capability and improved ruggedness compared to the first generation. This allows them to handle higher start-up inrush and over-currents, making them suitable for PFC applications.

Fairchild Semiconductor introduced the FAN7528, a PFC controller IC that reduces standby power as much as 320mW in switch-mode power supply designs under 250W, such as notebook adapters. The company also added three new Smart Power Modules (SPM) designed for full switching power factor correction in motor drive applications in the 3-6kW power range.

An advanced double-ended controller designed specifically for the series-resonant half-bridge topology was recently announced by STMicroelectronics. The L6599 includes a dedicated output for direct PFC connection and is suited for use in liquid crystal display and plasma display panel TVs, high-end ac-dc adapters for laptops and game consoles, 80+ initiative-compliant ATX silver boxes, servers and telecom switch-mode power supplies.

International Rectifier offers a motor control platform for air conditioning applications that enables 95% efficiency. The iMOTION integrated power design platform features a proprietary algorithm for interior permanent magnet synchronous motors in the compressor as well as the fan, and includes power factor correction.

For more information on Power Factor Correction, Potential Market Forecasts, Application Trends and Competitive Environment go to: http://www.darnell.com/consulting/study.php?mc_id=30

www.darnell.com

High Current low $R_{DS(on)}$ Trench MOSFET SIX-PACK

New DCB based surface mount package for automotive applications

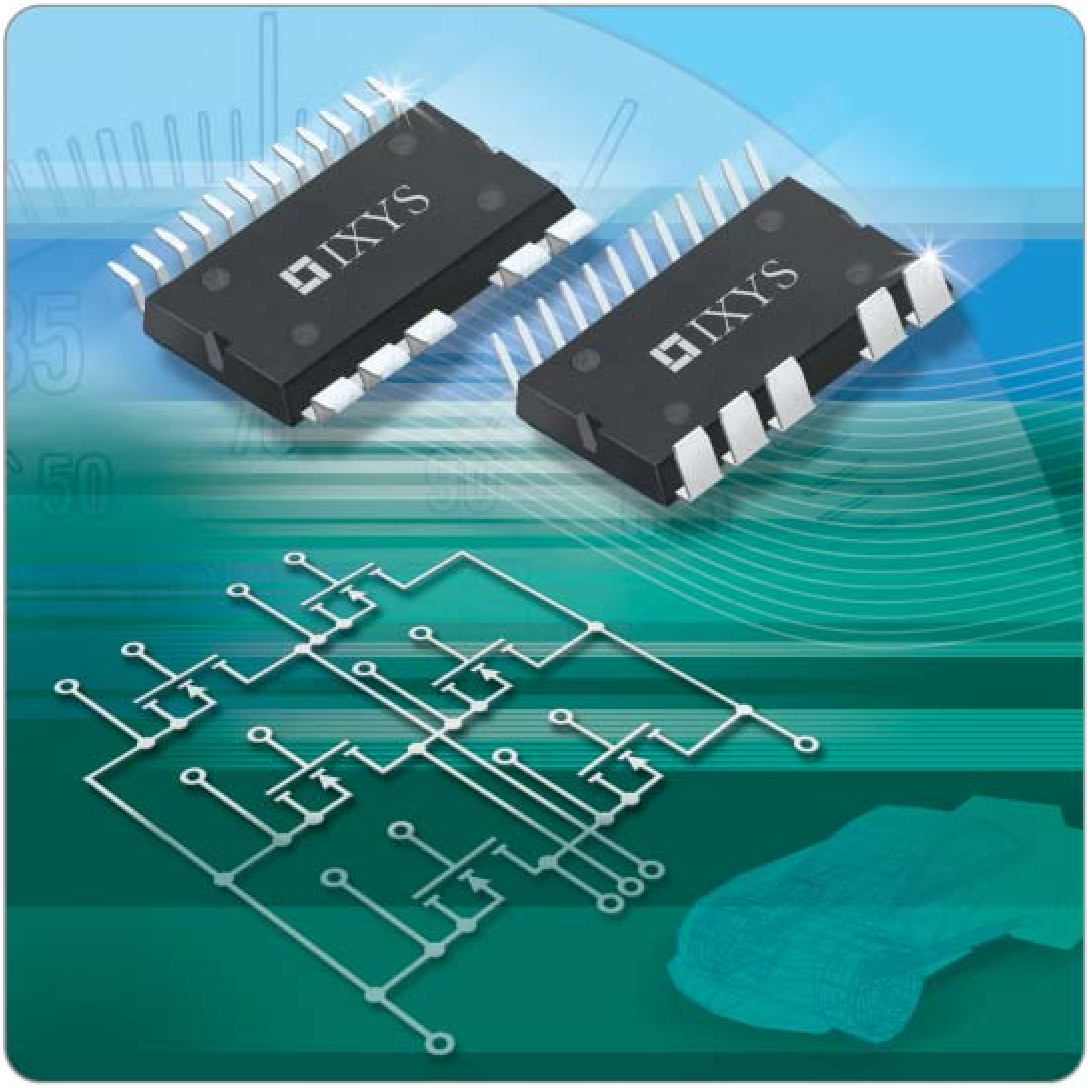

Features

- Low $R_{DS(on)}$
- Optimized intrinsic reverse diode
- High level of integration
- Multi chip packaging
- High power density
- Auxiliary terminals for MOSFET control
- Terminals for soldering (wave or re-flow) or welding connections
- Isolated DCB ceramic base plate with optimized heat transfer

Applications

- Electric power steering
- Active suspension
- Water pump
- Starter generator
- Propulsion drives
- Fork lift drives
- Battery supplied equipment

TYPE	V_{DS} Max V	$I_{D(cont)}$ T_c=25°C A	I_{D90} T_c=90°C A	$R_{DS(ON)typ}$ T_c=25°C mΩ	$Q_{G(on)}$ typ nC	t_{rr} typ ns	Lead Options (Note: xxx defines Lead Option)
GWM 220-004P3-xxx	40	190	145	2,0	94	70	BL - Bent Leads
GWM 160-0055P3-xxx	55	160	120	2,3	86	100	SMD - Surface
GWM 120-0075P3-xxx	75	125	95	3,7	91	90	Mount Device
GWM 70-01P2-xxx	100	70	50	11	110	80	SL - Straight Leads

Surface Mounted Device

Bent Leads

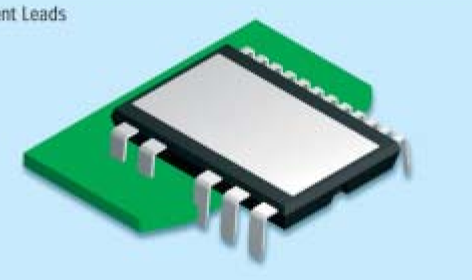

Benefits

- Highest reliability
- Easy assembly
- Optimized EMI behavior
- Extreme low power loss

www.ixys.com

Efficiency Through Technology

EUROPE:
IXYS Semiconductor GmbH
e-mail: marcom@ixys.de

USA:
IXYS Corporation
e-mail: sales@ixys.com

IXYS

The Help of Thermal and Mechanical Analysis

Modules to handle higher power levels

Power electronics applications continue to demand cost-effective power modules with ever-increasing efficiency and performances and efficiency. Semikron is meeting this need by introducing the SEMITOP 4 "baseplateless" module.

By Fabio Brucchi, Semikron Italia

This device retains the SEMITOP family's "one screw mounting" technique, while handling up to 22 kW motor power from a 58.5×53mm footprint (590 W/cm³).Power electronic applications are continuously demanding cost-effective power modules with increased efficiency and performances Current density in power modules has shown a continuous linear growth throughout the last decade. For example, 600V IGBT dice increased from 120A/cm² in 1996 to over 190A/cm² in 2005. In the same way, 600V fast CAL diodes were developed from 160A/cm² in 1992 to 230A/cm² in 2004.

This continuous need is met by introducing the "baseplateless" one screw mounting SEMITOP®4 module. The minimum specification to make this module attractive to the market (keeping the same reliability level as the smaller SEMITOP modules) was:

Power rating: Twice the power rating of SEMITOP 3;
Power density: 30% higher than SEMITOP 3;
Thermal resistance (junction-to-sink): 20% less than SEMITOP 3;
Topologies:
Six-pack (IGBTs and MOSFETs) and Converter Inverter Brake.

The trend of increased power density of power electronics applications coupled with the need for cost containment of power electronic applications has brought about reductions in electrical and safety margins.

Figure 1 shows the well-known dependency of the number of cycles with temperature swings (LESIT curves) for a power electronics module, and emphasises the importance of a correct thermal design.

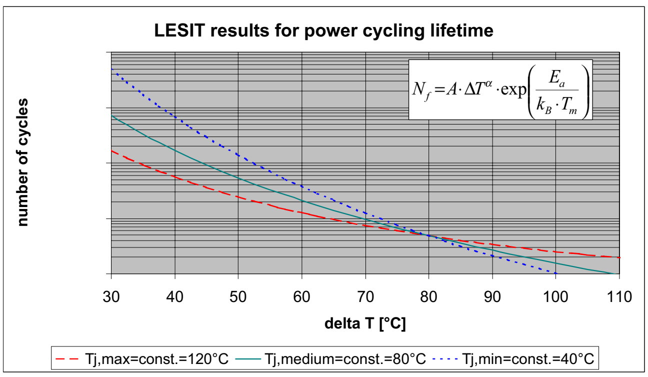

Figure 1. LESIT Curves for reliability of power modules.

N_f = Number of power cycles;
k_B = Boltzmann constant =1.38·10-23 J/K
E_a = Activation energy = 9.891·10-20 J
A = constant = 302500 K^{-a}
α = constant = -5.039
T_m = medium junction temperature.

For this reason, in order to achieve a successful and reliable power module, many thermal phenomena (such as thermal interference, temperature contour distortion and border effect) which have often been considered to be of secondary importance (or sometimes even neglected) have been considered now.
Due to the fact, that the housing also functions as a pressure system, an accurate mechanical dimensioning study has also been performed.

Mechanical simulations and design
To meet increased quality requirements and to avoid critical aspects in terms of the substrate's mechanical stress, a finite element mechanical analysis has been performed on different shapes, structures and housing materials.

This analysis reduced the expensive tests usually necessary to verify the trial housings made by milling machines and reduced the testing of plastic mould tooling.

Moreover, these simulations also reduced the time for prototyping and the number of revisions of the final tooling.

Figure 2 shows an example of such a comparison. The high level of mechanical deformation of a SEMITOP 4 prototype housing screwed onto a heat-sink and made in standard polymer (ABS, Figure 2a) is compared to the final design made in GF reinforced polyimide (Stanyl, Figure 2b). It is easy to see that in the wrong design the applied torque to the centre screw leads to excessive deformation of the housing (over 1.3mm), while in the final design the maximum mechanical deformation is about 320µm. Furthermore, in

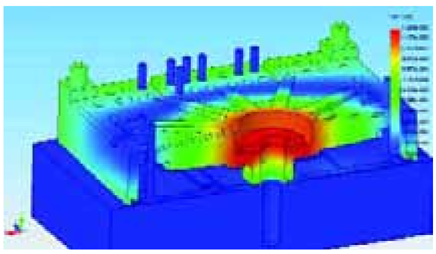

Figure 2a. Mechanical displacement of SEMITOP 4 with standard polymer

terms of mechanical pressure on the substrate, applying the nominal torque to the centre screw, the mechanical stress (according to Von Mises) was reduced from 500MPa (initial design) to less than 200Mpa (final design), which is broadly within the Weibull Modulus statistical limit of the ceramic bending strength failure (three point method).

Thermal Simulations and Design

To meet increasing power density requirements, more and larger dice populate the same area in today's modules. This makes it necessary to dissipate into the heat-sink the same (or even increased) power levels from ever-smaller areas.

This means that thermal interference, distortion of temperature contours and the interaction of all these phenomena have to be taken into consideration. This leads to a different approach to power electronics module design.

So, the typical coefficients used for $R_{th(j-s)}$ calculation have to be revisited as a function of the power module and as a function of the specific customer application.

With the introduction of user-friendly finite element analysis software and the increasing calculation power of PCs, finite element models (FEMs) can be generated very quickly. Starting from 3D-files or 2D-CAD files, complete and detailed substrate layout analysis can be produced in a few hours. This allows a time-effective generation of a great number of FEMs and the handling of huge amounts of data (which has been impossible up to now with standard FE software and PCs, which could take several days to produce a complete FEM).

It has been possible to verify the $R_{th(j-s)}$ distribution for each customised layout and to identify every possible thermal critical aspect. The potential critical points are then discussed with the final customer to evaluate the effective critical response in the real application.

Table 1 compares the measured maximum IGBT and FWD $R_{th(j-s)}$ values on trial housings vs. FEA results.

Measurements are based on the international IEC747-8/2.18 standard. This is an indirect method which uses the $V_{ce(sat)}$ to monitor the T_j. This value is a "sort of average" temperature of the die's junction temperature. For this measurement to be consistent with FEA, we used a weighted average chip temperature to get the T_j value and the heat-sink temperature T_s in the exact position where the temperature probe was placed during measurement.

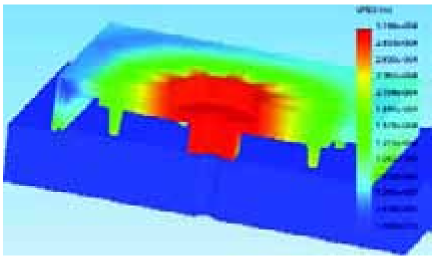

Figure 2b. Mechanical displacement of SEMITOP 4 with GF-reinforced polyimide.

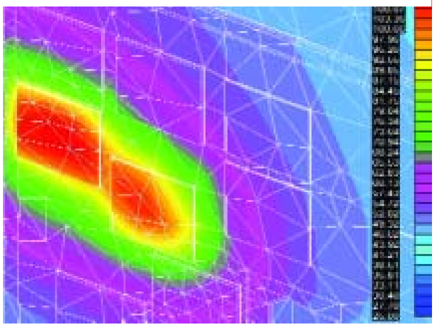

Figure 3a. Rth(j-s) measurement at PD=121.6W. Junction temperature contour (TJ(max)=111.47°C).

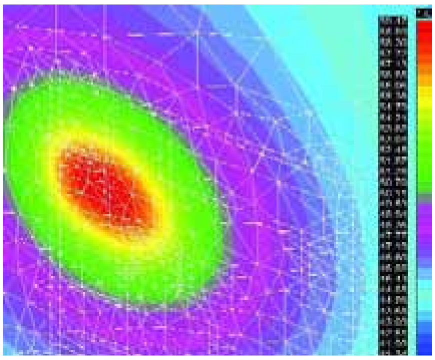

Figure 3b. Rth(j-s) measurement at PD=121.6W. Heat-sink temperature contour (Ts(max)=59.47°C) on switch IGBTTOP1 SK100GD126T.

It is important to specify this because the temperature across a silicon die (particularly in paralleled dice) can vary by several degrees (for example, in Fig. 3a T_j varies from 114°C to 96°C on the same die). The incorrect choice of measurement points can falsify the simulation result.

When running at high power dissipation, each die receives from the adjacent one a high thermal interference level. Furthermore, temperature contour distortion and border effect lead to an increased $R_{th(j-s)}$ level.

For example, Figure 4 shows this difference, using different power dissipation levels than those used for the $R_{th(j-s)}$ measurement and with lower die-to-die distances.

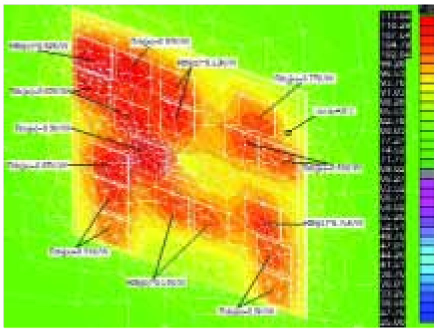

Figure 4. Simulation of SK100GD126T module running in application with specification of each Rth(j-s).

Figure 4 also shows the temperature sensor, which is positioned at the upper right corner of the power hybrid. With the FEA it is possible to check the real temperature "seen" by the temperature sensor (96°C, which is about 17°C lower than the hottest point in the module) and to compare it with the switch temperature to give a more accurate figure for T_j, instead of having the usual generic indication of the power hybrid's temperature.

Using this new design approach it has been possible to verify the $R_{th(j-s)}$ variations as a function of die-to-die distance, die shape and area and die-to-border distance for "baseplate-less" modules.

	I_C @ T_S=25°C	I_C @ T_S=80°C
GD126 Version		
3-Ø 1200V IGBT Inverter	100A	70A
3-Ø 1200V IGBT Inverter	77A	53A
3-Ø 1200V IGBT Inverter	65A	43A
GD066 Version*		
3-Ø 600V IGBT Inverter	155A	110A
3-Ø 600V IGBT Inverter	117A	82A
3-Ø 600V IGBT Inverter	84A	55A
DGDL126 Version		
CIB 1200V	60A	40A
CIB 1200V	45A	30A
DGDL066 Version*		
CIB 600V	90A	70A
CIB 600V	75A	56A
MD Version		
3-Ø 100V MOSFET Inverter	165A	125A
3-Ø 55V MOSFET Inverter	225A	170A

* $T_{J(MAX)}$ = 175°C

Table 1. Comparison between measured Rth(j-s) and simulated Rth(j-s) for each IGBT and FWD (SK100GD126T).

In particular, Fig. 5 shows $R_{th(j-s)}$ as a function of die distance for two paralleled dice (keeping a minimum die-to-border distance of 5mm in order to avoid border or temperature contour distortion effects). The consistency of these graphs has been cross-checked by comparing measurements on SEMITOP®3 and SEMITOP®2 modules following the IEC 747-8/2.18 international standard for R_{th} and Z_{th} measurement.

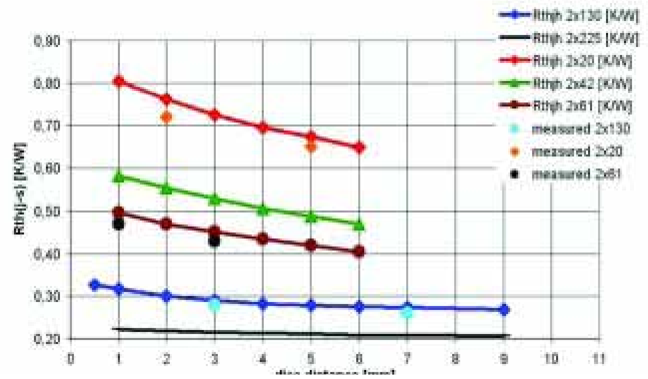

Figure 5. Rth(j-s) as a function of dice distance for two paralleled dice and different die size.

In addition, it was found that border effects and even die shape are not negligible when die-to-die distance is less than 3-4mm in a "baseplateless" module. In fact, we found that when two or more dice are paralleled, $R_{th(j-s)}$ is strongly influenced by the length of the adjacent die's parallel side. For example, three rectangular dice can be paralleled with adjacent short sides or adjacent long sides. In the second case, the $R_{th(j-s)}$ value was over 17% greater than when we paralleled the three dice with short adjacent sides. This is mainly due to the combination of deformation of temperature contours and thermal interference phenomenon (the simulation was performed trying to avoid border effect, then using a die to border distance greater than 5mm).

It is then easy to see that $R_{th(j-s)}$ in paralleled rectangular dice having adjacent shorter sides is smaller than $R_{th(j-s)}$ in paralleled squared dice at the same measurement conditions and at the same total switch silicon effective area.

In our research, we found that $R_{th(j-s)}$ can shift from its typical value by over 40% in a power module with high die density, because of thermal interference and the border effect.

SK100GD126T IGBT=2×57mm^2 FWD=61mm^2	**Measured $R_{th(j-s)}$ [K/W]**	**FEA $R_{th(j-s)}$ [K/W]**	**Diff [%]**
IGBT (top 1)	0,42	0,427	1,6
IGBT (top 2)	0,39	0,397	1,8
IGBT (top 3)	0,41	0,403	-1,7
IGBT (bottom 1)	0,44	0,437	-0,7
IGBT (bottom 2)	0,39	0,393	0,8
IGBT (bottom 3)	0,43	0,436	1,4
FWD (top 1)	0,62	0,625	0,8
FWD (top 2)	0,61	0,621	1,8
FWD (top 3)	0,69	0,686	-0,6
FWD (bottom 1)	0,67	0,674	0,6
FWD (bottom 2)	0,68	0,669	-1,6
FWD (bottom 3)	0,68	0,675	-0,7

Table 2. Thermal Resistance Measurement and Simulation

SEMITOP 4 – The Technology

To achieve the design aims, and keeping in mind the new FEA simulation, a new substrate has been used. This has different thicknesses of insulator and copper topside/backside, and improved thermal performance, compared to the smaller SEMITOPs. The substrate chosen has a thickness of 0.38mm Aluminium Oxide (Al_2O_3) with Curamik pre-bent technology. It is especially suitable for modules without a "baseplate" and allows an even thermal paste distribution while still only using one central mounting screw.

The thermal paste thickness does not need to be increased, compared to SEMITOP 3.

The module outline dimensions are: W=60mm, L=55mm, H=12mm. It is fully compatible with SEMITOP 1, 2 and 3; i.e. it is possible to use it in combination with the existing SEMITOP 1, 2 and 3 on the same circuit board and on the same heat-sink.

The module is available in three-phase IGBT (and MOSFET) inverter (from 65A/1200V up to 155A/600V at T_J 25°C) and in Converter Inverter Brake (from 45A/1200V up to 90A/600V at T_J 25°C) topologies.
The following are the results achieved with this technology:
Topologies: Six-pack (IGBTs and MOSFETs).

Converter Inverter Brake.
Power rating compared to SEMITOP 3:
3.6 times more for the 600V IGBT inverter;
3.1 times more for the 1200V IGBT inverter;
3.8 times more for the 600V IGBT CIB;
3.5 times more for the 1200V IGBT CIB.

Power density compared to SEMITOP3:
38% higher than 600V three-phase IGBT inverter;
47% higher than 1200V three-phase IGBT inverter.

Thermal resistance (junction-to-sink)

A SK100GD126T inverter in SEMITOP 4 (1200V/75A at T_s=80°C) has a typical thermal resistance of 0.39K/W. The same silicon dice mounted into SEMITOP 3 show a typical $R_{th(j-s)}$ of 0.49K/W. This is a reduction of about 20%.

SEMITOP 4 brings more power to the existing SEMITOP range of modules (without "baseplate", one centre-screw mounting). The higher power range allows for applications such as drives and power supplies up to 40kVA inverter power.

Conclusion

A different substrate with improved thermal performance has been used. The maximum power rating of IGBT inverter in SEMITOP 4 is over three times greater than existing SEMITOP 3 inverters. These modules have been designed using mechanical and thermal finite element simulation software to meet any critical mechanical and thermal factors, even in the worst environments. With the help of this software, a different approach to power electronics design has been implemented.

www.semikron.com

Innovative Cooling Concept for Power Modules

High thermal performance gives high reliability solutions

ShowerPower, a newly developed cooling concept, solves the key problems related to liquid cooling namely the high cost and the inhomogeneous cooling. The challenges for future liquid cooled power module assemblies, especially in hybrid electrical vehicle traction applications, can be met by the ShowerPower cooling principle.

By Klaus Olesen, Danfoss Silicon Power GmbH

Requirements for liquid cooling systems
In order to increase thermal performance and lifetime the manufactures of power electronic assemblies request:

High cooling performance, which saves silicon and ensures long life.
Homogenous cooling, which enables paralleling of several power semiconductors.
And all this at a low cost of course.

Present cooling technologies can not meet these requirements; performance and cost follow each other in state of the cooling technology. Even the step from coldplate technology to open pin fin coolers, that eliminates the need to use thermal interface materials between power module and cooler, does not solve the problems. However at Danfoss Silicon Power we have developed a cooling principle which is highly efficient (better than pin fin coolers), offers homogenous cooling across even large surfaces (temperature gradients are fractions of a °C), and at a low cost since the key part of the concept is a simple plastic part.

In a traditional liquid cooled system the heating up of the coolant causes a temperature gradient in the power module, see the left part of Figure 1.

ShowerPower™, the basic idea
The fundamental idea is to turn the direction of the coolant flow by 90° and to introduce coolant having the same temperature all over the surface to be cooled, which can be perfectly flat having no structuring, see the right part of Figure 1 below. The name of the concept originates from the conceptual resemblance to using a common shower-head from a daily life bathroom. But as opposed to other jet impingement coolers the trick here is to get rid of the coolant before large temperature gradients are generated.

Metal-to-plastic conversion
Parallel injection of coolant perpendicular to the surface to be cooled is obtained by a simple plastic part manufactured by e.g. injection moulded, the cost typically a fraction of one EURO. This metal-to-plastic conversion offers a very large cost reduction potential since the costly processes involved in standard coldplate- as well as pin fin manufacturing have been transferred to a simple low cost plastic part.
Several cooling cells on the top side of the plastic part guide the coolant to the baseplate surface; the meandering structure of the cooling channels ensures high heat transfer.

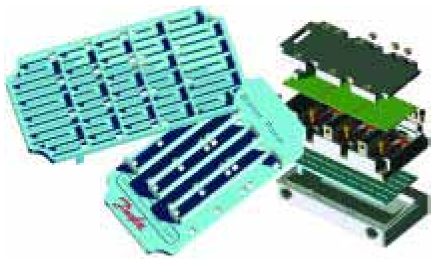

Figure 2. A simple plastic part acts as a guide for the coolant. Front and back of the plastic part are shown.

Homogenous cooling
To obtain homogeneous cooling the cooling cells are supplied with coolant that have the same inlet temperature; this is accomplished by the manifold structure on the backside of the plastic part.

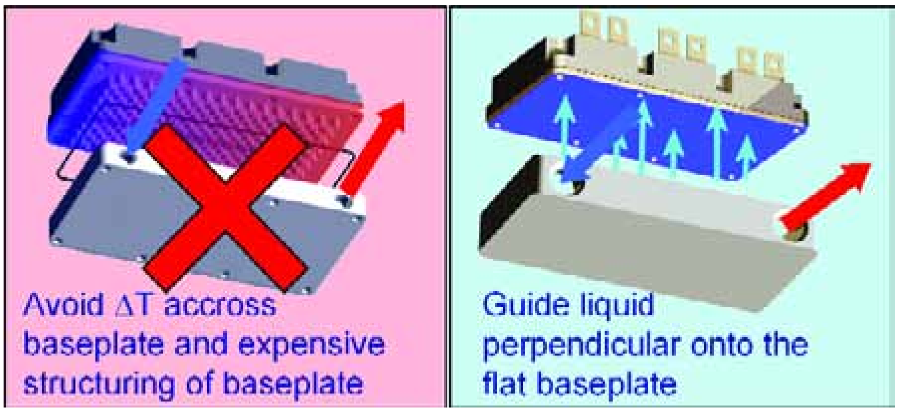

Figure 1. Turning the flow direction by 90° eliminate temperature gradients.

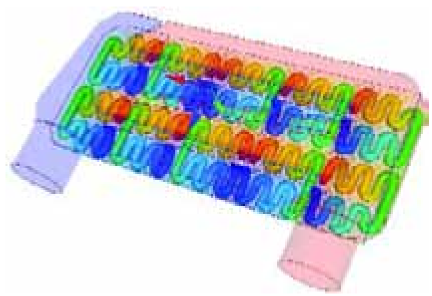

Figure 3. The fluid flow inside the cooler. The flow in the main manifolds is shown dimmed.

Figure 3 illustrates the principle: the pressure distribution in each meandering cell are identical and the inlet manifold feed (dimmed red) the channels whereas the outlet manifold (dimmed blue) guide the coolant away from the cooling cells.

Thus the concept offers true homogenous cooling with the ability to remove temperature gradients over arbitrarily large areas.

Tailored cooling

The concept can be used to solve specific thermal problems, e.g. if a particular hot spot in a power module needs special attention, the cooling channels of the cooler are simply adjusted locally. In other words the concept offers total design freedom to tailor the temperature gradients across the surfaces to be cooled.

Typical performance

Numerous tests have been conducted, in-house as well as externally at customers and research institutions. Typical performance parameters are heat transfer coefficients in the excess of 10.000W/(m2K) with pressure drops of a few hundred mbar's using ethylene-glycol/water 50%/50% as coolant. The chart below shows the thermal comparison between a pin fin cooler and a ShowerPower™ cooler, measured by Ernst Schimanek, Fraunhofer IISb- Erlangen. It shows the thermal resistance, junction to coolant, and pressure drop vs. the volume flow rate through the coolers.

It is seen that especially at lower flow rates that the ShowerPower™ performs better than the pin fin cooler.

ShowerPower™ offers:

- Uniform cooling of the power module, the temperature gradients are gone; alternatively tailored cooling is possible
- High thermal performance yielding more reliable cooling solutions
- Metal-to-plastic conversion drives down the cost significantly
- The direct cooling eliminates the need for a thermal interface material.

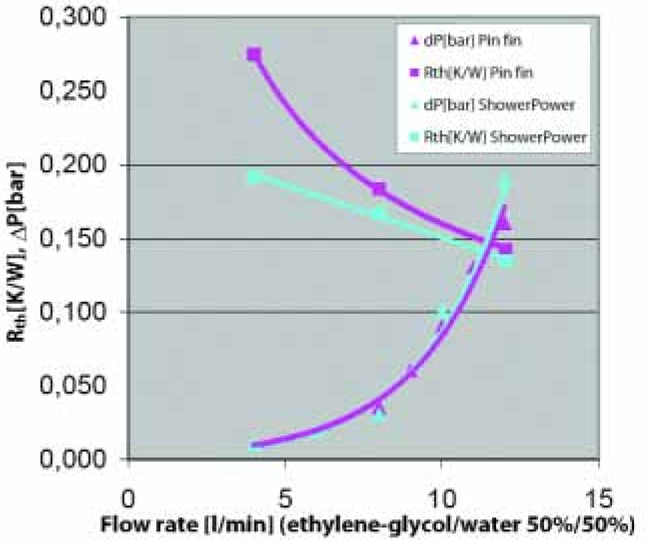

Figure 4. The thermal performance of a pin fin cooler compared with a ShowerPower cooler.

Applications for liquid cooling
The potential applications for liquid cooling and thus ShowerPower™ are numerous especially where high power densities represent a thermal challenge, and where liquid coolant is available. A dozen potential customers are performing or have done tests on ShowerPower™ coolers ranging from automotive applications to CPU coolers. Some examples:

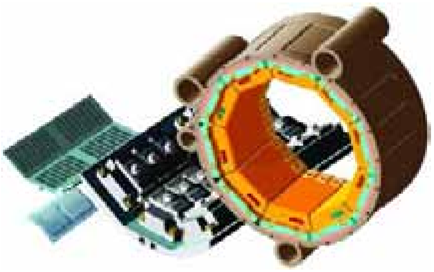

Figure 5. Assembly for a hybrid electric vehicle traction converter module, the shape of the ShowerPower coolers are adapted to needed application, e.g. a cylindrically shaped motor.

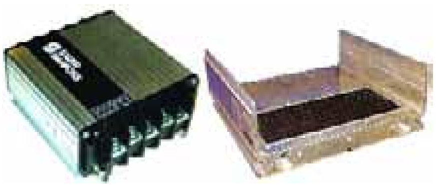

Figure 6. Battery driven inverter, BPI (Sauer-Danfoss); the Al baseplate (right) having integrated the ShowerPower cooler; intended mainly for forklift truck applications.

Figure 7. CPU cooler with a one-part ShowerPower cooler, (to the right the front and backside of the cooler is shown).

Designing a cooling system
When designing a cooling system it is necessary to understand the physics of the problem.

Characterising the system: hydrothermal performance
The requirements for a cooling system of course vary greatly from application to application. Nevertheless two main parameters are needed for characterising the hydrothermal performance of a cooling system namely the heat transfer coefficient (also called the convection coefficient) and the pressure drop. The latter is directly linked to the system cost since a high pressure drop requires a strong=expensive pump. Most often the maximum allowed pressure drop is specified along with the required thermal performance for a specific application and the task then is to design the cooling system accordingly.

When comparing the performance of different coolers, or when optimising a specific cooler, it is necessary to consider both parameters: the heat transfer coefficient and the pressure drop since the hydrothermal performance is always a trade-off between the two: a higher thermal performance most often means a higher pressure drop and vice versa. It is also much more convenient to consider the heat transfer coefficient than e.g. temperature since temperature depends on a number of additional boundary conditions related to the thermal stack (materials and geometries) that makes the comparison complicated.

Trade-off between thermal performance and pressure drop
As discussed in the previous section the hydrothermal performance is a trade-off between thermal performance and pressure drop. The chart below plots the pressure drop vs. the thermal performance for a large variety of meander channel geometries where channel width and length have been varied. It turns out that the results basically follow the same hyperbolic curve. Note that the thermal performance here is given as normalised thermal resistance, which basically is the reciprocal of the heat transfer coefficient.

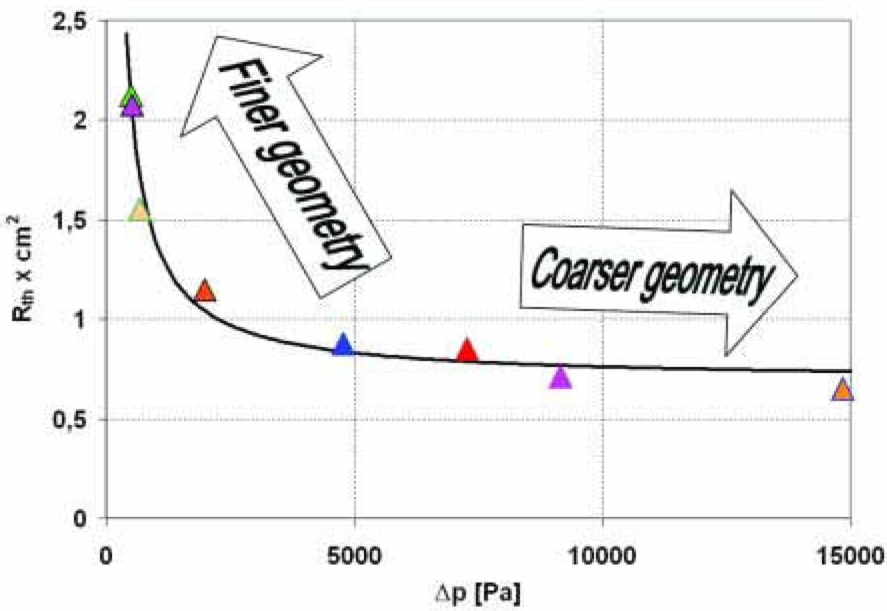

Figure 8. Varying the channel geometry influences the hydrothermal performance.

It is seen that coarser channel geometry results in lower pressure drop but also a higher thermal resistance and vice versa.

Optimising the performance
Improving the hydrothermal performance of a cooling system is a challenge: how to improve the ability to remove heat without sacrificing the pressure drop. This is equivalent to find other hyperbolic curves in the same way as in Figure 8 that features lower pressure drops at lower normalised thermal resistances.

In many cases simple empirical formulas applying dimensionless parameters like the Reynolds-, Prandtl- and Nusselt-numbers can be used to get a first assessment of the hydrothermal properties, but for more thorough investigations CFD (computational fluid dynamics) is a must.

Simulation strategy
The ShowerPower™ is unique in that sense that it is based on identical cooling channels supplied with coolant in parallel, this means that it is only necessary to consider the cooler on single-cell level which makes simulations and optimisations much simpler.

Optimisation example
As an example of how the hydrothermal per-

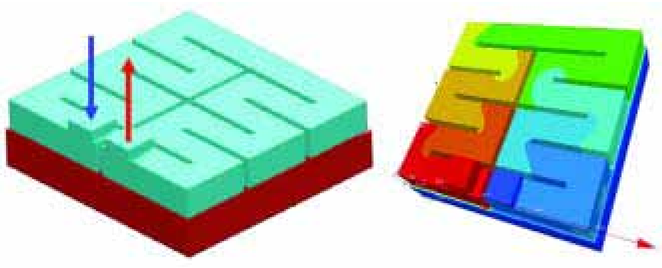

Figure 9. A unit meander cell, the liquid (blue) is placed on a piece of baseplate. To the right the pressure distribution is shown, found from a CFD simulation.

formance of the ShowerPowerTM cooler can be optimised, the introduction of small bypass flows is presented.

Small gaps between the plastic part and the power module baseplate allow fluid flow over the top of the walls separating the “legs” of the meander channels. The sketch below illustrates the idea.

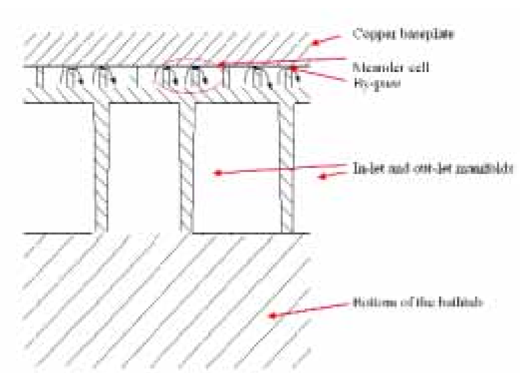

Figure 10. A gap between the walls of the channels and the baseplate allows a bypass flow.

The CFD simulation result below shows the fluid velocity distribution in a meander channel having gaps between wall and baseplate of 0,25mm. It is seen that the fluid velocity is quite high in the bypass area.

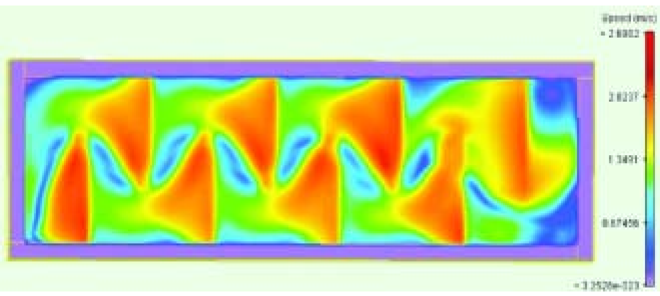

Figure 11.
The fluid flow velocity in a meander cell having a bypass flow.

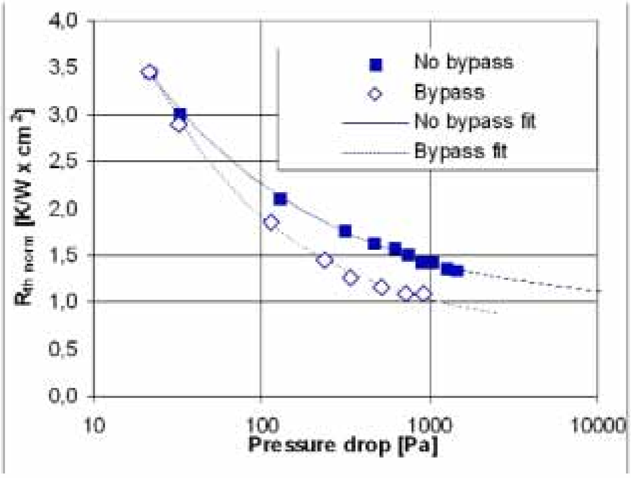

Figure 12. Normalised thermal resistance vs. pressure drop for meander channels with- and without the bypass flow. CFD simulations and fit curves.

Varying the channel geometry of the meander channel, i.e. channel width, height and length, with- and without the bypass gap and plotting the normalised thermal resistance vs. the pressure drop yields two hyperbolic like curves as seen in figure 12.

The two curves represent the CFD results for meander channels having meander-channel lengths from 0 to 9,5mm, with and without a bypass of 0,25mm. The upper left point represents the straight channel having no bends, therefore the two sets start at the same point (a straight channel can not have any bypass). As soon as the bend length increases the thermal resistance decreases but at the cost of increased pressure drop, but the meander cells having a bypass drops faster meaning that the overall performance is better for this cell type.

Also shown in the chart are two curves that represent the best fit to the individual CFD results, the fit-function being a power function.

The conclusion is that by introducing a bypass flow gives a better hydrothermal performance: lower thermal resistance at lower pressure drops.

Summary

It has been demonstrated how the shortcomings of conventional liquid coolers such as inhomogeneous cooling and high cost have been overcome by a metal-to-plastic conversion of costly mechanical features in the metal parts of power modules and liquid coolers into simple plastic parts. This metal-to-plastic conversion offered by ShowerPowerTM has even brought along further features that are not available in conventional coolers: the ability to tailor the cooling thereby giving true design freedom. Additionally the high thermal performance gives high reliability solutions, which are especially important in the hybrid traction vehicle area.

http://Siliconpower.danfoss.com

The SmartRectifier in Practical Design

A step forward for secondary-side rectification

Power supply architecture has become a major issue in product design over recent years. At the core of this trend has been the decrease in digital IC voltages, while overall power densities have moved in the opposite direction.

By Mario Battello, International Rectifier

Change has also been driven by the constantly developing nature of end products, all with different current and voltage requirements, and many representing not just evolutions, but whole new device categories. LCD monitors, laptop computers, home-theatre setups, “headless” mini-PCs, games consoles, LCD and PDP TVs; all have unique requirements that the power designer needs to understand.

Last but not least has been a growing awareness of the need to conserve energy so as to make prudent use of natural resources. Not far down the road, legislation such as Europe’s EuP (energy-using products) Directive will lay down the law on requirements for efficient use of energy. These will sit alongside specifications such as EnergyStar and the IEA’s 1W Standby initiative.

As a consequence, power-supply-rectification architectures have, like the products in which they are used, also come a long way. The basic half-wave diode rectifier, with its bulky heatsinks and high power dissipation, has given way to the use of more efficient synchronous-rectification schemes using MOSFETs. A typical cost-effective flyback converter serves as an example. In Figure 1, the schematic on the left utilizes a diode rectifier whereas the schematic on the right uses a synchronous-rectifier MOSFET. Assuming that the voltage across the diode in conduction mode is 0.6V, that the FET RDSon @ 100 C is 10mOhm, and that the IRECTRMS is 5A the power loss of each device is as appears in the Table 1.

	Calculation	Power Loss (W)	Size
Diode	$V_F \times I_{AVGRECT}$	3.0	Slightly large
MOSFET	$R_{DSon} \times I^2_{RECTRMS}$	0.25	Reduced by ~90%

Table 1: Comparing the characteristics of a diode rectifier and synchronous-rectifier MOSFET

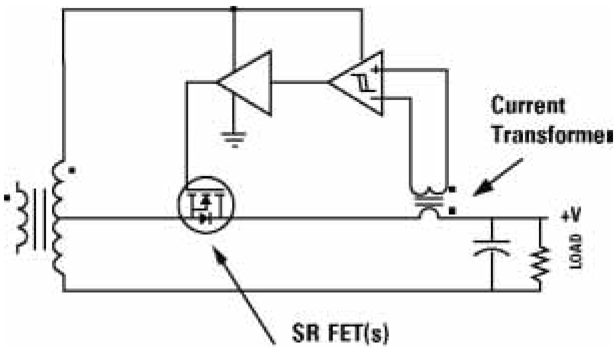

Figure 2: conventional current sensing architecture

Under the same operating conditions, the synchronous-rectifier MOSFET has a smaller power dissipation compared with the diode rectifier during the on phase. Due to lower device temperature the size of the solution can be reduced so increasing power density. For larger currents, using the synchronous-rectifier MOSFET to perform secondary side rectification is necessary.

A subsidiary benefit is that the components can be smaller, improving power density. And the advantages become accentuated at higher current levels, since the diode on-voltage is fixed.

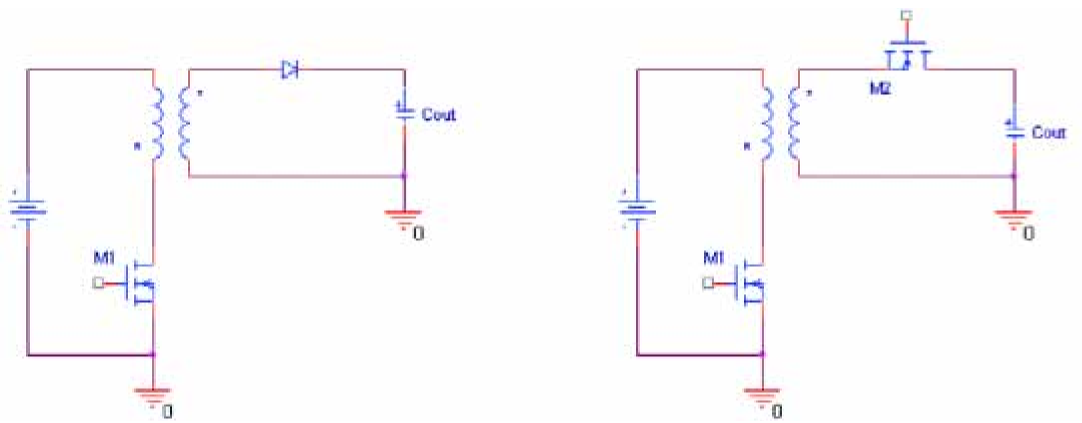

Figure 1: Synchronous-rectifier MOSFET replaces a diode rectifier

The challenge in implementing such FET architectures, however, is that they require relatively complex circuitry to control the MOSFET switch. One approach is to derive the required timing signals from the primary-side waveform. However, practical circuits that use this principle tend to perform poorly under light load conditions, and struggle to comply with targets such as 1W Standby.

The alternative is to use the secondary side as the source of control. Flyback converters commonly include a current transformer on the secondary side for this purpose (see figure 2).

This technique improves overall system efficiency, but still has its drawbacks. The topology triggers the MOSFET's off interval after the reverse current has developed to a sufficient amplitude - a phenomenon analogous to a diode with a stately recovery time. The resultant circulating current does nothing but reduces the overall supply efficiency, which adds to the design's thermal load, and increases the output ripple for a given charge storage capacity.

As a result of these shortcomings, International Rectifier has

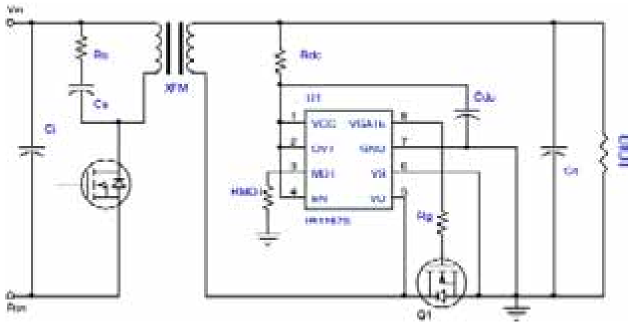

Figure 3: Flyback Converter using IR1167 SmartRectifier Control

developed a topology known as SmartRectifier, which works by measuring the voltage across the synchronous rectifier switch. The result is an efficient, fast design, with low parts count.

The principle is to ensure that the synchronous rectifier FET is switched very near the current's zero crossing. IR has introduced an IC implementation of the architecture, the IR1167, which includes a pair of high-speed 200V comparators that sense the FET's drain-source voltage: during the ON interval, this provides a reflection of the current through the FET's on-resistance.

When used in a typical flyback converter design (see figure 3), the IC differentially senses this drain to source voltage and compares it to three voltage thresholds – VTH1, VTH2, and VTH3 – to determine the correct time to turn on or turn off the SR switch (see figure 4).

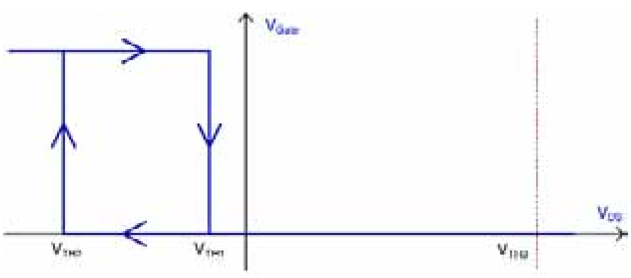

Figure 4: IR1167 voltage thresholds

The operation of the circuit can be analysed in three stages, starting with the decision to turn the SR switch on. This process begins when the primary switch turns off, forcing current through the parasitic diode in the SR switch. This creates a larger (negative) voltage value than the voltage drop caused by current flowing through the MOSFET on-resistance. When this voltage reaches the VTH2 of the IR1167, the switch will turn on, allowing current to flow from drain to source and decreasing VDS.

For a flyback converter in DCM/CrCM (discontinuous or critical conduction mode, see figure 5), the rectified current decreases after the switch turns on. The absolute value of VDS also decreases until it reaches VTH1: at this point the switch is turned off again.

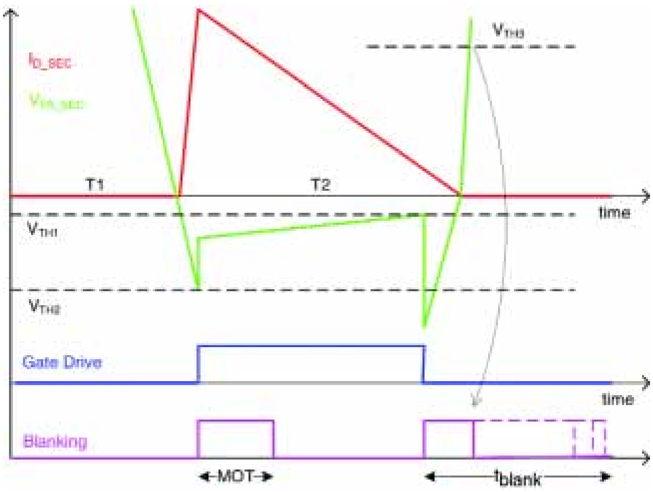

Figure 5: Flyback Converter Secondary side DCM/CrCM operation

There are several fine-tuning points within this cycle. First, circuit resonances at switch-on can allow the drain-source voltage to dip below VTH1 and turn the switch off. The IR1167 therefore includes a programmable minimum on-time (MOT) to prevent such spurious effects, simultaneously limiting the minimum duty cycle of the secondary side as well as the maximum duty cycle of the primary side switch.

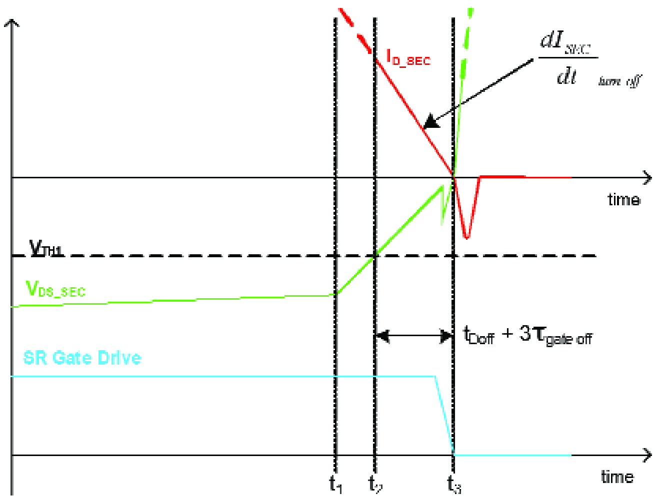

Figure 6: Flyback Converter Synchronous Rectification turn off waveforms in CCM

Second is the danger of a false trigger for the turn-on threshold. This can occur because once the drain-source voltage falls below VTH1, residual current flows through the body diode, possibly allowing the drain-source voltage to reach VTH2. To prevent this, the IR1167 inserts a blanking time after turn-off, during which the IC is inactive. When VDS reaches VTH3 after the blanking period ends, the device resumes operation.

The situation is slightly different in continuous current mode (CCM, see figure 6). During the conduction phase the current decays and the drain-source voltage decreases. When the primary switch turns back on, the current through the secondary FET rapidly decreases. This forces the drain-source voltage beyond VTH1, turning off the FET, and sending residual current freewheeling back into the primary side.

This means that timing the turn-off is critical in preventing cross-conduction. Timing the turn-off to match as closely as possible to the point where the current reaches zero also helps to reduce power losses in the switch.

The IR1167 is designed to help designers working under a broad range of circuit design constraints. Its gate drive can source peak currents of 2A and sink up to 7A, into and out of a 10nF gate capacitance. Two versions of the device are available, giving the choice of 10.7V and 14.5V internal clamping voltages.

The IC provides other features required by designers of modern power controllers. These include a sleep mode that reduces standby current to 200µA for compliance with the IEA's 1W-standby initiative, Energy Star, and CECP.

The SmartRectifier principle produces a number of circuit design benefits for the engineer. Firstly, switching losses are reduced, because the circuit allows current to flow through the body diode before the switch is turned on. The effect is to reduce the gate-charge required for switch-on.

The second consequence – produced by a combination of the architecture and the level of integration of the IC itself – is that the parts count for a typical secondary circuit is reduced to six, including the SmartRectifier controller. This 75% reduction relative to a current-transformer based design reduces PCB area, BOM and assembly costs: just as importantly for modern consumer goods, it allows designers to reach new levels of power density.

A 1% increase in efficiency also contributes a further power density improvement: although this may seem like a very small step forward, it should be remembered that the efficiency of such designs has in recent times increased by, on average, around 0.5% per year. A 1% advance therefore represents two years' development.

Market and regulatory developments mean that power supply design is now well and truly on the map. New developments such as SmartRectifier will allow designers to continue producing innovative products, whilst satisfying increasingly stringent legislation and customer demands in terms of power consumption.

www.irf.com

All the power you need...

For a better environment

IPM Modules	IGBT Modules	DIP-CIB Modules
		

Mitsubishi's service-proven product ranges with the latest chip and production technologies for best efficiency, highest reliability and, needless to say, good environmental compatibility.

Mitsubishi offers a large variety of RoHS compliant series for your industrial application. And compatibility with previous product generations is always assured.

MITSUBISHI ELECTRIC

Changes for the Better

semis.info@meg.mee.com · www.mitsubishichips.com

Interleaving Enhances Power Factor Corrector Performance

Interleaving reduces dramatically the ripple current amplitude

To limit the input current harmonics drawn by the off-line equipment, several international regulations, such as the EN61000-3-2 are in place. In order to limit the harmonic currents, power factor correction (PFC) circuits are used.

By Marcus Zimnik, Texas Instruments

The need for power factor correction (PFC)
Most electronic equipment is supplied by 50/60 Hz utility power, and more than 50% of the power is processed through some kind of power converters. Usually, most of the power conversion equipment employs a diode rectifier with a bulk capacitor to convert AC to DC voltage before processing it. Such rectifiers produce input current distortion and current harmonics, which pollute the power system.

To limit the input current harmonics drawn by the off-line equipment, several international regulations, such as the EN61000-3-2 are in place.

Another reason to limit harmonic currents is the ability to use the full rated current from the available power source. For example, if you have a typical 16A service (single phase 230V) and your rectifier is 98% efficient with 55% power factor the maximum load you can draw is 1984W. This assumes using 100% of the rated breaker current, which is unlikely. If the power factor improved to 99% the load increases to 3570W, an increase of almost 80%.

In order to limit the harmonic currents, power factor correction (PFC) circuits are used.

The Boost Converter
Most PFC circuits for higher output powers are based on the boost converter (Figure 1). The reasons for using the

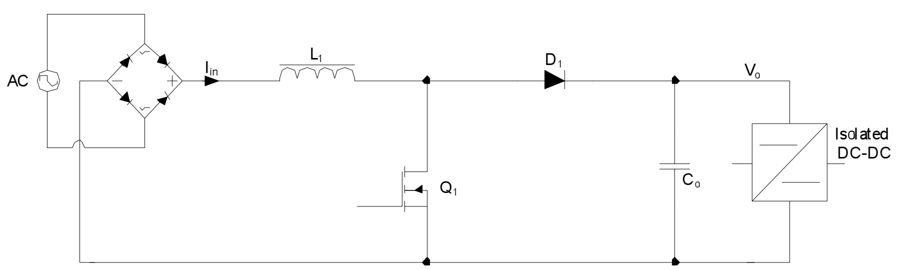

Figure 1: PFC based on boost converter

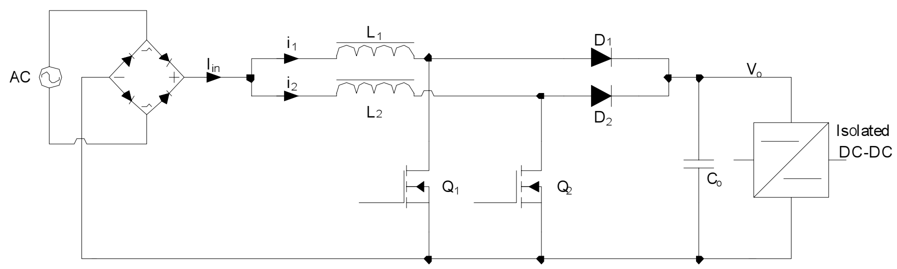

Figure 2: PFC based on a Two cell interleaved boost converter

boost converter are the simplicity in circuit and system design, reduced voltage stress on devices, and high conversion efficiency compared to the other topologies. Further, the step-up conversion makes it suitable for universal input voltage application (90…264 V).

The boost converter can operate in two modes, continuous conduction mode (CCM) and discontinuous conduction mode (DCM). PFC boost converters operating in CCM have better utilization of power devices, lower conduction loss, and lower input current ripple. On the other hand, boost converters in DCM have lower boost-rectifier reverse-recovery loss and lower transistor switching-on loss.

Qualitatively the CRM boost has an advantage in losses for low to medium power applications, while the filtering requirement is not so severe as to be a big disadvantage.

The CCM boost is a better choice for medium to high power applications. The peak currents are significantly lower which reduces conduction losses while the lower ripple current reduces filter requirements.

PFC based on Interleaved Boost Converters (IBC)
As the power rating increases, it is often required to associate converters in series or in parallel. This is mainly due to the lack of a single device that can withstand the voltage and/or current stresses of high power applications. For high power applications, the interleaved boost converter is preferable (Figure 2).

It consists of a phase shifting of the control signals of several cells in parallel operating at the same switching frequency. As a consequence of the interleaving operation, the aggregated input current and output voltage waveforms exhibit lower ripple amplitude and smaller harmonic contents than a single boost converter. The cancellation of low-frequency harmonics allows, eventually, the reduction of size and losses of the filtering stages. In addition, switching and conduction losses through the switches are just a fraction of the input current and as a consequence EMI levels decrease significantly. Figure 3 shows the inductor current waveforms of a two cell interleaved boost converter.

Figure 3a shows operation at 50% duty-cycle which results in a complete cancellation of input ripple current and figure 3b shows operation at 30% duty-cycle. Here the aggregated input ripple current is twice the individual cell switching frequency.

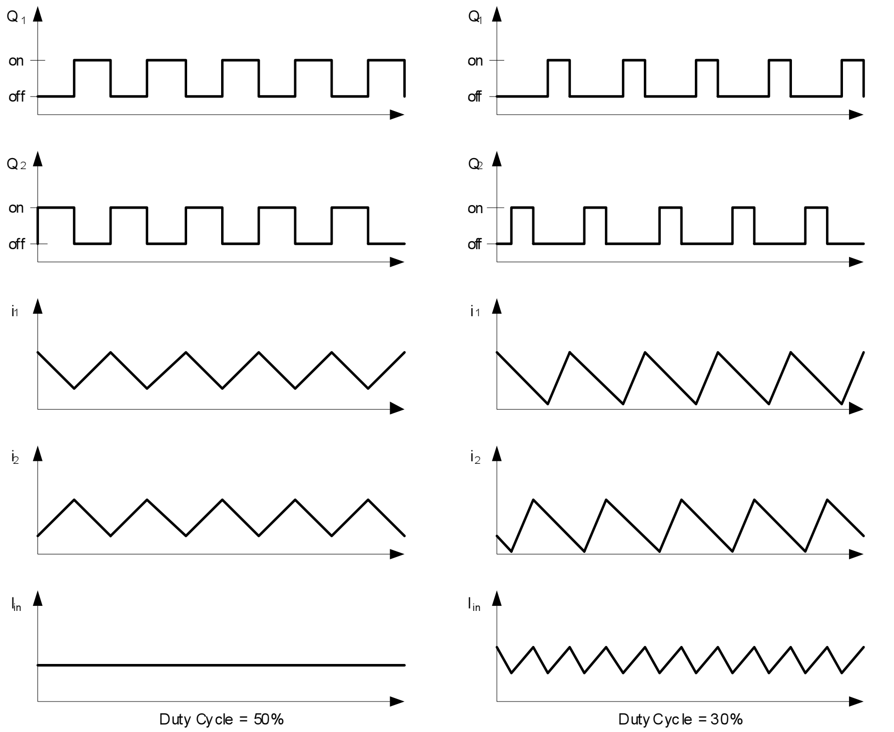

Figure3:
Inductor current waveforms of a two cell interleaved boost converter at different duty-cycles

Trade-offs offered by interleaving PFC converters
There are many benefits for using the interleaving technique in PFC systems. First, interleaving two boost cells with 180° phase shift cancels the weaker odd harmonics while doubling the evens. Therefore, for the same net ripple amplitude and EMI specification, the parameter values of the input EMI filter can be made smaller by a factor of 2. On the other hand, for a fixed input ripple frequency f, the switching frequency of the individual boost cell can be reduced to f/2, which may lead to substantial reduction of switching losses. Second, by splitting the total power into 2 paralleled boost cells, each boost cell input/output current is reduced by 1/2. Correspondingly, the ripple current is reduced by 1/2. On the other hand, if we keep the same current ripple amplitude, the inductance in each boost cell can be reduced by 1/2. This could reduce the converter size. For example, it becomes possible to reduce the switching frequency by a factor of 2 (to increase conversion efficiency) and to reduce the inductance per boost cell by a factor of 2 (to reduce converter size). The resulting system will have a per-cell ripple 22 times larger than a single boost converter, but the net interleaved ripple will remain unchanged. In this manner, interleaving can be used to increase conversion efficiency and power conversion density as well as to reduce ripple amplitude. Third, interleaving can be used to dramatically reduce the ripple current amplitude at the boost converter input and output. Figure 4 shows the input current ripple of a single and dual-phase interleaved boost converter [9].

Figure 5 shows the relative output voltage ripple of a single and dual-phase interleaved boost converter [9].

The main challenge found when implementing an interleaved PFC converter are current unbalances resulting from intrinsic device parameters variations and differences, which is specially critical when operating in CCM and the increased circuitry complexity when compared with a conventional boost converter.

EVM available featuring interleaved PFC
Texas Instruments has developed an evaluation module (EVM) that allows engineers to explore the benefits of an interleaved PFC converter. The circuit diagram is depicted in figure 6 and 7, respectively. The control circuitry uses a State-of-the-Art UCC28528 PFC/PWM combination controller to shape the input current wave to provide power factor correction. This device also controls a 2-W auxiliary bias supply that can be used to control external circuitry. The UCC28528 features an improved multiplier and the use of a transconductance amplifier for enhanced transient response. The UCC28528 has a highly linearized multiplier circuit capable of producing a low distortion reference for the line current over the full range of line and load conditions. The output voltage error is processed through a transconductance voltage amplifier. The transient response of the circuit is enhanced by allowing a much faster charge/discharge of the voltage amplifier output capacitance when the output voltage falls outside a certain regulation window. A number of additional features such as under voltage lock out (UVLO) circuit with selectable hysteresis levels, an accurate reference voltage for the voltage amplifier, zero power detect, over voltage protection (OVP)/enable, peak current limit and power limiting characterize the PFC section of the device.

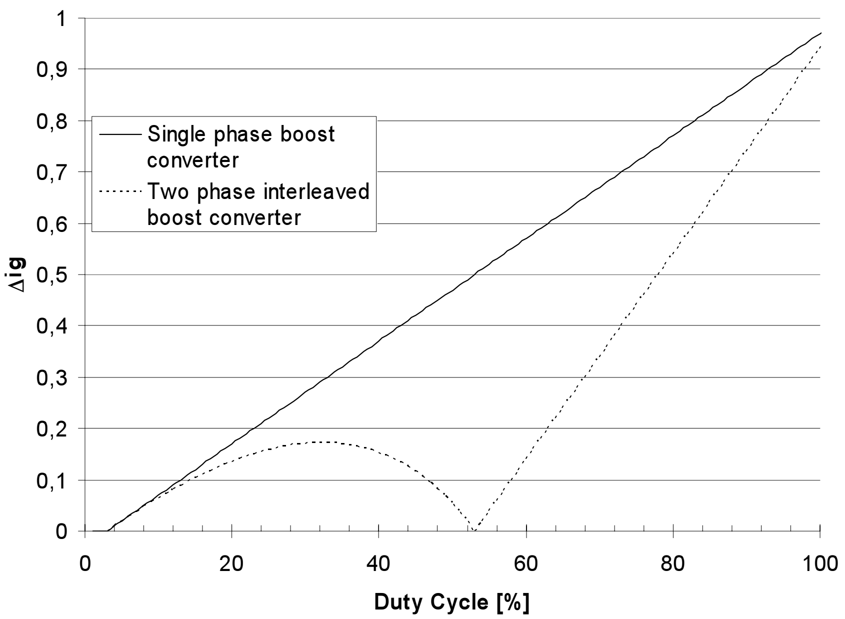

*Figure 4: Input current ripple of a single and a dual phase interleaved boost converter (*Vin/(fs*2L))*

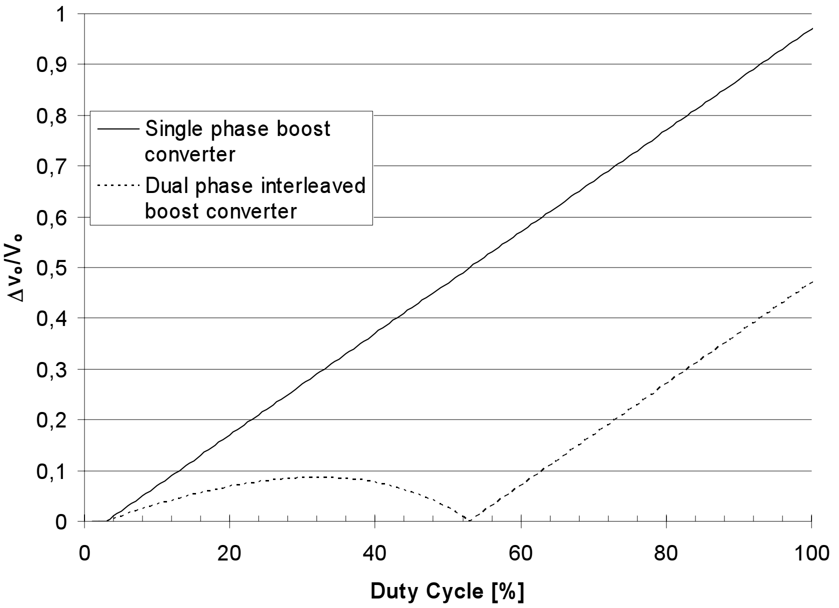

*Figure 5: Relative output voltage ripple of a single and dual-phase interleaved boost converter (*1/(fs*2RLoadCo)*

The UCC28220 interleaved PWM provides OVP protection and current sharing between the two interleaved boost converters. The UCC28220 is a BiCMOS interleaved dual channel PWM controller. Peak current mode control is used to ensure current sharing between the two channels. Additional features include a programmable internal slope compensation with a special circuit which is used to ensure exactly the same slope is added to each channel.

Figure 8 shows the individual inductor current waveforms and the aggregated input current of the EVM.

More waveforms and information is available in the EVMs user's guide.

The interleaved PFC regulator is an interesting alternative and choice for high current applications. Interleaving permits a significant reduction in the magnetic energy storage inductors and the differential-mode EMI filter. Interleaving can also significantly reduce the switching losses. The main advantage of interleaving is that it effectively

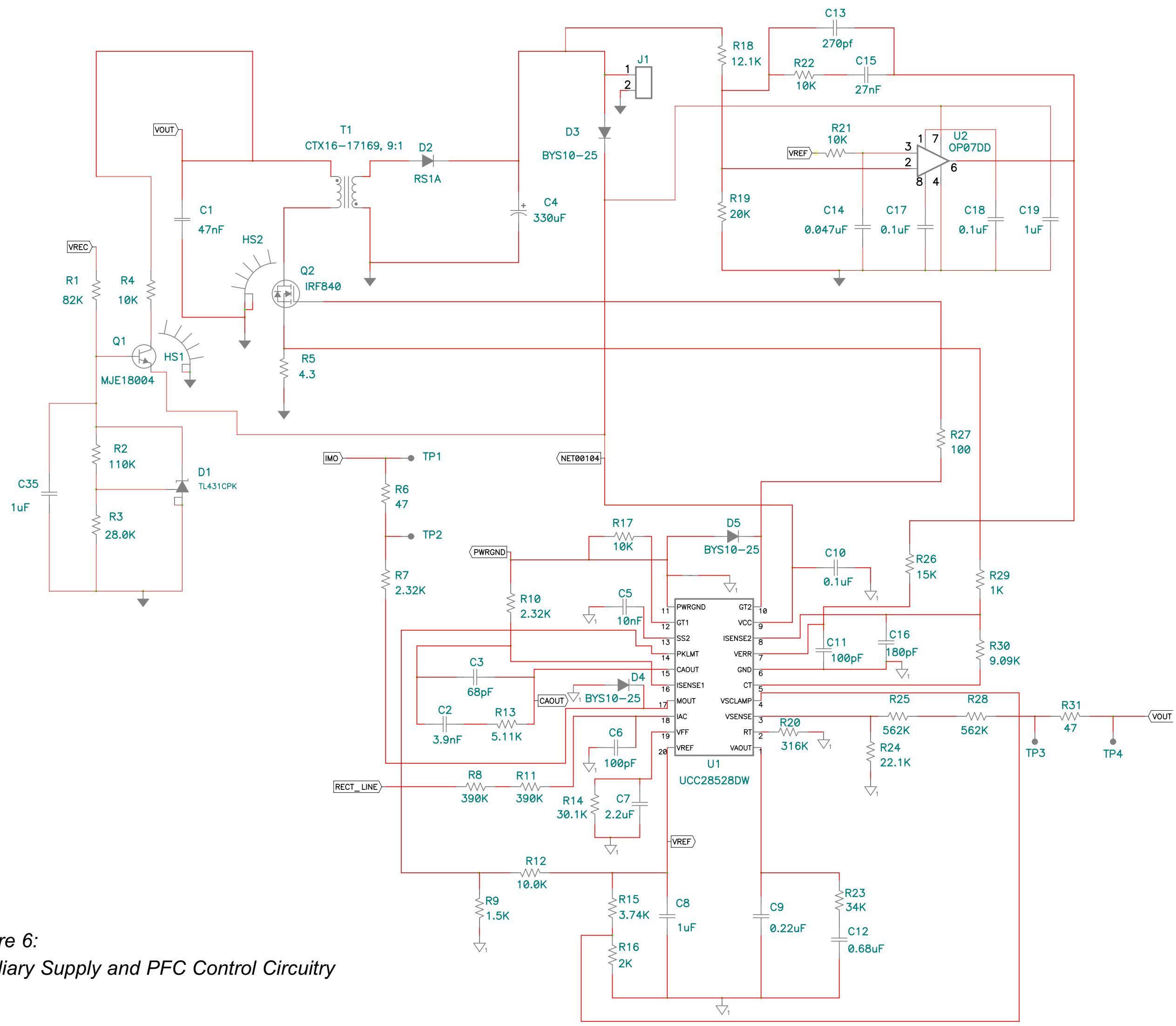

Figure 6:
Auxiliary Supply and PFC Control Circuitry

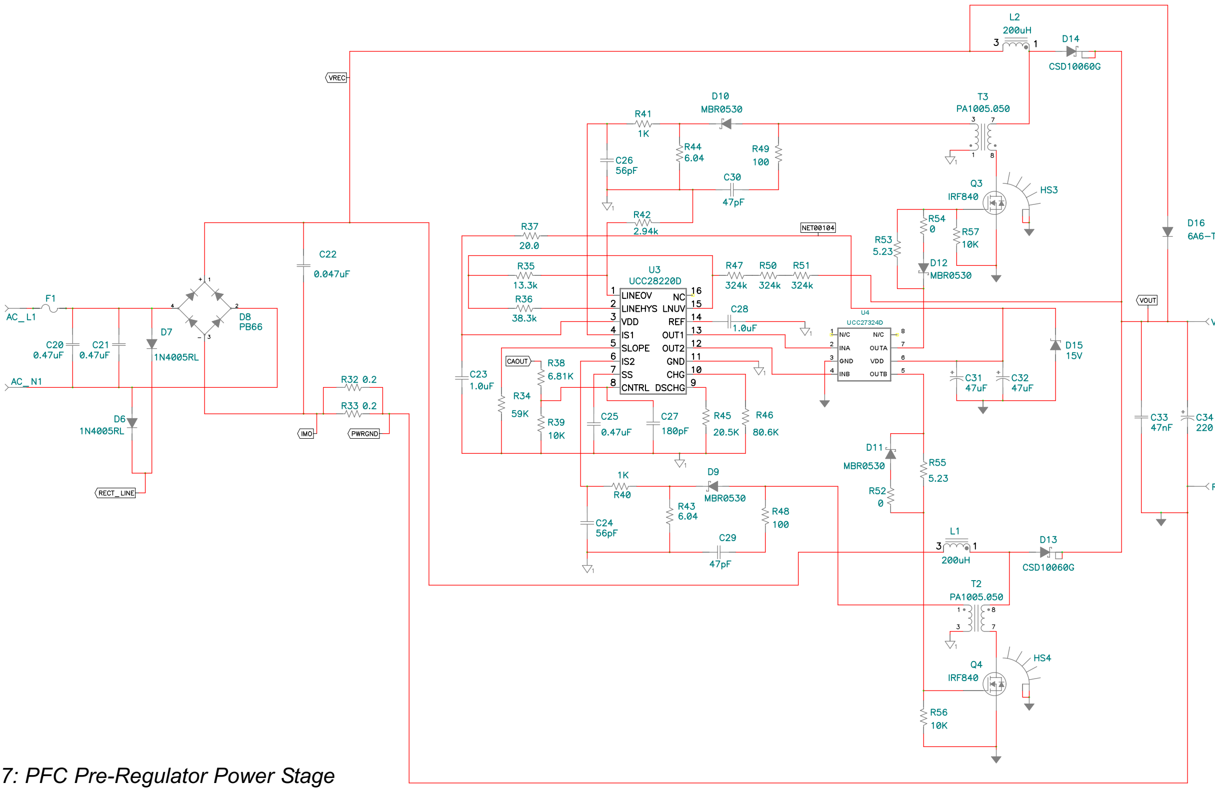

Figure 7: PFC Pre-Regulator Power Stage

increases the switching frequency without increasing the switching losses. The obvious benefit is an increase in the power density without the penalty of reduced power-conversion efficiency. An EVM board available from Texas Instruments allows engineers to explore the benefits of an interleaved PFC regulator.

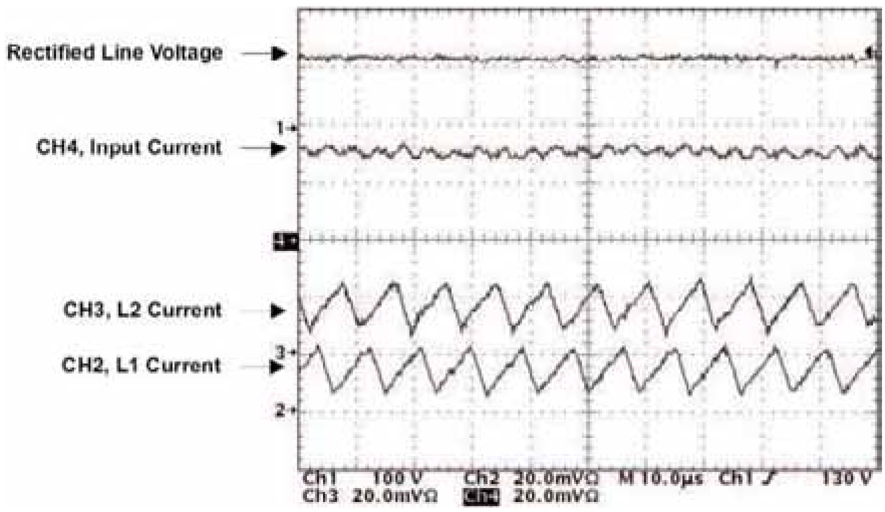

Figure 8: Input Current and Inductor Currents

References

[1] L. H. Dixon, "High Power Factor Preregulators for Off-Line Power Supplies", Unitrode Power Supply Design Seminar Manual SEM600, 1988
[2] L. H. Dixon, "Optimizing the Design of High Power Factor Switching Preregulator", Unitrode Power Supply Design Seminar Manual SEM700, 1990
[3] J. P. Noon, "Designing High-Power Factor Off-Line Power Supplies", Texas Instruments-Unitrode Power Supply Design Seminar Manual SEM1500, 2002
[4] L. Balogh, R. Redl, "Power-Factor Correction with Interleaved Boost Converters in Continuous-Inductor-Current Mode," APEC Conf. Proc., 1993, pp. 168-174.
[5] José R. Pinheiro, Hilton A. Gründling, Dalton L. R.Vidor and José E. Baggio, "Control Strategy of an Interleaved Boost Power Factor Correction Converter", PESC'99, Vol.1, pp. 137-142
[6] B. A. Miwa, D. M. Otten and M. F. Schlecht, "High efficiency power factor correction using interleaving techniques"-Proceedings of APEC'92, pp. 557-568, 1992.
[7] H. A. C. Braga and J. Barbi, "A unity Power Factor Rectifier Based on a two cell Boost Converter Using a New Parallel-Connection Technique", PESC'96, pp. 1620-1626, 1996.
[8] Giral, R., Martinez-Salamero, L., Leyva, R. and Maxie, J, "Sliding-mode control of interleaved boost converters", IEEE Trans. Circuits and Syst. I Fundam Theory Appl., 2000, 47, (9), pp. 1330–1339
[9] H. B. Shin, J. G. Park, S. D. Chang and H. C. Choi, "Generalized analysis of multi-phase interleaved boost converter", International Journal of Electronics, Vol. 92, No. 1, January 2005, pp. 1-20
[10] C. Chang and M.A. Knights, ''Interleaving technique in distributed power conversion systems'', IEEE Transactions on Circuits and Systems—I: Fundamental Theory and Applications, 42, pp. 245–251.
[11] Texas Instruments Datasheet "UCC28528", TI literature number SLUS608D, www.ti.com
[12] Texas Instruments Datasheet "UCC28220", TI literature number SLUS544A, www.ti.com
[13] Texas Instruments EVM User's Guide "HPA117 350-W Interleaved PFC Pre-Regulator", TI literature number SLUU228, www.ti.com

Analog Transmission Across Digital Barriers

An RF carrier is modulated instead of light

Acquiring high quality analog signals from extreme and often hazardous environments while protecting the operator can be a difficult task. This article investigates various methods to acquire analog signals in hazardous environments while using opto-couplers or novel digital isolator technology.

By Keith Coffey, Silicon Laboratories Inc.

Industrial plants are noisy and often hazardous environments. Nevertheless, critical analog nodes, such as temperature, pressure, flow rate and gas concentrations, must be attained to ensure the safety of the control system and its operator. As shown in Figure 1, numerous modulation techniques are used to first encode an analog signal then transmit the signal across the barrier. Once across the barrier, a filter or demodulator reconstructs the analog signal. Systems like this might directly drive a safety shutdown circuit and automatically shut down a system once a preset threshold is exceeded. Reaction time is critical in these systems and is usually dictated by the propagation delay of the isolator.

Numerous other systems, (Figure 2) such as audio, video and motor control also use isolation. However, these systems typically use isolation to minimize ground loops and thus enhance the integrity of data transmission across the system. These systems generally use discrete, high-resolution, 8 to 16 bits (high fidelity audio systems use 24-bits) analog-to-digital converters (ADCs) and/or digital-to-analog converters (DACs) with 100 ksps to tens of mega samples per second (Msps) throughput.The ADC/DAC that is chosen depends on the quality and budget constraints of the system being designed. For instance, in the typical audio system, a DSP acquires the digital content from a CD. The DSP then processes the information add the appropriate sound effects (2, 4 or 8 channel audio) and then transmits the post-processed digital bit stream to an audio DAC (Filter/demodulator in Figure 1). The analog signal from the DAC is then routed to the speakers to recreate the desired sound. As mentioned, many audio systems (especially 24-bit hi-fidelity systems) like to isolate the DSPs processing ground planes from the power (speaker) planes. This technique is used to minimize ground loop pickup and hence reduces background noise and audible humming.

Audio and video systems also require very high-speed isolated data transmission with minimal propagation delay to ensure a high quality reproduction of the original audio or video content. Audio systems typically use 48 ksps ADCs, while video systems require much higher data converters, typically using a minimum of 1 Msps to as high as 10 Msps data converters. To transmit a serially-encoded 14-bit, 10 Msps data stream across an isolated barrier requires a 140 Mbps isolator. Only a modern digital isolator can accomplish this task.

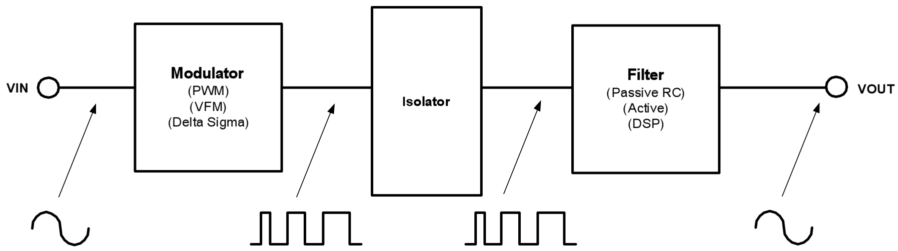

Figure 1. Isolated Analog Acquisition

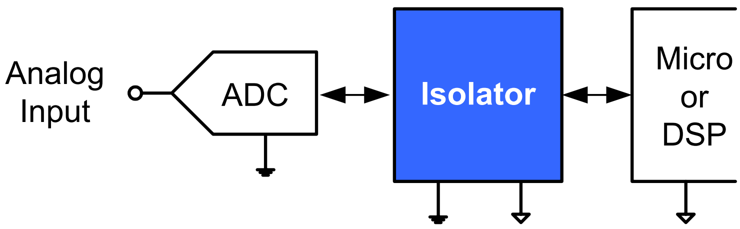

Figure 2. Isolated Discrete ADC to Processor Control Example

Opto-Couplers vs. Digital Isolators

Both opto-couplers and digital isolators are used to isolate and provide a communication link across a barrier. There are inherent advantages to using each technology.

Opto-Couplers

Opto-couplers are devices used for communicating across isolation barriers. They consist of a light-emitting element and a photo detector element (see Figure 3). Both elements are usually integrated into the same package; however, no electrical or physical connection exists between the two elements, just a beam of light. The light emitter element is usually an LED (light-emitting diode). The photo-detector elements could be one of a number of elements but usually consist of a photodiode or phototransistor [1].

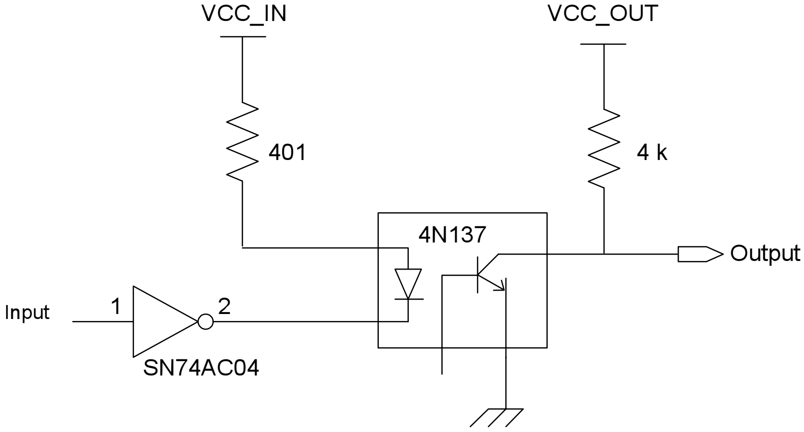

Figure 3. Typical Opto-Coupler Connection Circuit

Opto-couplers have been the workhorse for isolation in intrinsically safe systems for decades. They are relatively economical, especially if ones transmission speed stays below 100 kbps and can transmit analog signals across the boundary. Unfortunately, optos consume large amounts of real estate (typically one channel per package with numerous discrete components required) and suffer from limited throughput (up to 10s of Mbps max). Moreover optos require numerous discrete components, and performance degrades as the ambient temperature increases.

As system temperature increases, the required drive current on the opto in many cases doubles because the CTR (current transfer ratio, a ratio that indicates the amount of input signal transferred to the output) can degrade by up to 60 percent as temperature deviates from 25ºC to 100ºC. This increases opto current drive needs and system cooling demands. Such temperature gradients are common in motor control applications [2]. Regardless of their limitations, they typically provide 3 kV of voltage isolation and only consume 100s of milli-watts.

Digital Couplers

The operation of digital isolators is analogous to that of an opto-coupler, except an RF carrier is modulated instead of light. This simple architecture provides a robust isolated data path and requires no special considerations or initialization at start-up. A simplified block diagram for a single Si8440 channel from Silicon Laboratories is shown in Figure 4. A channel consists of an RF transmitter and receiver separated by a transformer. Referring to the transmitter, input A modulates the carrier provided by an RF oscillator using on/off keying and applies the resulting waveform to the primary of the transformer. The receiver contains a demodulator that decodes the input state according to its RF energy content and applies the result to output B via the output driver.

Digital isolators provide unidirectional, high sensitivity and stable, repeatable switch points. Their integrated transformers use standard CMOS chip-scale technology utilizing silicon dioxide to provide galvanic isolation. RF couplers have a higher peak data rate of up to 150 Mbps, more than 10 times faster than traditional opto-couplers. Further, note, that RF coupler technology is CMOS scalable to even higher throughput rates [3].

RF couplers provide transient immunity of better than 30 kV/µs, compared to 10 kv/µs for opto-couplers. They also provide up to 2500 V_{RMS} of isolation. RF couplers are also more immune to temperature than opto-couplers as their process parameters are not as subject to process effects. Many easily operate up to 125ºC. Again, the biggest advantage RF couplers have over opto-couplers is size. They are typically fabricated in a small die area per channel and many are available in SOIC packaging allowing multiple channels per package [3]. A drawback of RF couplers is their limited operating voltage range, which significantly limits their use in high-voltage applications. They are typically limited to operate from a 5 V supply.

Figure 5 illustrates the PCB real estate impact digital isolators have.

Table 1 illustrates the energy savings and throughput enhancements of digital isolator over opto-couplers.

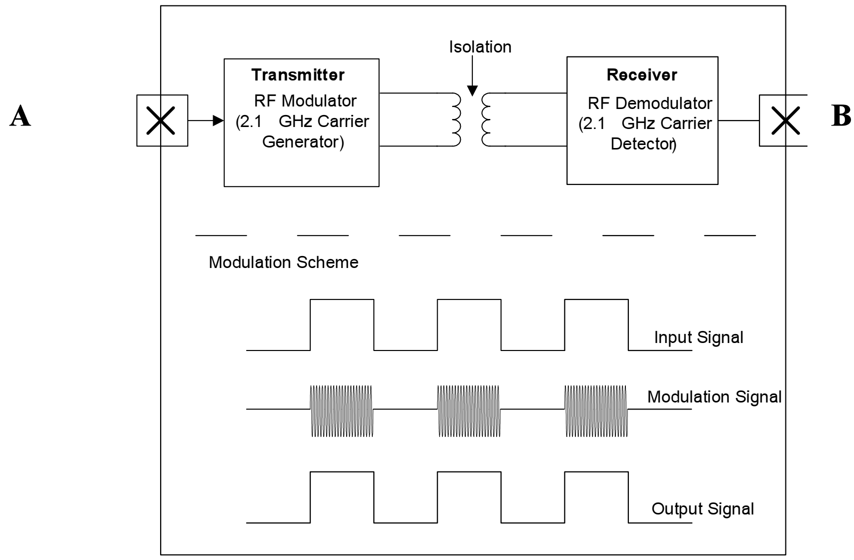

Figure 4. RF Coupler Overview Diagram

Safety Considerations

To protect users from electric shock, the majority of these applications (especially those that require intrinsic safety) will require 2500 V_{RMS} isolation capabilities. For example, 220–240 V applications require double protection to ensure operator safety. To achieve double protection isolation, the end system must have no copper traces within an 8 mm isolation boundary area between the safety extra-low voltage (SELV, voltages < 30 V_{RMS}) and the hazardous voltage (voltages >30 V_{RMS}). This boundary should have a conformal coating, such as solder resist, and any device that crosses the boundary must provide 2500 V_{RMS} isolation minimum. To satisfy these opportunities, an 8 mm wide package must be used. Moreover, two commonly used product-safety standards for end-equipment certifications include the IEC61010-1 for test-and measurement instruments and the IEC60950-1 for information-technology equipment.

To reduce the time and cost of end-product certifications of IEC61010-1 and 60950-1, isolators are typically certified to Component Programs at Underwriter Laboratories, CSA International and VDE Testing and Certification Institute. The process to achieve component certification approvals is rather stringent. It typically entails JEDEC type qualification as well as high potential (hi-pot) testing at the rated isolation voltage for 60 seconds at an independent testing body. After the initial qualifications, a site inspection at manufacturer's facility occurs where the isolation device is inspected to undergo a production hi-pot test for 1 sec at the rated isolation voltage to ensure compliance. Common component certifications include: UL1577, CSA #5A and VDE60747-5-2.

Digitally-controlled systems mandate faster isolation technologies. As this paper discusses, there are a number of bandwidth bottlenecks currently encountered when implementing high-speed isolation barriers in various audio, video and industrial systems. One can implement an intrinsically safe system using two architectures to solve the bottleneck issue caused by the isolator. Of all the couplers, only the emerging silicon isolator

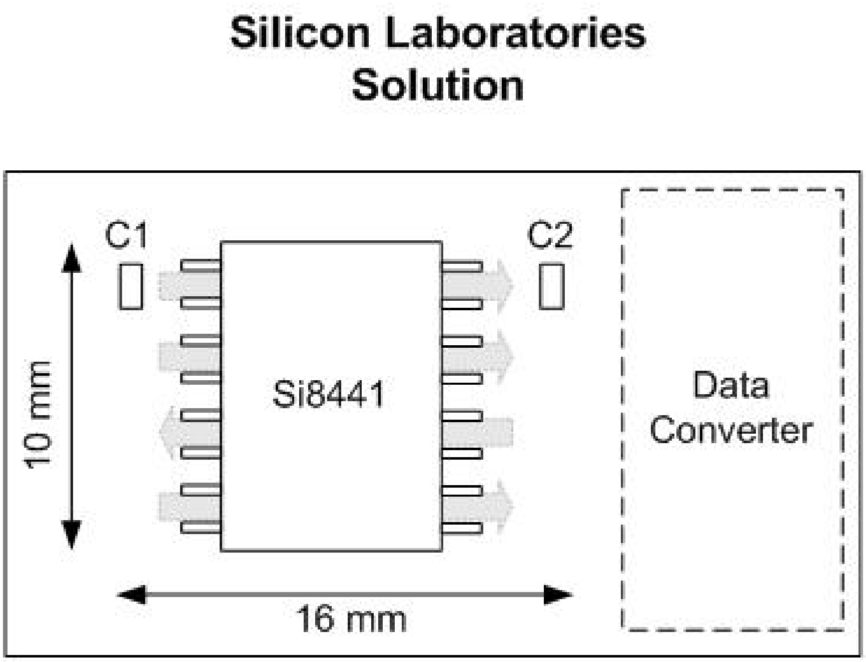

Figure 5. Layout Comparison of Opto-Coupler vs. Digital Isolator

Part	mW/ch	Mbps	mW/Mbps
Si8440	12	150	0.1
Opto-Coupler 1	160	80	2.0
Opto-Coupler 2	40	6	6.7
Opto-Coupler 3	90	10	9.0
Opto-Coupler 4	40	1	40.0
Opto-Coupler 5	55	0.1	550.0

Table 1. Opto-coupler vs. Digital Isolators

technologies solve the isolated data throughput problem. In sum, digital isolator technology provides the lowest cost, lowest latency, highest bit rate, and most integrated isolation path. This emerging and scalable technology overcomes the digital barriers using isolated analog data transmission.

References

[1] Horowitz, Paul and Winfield Hill. The Art of Electronics. 2nd ed. New York: Cambridge University Press, 1995.
[2] Opto-isolators v 2.04. Which Online. August 4, 2004.
[3] Si8440/1/2 Datasheet. Silicon Laboratories, Preliminary Rev. 0.3 April 2006.

www.silabs.com

New Applications for Hall-Effect Current Sensors

Sectors where sensors provide optimal solutions

Hall-effect current sensors offer an inherent benefit over other solutions in that there is isolation between the current path and the sensing and interface electronics.

By Andreas Friedrich, Allegro MicroSystems Europe

The innovative packaged current-sensing solutions featured in this article are based on a low-resistance primary current path and a monolithic linear Hall IC which integrates the Hall element and state-of-the-art BiCMOS interface circuitry (Figure1). The sensors cover a measurement range of up to ±200 A, and can also be designed into higher current applications by using a current divider configuration. They also offer the benefits of low cost, high accuracy, and small size. This article describes two application sectors where these current sensors provide optimal solutions.

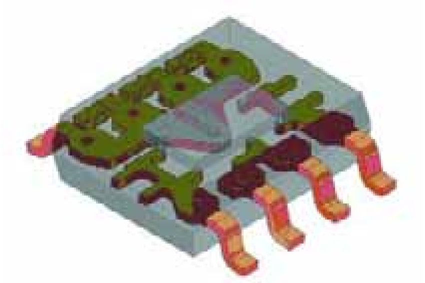

Figure 1a. Hall-effect current sensors. Low-profile surface-mount device for currents up to 20 A

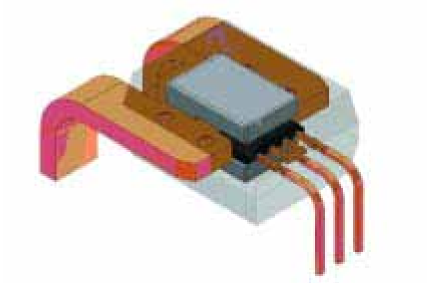

Figure1b. Hall-effect current sensors. High-current (200 A) sensor showing primary conductor, flux concentrator and linear Hall IC

Battery monitoring

Smart battery systems require circuitry to monitor cell voltages, temperatures, and currents. For capacity monitoring applications, all these measurements are critical. The most difficult to design in properly is the current measurement. The reasons for this are accuracy, power dissipation, and solution size.

Current measurement accuracy is essential to ensure that the capacity monitoring algorithms are working well. The traditional method of measuring this current is with a shunt in the ground path or on the low side. The key problem with this is that to minimise I^2R losses, the value of the shunt needs to remain very small. With this approach, low-current measurement accuracy becomes compromised. What it means for notebook applications is that, during suspend, hibernate, or other low power states, it is difficult for the battery to accurately monitor the current flowing into the system.

If the battery is using a 10 mOhm sense resistor to minimise power dissipation at nominal loads in a low power state with only 50 mA of power draw, the voltage across the shunt would be 500 mV. This voltage is very difficult to resolve, and so complicated algorithms for estimating the residual capacity must be developed for the battery to compensate for this effect. These routines are conservative in nature, meaning that they tend to assume that they lose a bit more capacity than is calculated. This can result in the battery appearing to lose capacity over time.

Depending on the battery and the application, 1-2 W sense resistors would be required to monitor the currents. Typically, in portable solutions, there is not enough space for 2 W resistors, and so the solution is usually limited to 1 W resistors. For higher current solutions, multiple resistors are used in parallel to keep the power ratings within the devices limitations. Both solutions have a large impact on the available board space required to fit these components.

By using a Hall-effect device as a shunt solution in the battery pack, the power dissipation in the pack can be reduced. The advantage of using Hall-effect devices is readily apparent with the low insertion loss of the device. For the latest SOIC-8 packaged devices, the lead-frame insertion loss can be as low as 1.5 mW. The difference in power consumption over a range of load current is shown in Figure.2.

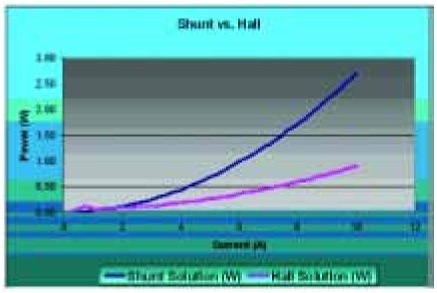

Figure 2. Power loss in a shunt compared with a Hall-effect current sensor in battery monitoring applications

The use of a Hall-effect device can also increase the accuracy of the current measurements, as shown in Figure 3. This block diagram shows a high current path and a low current path – the latter being enabled for better accuracy when monitoring small currents.

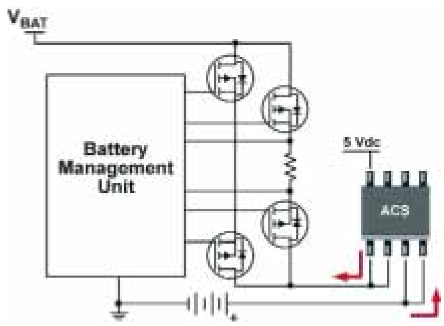

Figure 3. Improved accuracy and efficiency in battery monitoring with Hall effect devices

Not only does the solution shown in Figure 3 provide higher accuracy for lower charge and discharge currents: it also provides more signal than the shunt solution over the measurement range. Assuming that the Hall effect device has a gain of 100 mV/A, this signal is much larger than the resulting signal across a shunt resistor (Figure 4).

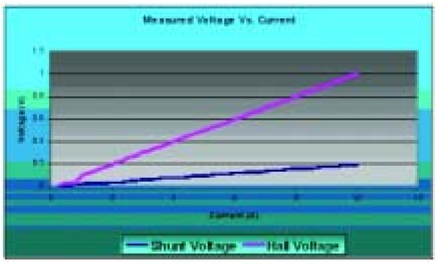

Figure 4. Output voltage of a Hall-effect current-sensing solution compared with a 20 mOhm shunt

The step increase in gain with the Hall-effect solution assumes that the application allows the high-current path shown in Figure 3. The actual threshold for the transition and level of hysteresis desired will be a function of the application as well as the value of the shunt employed.

The use of Hall-effect devices in battery systems can help to reduce the PCB area required for a shunt sensing solution and allows high-side sensing which does not interrupt the ground path. The two major benefits in using a Hall-effect device will be in improving current measurement accuracy over a wider current range, and reducing power consumption by significantly reducing the I^2R loss of the shunt.

UPS and invertor applications

Both Hall-effect devices and current transformers are used for current sensing in UPS systems. While current transformers are seen as low-cost solutions, they actually require more support components than a Hall-effect solution, and are strictly limited to AC applications. Another secondary cost involved when using current transformers to monitor the AC line voltage is the additional circuitry to manage the effects of inrush and possible core saturation during an inrush event.

UPS systems use the line voltage to charge a battery that is used to supply line voltage for a system in the event of a power failure. The goal of the UPS is to supply as much energy as possible with the maximum efficiency. For example, a 2200 VA UPS requires a typical 3-hour charge time. This same UPS can only supply around 24 minutes of power at half load (990 W) and 6.7 minutes at full load (1980 W). The input and output currents are monitored both for protection and to be able to show the battery state of charge with a level of confidence.

A high-performance Hall-effect current sensor is ideal for monitoring the input power or battery charge current for several reasons. The obvious benefits for a small form factor Hall-effect solution are:

The volume required is a fraction of the equivalent current-transformer solution the elimination of gain and additional protection components, resulting from the fact that the Hall sensor cannot overshoot the voltage on the isolated side of the device.

When powering the invertor stage at high loads, the optimal place to have the Hall-effect sensor is at the line voltage itself to monitor the load currents directly. The reason is that the line voltage current may be as high as 15-20 A RMS, whereas the battery sourcing current may be in excess of 50-60 A, depending on the voltage of the battery stack and the efficiency of the convertor.

Figure 5 shows how a Hall-effect device can be used in an UPS power train.

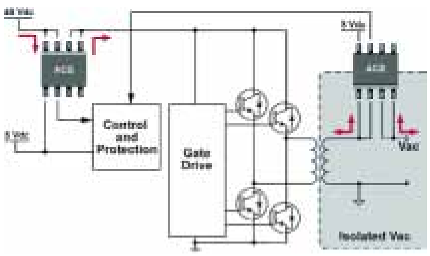

Figure 5. Using Hall-effect current sensors in a UPS power train

This latest generation of Hall-effect devices is helping to resolve known issues with current transformers and to improve the reliability of the system. By using Hall-effect devices in the battery charging system and invertor power train, the efficiency of the convertors can be optimised. This can help to reduce the overall size of the system as well as saving costs.

www.allegromicro.com

Ultracapacitors - Powering the Shift to Hybrid Electric Vehicles

Long cycle life and excellent cold temperature performance

Today, car manufacturers and suppliers are increasingly aware of ultracapacitors for use in automotive power-trains and subsystems, and the advantages of the product in meeting their business and technical requirements.

By Jürgen Auer, Maxwell Technologies

Ultracapacitors are becoming a standard energy and power storage option.

The development of electric and hybrid vehicles (EV/HEVs) is a response to the growing global pressure on improving the environment and the subsequent search for significantly cleaner and more efficient vehicles. The success of these new vehicle architectures depends on the development of advanced energy storage technologies, including batteries and ultracapacitors.

Most vehicle systems in development today rely on battery technology because of its relatively high energy density, its relative maturity, and its familiarity to designers. Since ultracapacitors and batteries have significantly different characteristics, few current designs can immediately replace the battery with an ultracapacitor, and new design approaches are required. The unique characteristics of the ultracapacitor allow additional dimensions in design to be explored, and open up opportunities for the development of new powertrain and subsystem architectures which can improve on the goals of performance, efficiency, and cleanliness.

Subsystems with variable voltages will ultimately be a part of all vehicles, including traditional combustion engine vehicles. In these systems, ultracapacitors can be used not only to provide power for acceleration purposes, but also to provide the possibility of capturing regenerative breaking energy.

Examples of vehicles using ultracapacitors in the powertrain include BMW's hybrid X5 and Volkswagen's fuel cell powered Bora prototype vehicles, and Honda's IMA and Toyota's ES production vehicles. The reason for the acceptance of ultracapacitors in vehicle propulsion systems is their high pulse power capability, fast transient response, and high efficiency during charge and re-charging plus full charge cycling in excess of 500,000 cycles.

Figure 1: BMW X3, Hybrid concept car shown at IAA Auto show 2005

Ultracapacitors in Hybrid Electric Vehicles (HEV)

Perhaps the most promising near-term solution is the Hybrid Electric Vehicle (HEV). HEV technology combines the best characteristics of fuel-driven engines, electric motor drives, and energy storage components. It is designed with a combustion engine as the primary power source, and an electric power storage system as the secondary power source.

The presence of the secondary power source allows designers to size the combustion engine for cruising power requirements. The secondary source handles peak power demands for acceleration. It is also used for capturing regenerative breaking energy and applying this energy for further acceleration or for the basic energy needs of supplementary electrical systems. Through this basic design structure, HEVs promise to offer low maintenance, clean operation, and high fuel economy.

Ultracapacitors significantly improve power management in hybrid electric vehicles. In addition, ultracapacitors decrease emissions, optimize fuel-efficiency and improve electrical drive capabilities. Using ultracapacitors allows the HEV to recapture and reuse braking energy. Compared to conventional diesel engines the reduction of fuel consumption is estimated to be higher than 50%; reduction in particulate emissions is 90% or even more; as well as the reduction of nitrogen oxide emissions by 50%.

The fuel reduction for hybrid vehicles is based on:
- Start-stop
- Braking energy recuperation and
- Down-sizing of engine.

Depending on the power demands of the electric motor as well as the functions, one of the possible hybrid class is shown:

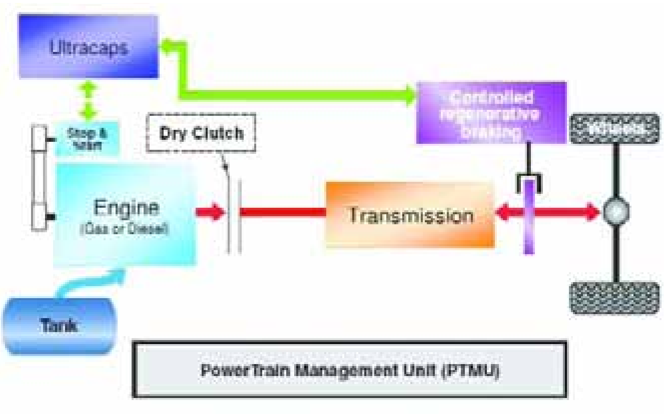

Figure 2: Micro Hybrid System Architecture

The systems differ by the power requirement for the energy storage system. The challenge for the HEV manufacturer is to reduce the peak power from the battery, which occurs during high power times such as during braking and acceleration as well as high power demands of additional electrical systems. Here the battery is exposed in general. If these peaks are covered by a secondary power source, the battery can be down-sized and its lifetime strongly be increased, therefore reducing cost.
Maxwell Technologies' ultracapacitors are designed to work with system batteries to improve power management and take away peak load stress from batteries. The ultracapacitor technology protects the battery, as it allows the battery to handle the energy requirements while the capacitors handle the high power requirements.

Ultracapacitors in start-stop systems
Idle-start-stop power train functionality is clearly an easy way to increase fuel efficiency and reduce pollution reduction by stopping the engine during normal idling conditions and restarting at accelerator tip in. The use of a 15V ultracapacitor module will support high pulse power loading imposed by high occurrence of engine warm restarts under idle-stop-start control. The use of engine start-stop and regenerative braking is expected to increase fuel efficiency by 7% to 15% while reducing pollution by an even higher percentage. Maxwell also makes its ultracapacitors available in module configurations, which is a good solution for start-stop applications. The company's 15V building blocks can store approximately 45kJ to meet the idle-start-stop requirement as well as capturing braking energy. This allows a 5kW braking charge to be absorbed for several seconds and then reused for several seconds of engine starting power.

Distributed power modules
Due to increasing power demand as well as the requirement for redundancy in new vehicle functions such as electric assist steering, electromagnetic valve control, electric door opening and electric braking require, there is a requirement for automotive engineers to develop new electrical distribution system architectures.
An electrical system architecture with modular and distributed power modules is one method of addressing the need for power and redundancy required by the safety critical and security systems in automotive applications.

Distributed ultracapacitor modules alleviate electrical distribution system voltage sag and transients by supplying high peak power locally, while requiring only the average power from the vehicle's primary power supply. This essentially decouples the high transient power load from the vehicle's power supply system.

A further requirement of safety critical applications is the need for a redundant power supply in the event of loss of the main electrical distribution system branch circuit for x-by-wire functions. Distributed power modules located at critical loads such as near the electric power assist steering system, or near electro-hydraulic brake modules, offer the vehicle designer additional redundancy for such safety critical applications.

Conclusions
All kinds of automotive applications require storage systems which are durable, with a long operating life and wide temperature ranges. And all of this must be provided at low cost! Batteries, even advanced technologies cannot meet this entire set of requirements. This is especially true in systems requiring high power and little energy.

Ultracapacitors offer long cycle life and excellent cold temperature performance down to
-40degC, and the basic materials used in their construction pose no significant barriers to affordable cost in quantities typical of the automotive market. The introduction of ultracapacitors into subsystems and "stepping-stone" power trains will accelerate the adoption of the technology into the automotive market, and will drive up the volumes, and therefore drive down the cost.

This volume-driven cost reduction combined with the ongoing performance enhancements will continue to make ultracapacitors an excellent solution for current and future power trains, local power nodes and electrically driven subsystems.

www.maxwell.com

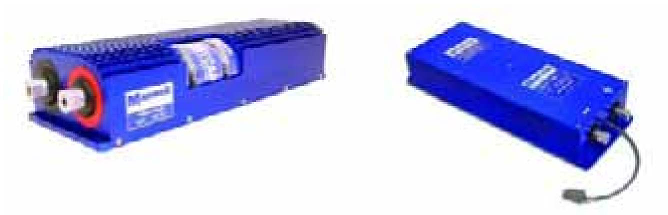

Figure 3: Maxwell module solution for micro hybrid

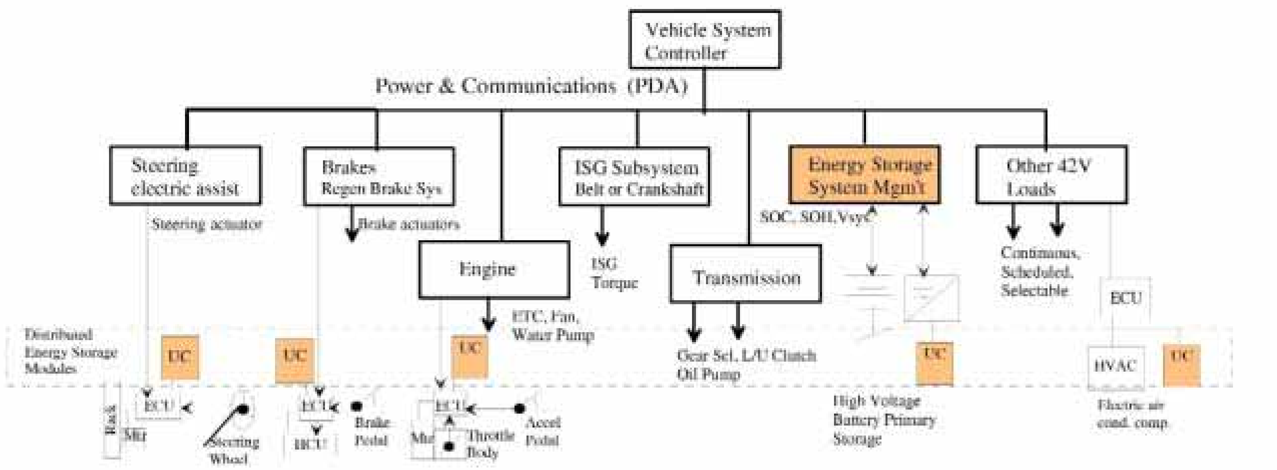

Figure 4: Distributed module architecture with ultracapacitor modules (UC) for vehicle safety critical and hybrid functionality

How to Select an Off-The-Shelf Current Transformer

A simple guideline can greatly help

In electronic systems applications such as switch-mode power supplies, current transformers are generally used for control, circuit-protection, and monitoring features.

By Ariel General, Senior Design Applications Engineer, Datatronics, Inc.

Engineers have relied on current sense transformers as the 'gold standard' for precise measurements in instrumentation applications for decades. They are accurate, easy to implement, and reliable under harsh environmental and thermal conditions. In electronic systems applications such as switch-mode power supplies, current transformers are generally used for control, circuit-protection, and monitoring features. With the increasing availability of OTS (Off-The-Shelf) current transformers, a simple guideline can greatly help in the selection of proper and cost-effective components for many applications.

Below is a simple chart outlining the steps in the current transformer selection process:

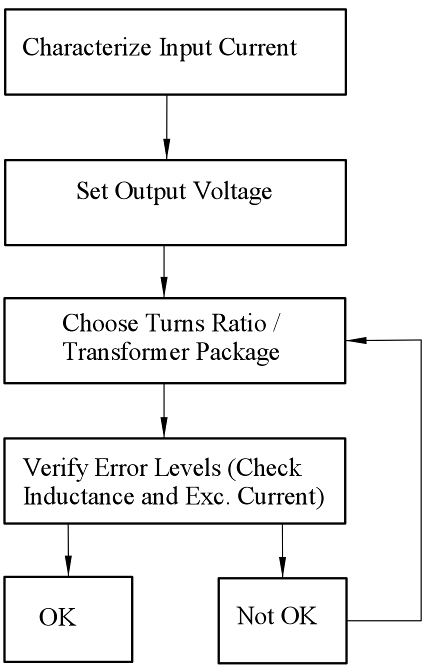

Figure 1:
OTS current transformer selection flow chart

Characterize the Input Current
The first step when selecting a current transformer is to define and verify key factors such as size, frequency, function and the range of current being sampled. These are important factors to verify since the accuracy and effectiveness will essentially be dependent on these parameters. Aside from the possibility of compromising the transformer's accuracy, using a current transformer above the manufacturer's rated current specification may saturate the transformer and may cause circuit failures due to an uncontrolled rise in operating temperature. On the other hand, a current transformer that is rated much higher than the "sample current" might be restrictively too large and expensive for its purpose. Typically, selecting a current-transformer that is rated approximately 30% above the expected maximum of the "sample current" is a prudent starting point.

The Turns Ratio
The most commonly available OTS current transformers have turn ratios ranging from 1:10 to 1:1000. The higher the turns ratio ($r = N_{sec}/N_{pri}$), the higher the resolution of the current measurement. However, care must be taken as too high of a turns ratio will necessitate an increase in distributed capacitance and leakage inductance which may decrease the transformer's accuracy and capability to operate at higher frequencies (due to self-resonance). However, if the number of turns is too low (lower inductance), the output signal may distort or "droop" (in positively sloped unipolar input signal) which may also cause instability in the control circuit and inaccuracies in measurements.

Inductance and Excitation Current
To determine the fidelity of the output for a particular current transformer, you must evaluate its secondary inductance. The value of inductance is inversely proportional to the excitation current – which is then subtracted to the "sensed current."

In order to ensure the maximum error tolerance of the transformer, the excitation current should be several times less than the magnitude of the sample current (a maximum of 10% is ideal for most switch-mode power supplies, SMPS, applications). For instance, if a circuit has to maintain a maximum of 10% loss for a sample current of 1 A to 20 A at 100 kHz, the excitation current must be set to a maximum of 100 mA (10% of the minimum sample current value). A 1 A sample current will yield an error of 10% while a 20 A sample will yield an error of 0.5%.

This equation can be used to calculate the excitation current, in the event that it is not specified in the manufacturer's data sheet:

$$e = -L\frac{dI}{dt} \;;$$

$$\left|\frac{dI}{dt}\right| = \frac{e}{L}$$

Where *e* is the set output voltage (V), L is the inductance (H), and |*dI/dt*| is the excitation current w/ respect to time (A/s).

The Output Voltage and "Burden Resistor"
Set the output voltage (Vo) as low as practically possible in order to minimize the insertion loss. Assuming 0.5 V is the optimum secondary output voltage in a circuit and the output current is 20 A, a 1:100 ratio transformer will yield a secondary current of ≅ 200 mA. Per Figure 2, the burden resistor should be:

$$Ro = \frac{Vo}{Is} = \frac{0.5}{0.200} = 2.5\ \Omega$$

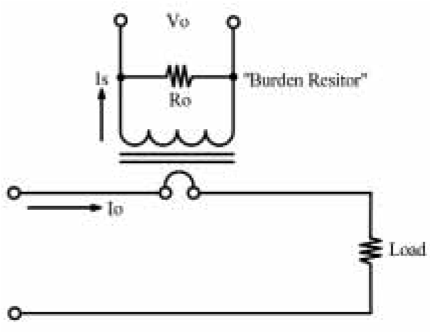

Figure 2: Current sense circuit.

Practical Example:
Definition of Requirements:

Input Current:	100 kHz, 1A – 5A
Output Voltage:	0.1 V → 1 A
	0.5 V → 5 A
	@ 10% accuracy
Package:	low-profile, surface-mount

Part Selection:
Using Datatronics' standard OTS catalog on their website, the CT317-100 current transformer satisfies the input current and package requirements – only the accuracy level and burden resistance are left to be determined.

Error Level Approximation:
For 10% Error (neglecting coupling losses), the primary excitation current must be less than 10% of the minimum input current – a maximum of 100 mA in this case;

I_{exc} (SEC) ≅ 1/f * e/L
≅ 1/100 kHz * 0.1/(2.5 mH)
≅ 0.4 mA

This yields an approximate current of 40 mA on the primary, 60 mA less than the 100 mA maximum.

Burden Resistor Calculation:
Ro = Vo/Isec = 0.1V / (1A/100) = 10Ω

For the given requirement, the Datatronics CT317-100 is an acceptable selection.

Conclusion
Off-The-Shelf components are typically low cost and readily available. However, as we've discussed, OTS components have definite functional limitations on their usage. There are applications where specific recommendations or even full customization may be required. It is therefore advisable to procure these components from reputable manufacturers that have strong engineering, manufacturing, and customer service capabilities.

References:

Billings, Keith H., *Switchmode Power Supply Handbook – 2nd ed.*, McGraw-Hill, New York, 1999.
McLyman, Colonel Wm. T., *Transformer and Inductor Design Handbook*, Marcel Dekker, New York, 1978.

About the Author

Ariel General is Senior Design Applications Engineer for Datatronics, Inc.,
28151 Highway 74, Romoland, CA 92585.
Phone: +1-951-928-7700
www.datatronics.com

Crystal Oscillator Design and Negative Resistance

Active elements must be able to function with crystals of varying parameters

There is a discrepancy, however, in the measured negative resistance in comparison to the simulated start-up negative resistance. Differences in signal and impedance levels coupled with circuit nonlinearities are a major part of the measurement discrepancy.

By Anthony M. Scalpi, Applications Engineer Senior Staff, Cypress Semiconductor

Timing is a critical part of almost every electronic application. Communication and data transfer generally requires a reference signal or source that enables system synchronization and signal generation. At the heart of most reference sources is the oscillator. An oscillator is a circuit that produces an output signal with no input signal. Oscillator start-up is achieved by the injection of energy composed of noise and or the transient power supply response. A crystal oscillator consists of a feedback network and an amplifier or gain element. Historically, both of these building blocks were designed and manufactured by companies specializing in frequency control products. Today, this paradigm has changed as separate companies design and manufacture the crystals and the amplifiers.

This article focuses on the ubiquitous Pierce oscillator configuration, although the analysis can be applied to other oscillator configurations. The Pierce oscillator consists of an inverting amplifier and two capacitors, all of which can be easily integrated with existing CMOS technology. The Barkhausen criterion is the most common design analysis tool or model that we have all become familiar with. Simply stated, the gain around the amplifying and feedback loop must be equal to or greater than one at the desired oscillation frequency. The phase shift through the loop must be 0 or some integer multiple of 2Π. An alternate and equally viable analysis methodology is the Negative Resistance model. This model is attractive in that it can be easily simulated with common analysis tools like Spice. A current source is used as part of the AC simulation. One does not need to break the loop in analyzing start up or small signal negative resistance.

A negative resistance measurement can be done in the lab using a Network Analyzer although the measurement methodology must be carefully examined. In the case of the Pierce, a two-port measurement can be acquired with the gain and feedback network left intact. Negative resistance measured across frequency can give valuable insight into the behavior of desired and unwanted modes of oscillation. The widely accepted series resistor method for calculating negative resistance is only valid at the frequency of operation. There is a discrepancy, however, in the measured negative resistance in comparison to the simulated start-up negative resistance. Differences in signal and impedance levels coupled with circuit nonlinearities are a major part of the measurement discrepancy. The measured negative resistance results using a network analyzer are lower than predicted by AC simulation; however, this will not be covered here. This article will provide a theoretical explanation and design methodology for negative resistance. Traditionally, generic rules of thumb were applied to calculating the required amount of negative resistance in proportion to the resistance of the crystal. Negative resistance is critical in the design of VCXOs where the gain and resonator impedance will change across the input control voltage range.

The term Negative Resistance has been historically associated with an active device such as a vacuum tube or a tunnel diode whose characteristics change when operated in a particular region of their IV curve. These active devices exhibit a dip in the IV curve such that an increase in voltage results in a decrease of current. This behavior called Negative Resistance is very useful in creating Microwave Oscillators in the case of a tunnel diode. The important concept to remember when considering these types of devices is that no other passive components are required to create the effect of negative resistance. There are bias networks that are necessary to select the region of operation and associated feedback networks that create an oscillator network, but it is the active device itself that supplies the negative resistance. The IV curve for a tunnel diode is illustrated in Figure 1.

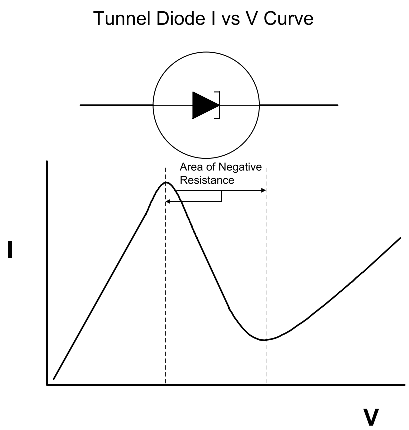

Figure 1 Tunnel Diode I-V Curve

The term negative resistance has been used in the oscillator industry for many years to model the required gain needed from the active network to design stable oscillators. Historically the end user would purchase an oscillator from a vendor and the vendor then had complete control in the selection of the crystal and gain block and would subsequently design, test, and deliver the oscillator without the customer ever being involved in the crystal or gain element design or specification. Negative resistance has gained a lot of attention recently due to the fact that the end user is purchasing the gain block separately and then choosing a crystal from a different vendor. The gain or amplifier block is now being integrated in silicon in order to offer greater functionality and flexibility.

This has created a new problem since the crystal vendor, semiconductor manufacturer, and the end user or customer determines the final design of the oscillator. They each may have different design guidelines and measurement methodologies. Negative resistance is a very important oscillator design parameter that can change based on the design guideline or measurement methodology employed. The end customer or isolated vendor may specify parameters that are not compatible for an overall successful oscillator design. The purpose of this article is to theoretically explain and quantify negative resistance when used in terms of oscillator design such that the crystal vendor, semiconductor manufacturer, and customer can have a common platform for communication and collaboration in designing a robust crystal oscillator.

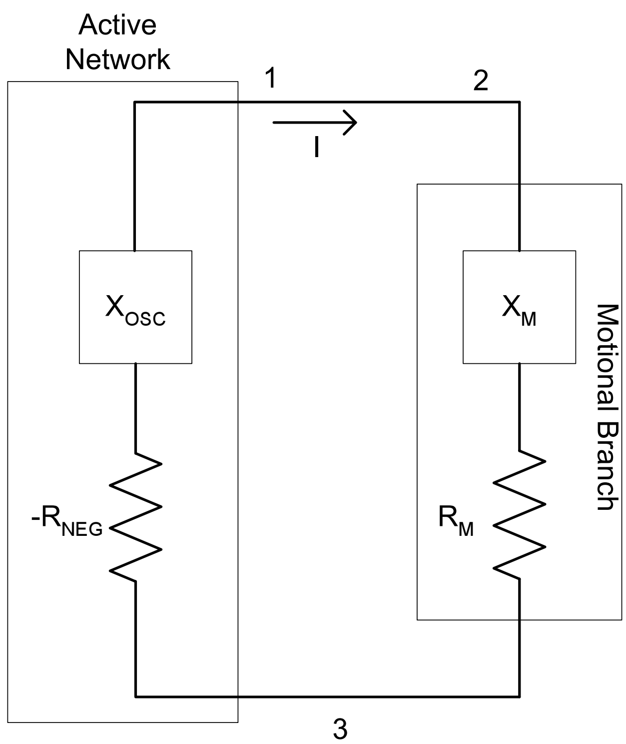

Figure 2 Negative Resistance Model

The first place to start is by defining a negative resistance model for an oscillator and the basic requirements for oscillation to take place. The basic model is shown in Figure 2.

The criteria for oscillation in the negative resistance model is analogous to that stated in the Barkhausen criterion. The condition at steady state is as follows:

$-R_{NEG}$ = RM

$-X_{OSC}$ = XM

The active network must produce a negative resistance that is equal to, in absolute value to the resistance of the motional branch. The reactive parts must cancel each other and it is at this point the frequency of operation is determined. When the signal amplitude is small, at start up, the negative resistance is greater than the motional resistance and then decreases as the signal swing increases finally settling at the steady state value described above.

Herein lies the design constraint that causes the greatest confusion between vendors and customers alike. How much negative resistance should my active network provide to the motional branch at start up? The motional branch that is commonly used is the quartz crystal. A quartz crystal provides a large Q tuned circuit that affords the end oscillator high frequency stability. As stated previously, this was not a problem when there was only one designer and vendor involved in the oscillator design, but now you have the crystal vendor, semiconductor manufacturer, and the end customer all collaborating in the design. As with any design, margin is built in to overcome design and process variations.
In the case of specifying negative resistance this is also the case, but in addition the amount of negative resistance is chosen to overcome crystal drive level dependency and optimize the oscillator start up time.

The main problem arises when generic rules of thumb are applied to specifying negative resistance. These rules of thumb evolved empirically over the years and may not have their basis in fact. A plausible scenario is that a design specification was given to a vendor and confusion generated by jargon and measurement methodology caused a subsequent failure. The root cause of the failure was never identified and the end user merely increased their rule of thumb margin for negative resistance. A specification for five times the motional resistance was increased to ten times and then used as a blanket requirement when specifying active networks. At this point in the discussion the obvious question arises. What are the drawbacks to increasing the negative resistance? Gain is a good thing so is increasing gain even better? This article will demonstrate that when used with a crystal, this is not the case, and an increase in negative resistance can have catastrophic consequences to the end oscillator design. Specific equations will be given for the maximum negative resistance that any active network will provide when connected to a quartz crystal to form a crystal oscillator.

We have described the motional branch in our circuit as a quartz crystal. Figure 3 is the electrical equivalent model of a fundamental mode quartz crystal.

C0 - Static capacitance. This is the capacitance of the metal electrodes, the dielectric constant of the quartz, and the holder. This is not related to the piezoelectric properties of the quartz and can also be measured by a C-I meter. It is sometimes referred to as the shunt capacitance, and is typically measured in Pico farads (pF).

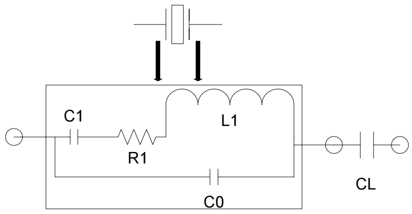

Figure 3 Equivalent Crystal Network

C1 - Motional capacitance. The capacitance that the resonator exhibits at series resonant frequency. This is a direct result of the piezoelectric properties of the quartz and is represented in the traditional lumped equivalent circuit and sometimes referred to as Cm. This is dependant on the size of the crystal electrode and is typically measured in Fempto farads (fF).

L1 - Motional Inductance. The inductance that the resonator exhibits at series resonant frequency. This is a direct result of the piezoelectric properties of the quartz and is represented in the traditional lumped equivalent circuit and sometimes referred to as Lm. This is transparent to the end user and taken into account when the crystal frequency and load are specified.

R1 - Resistance at series resonant frequency. The resistance that the resonator exhibits at series resonant frequency. This is a direct result of the piezoelectric properties of the quartz and is represented in the traditional lumped equivalent circuit and sometimes referred to as Rs or ESR, (Equivalent Series Resistance).

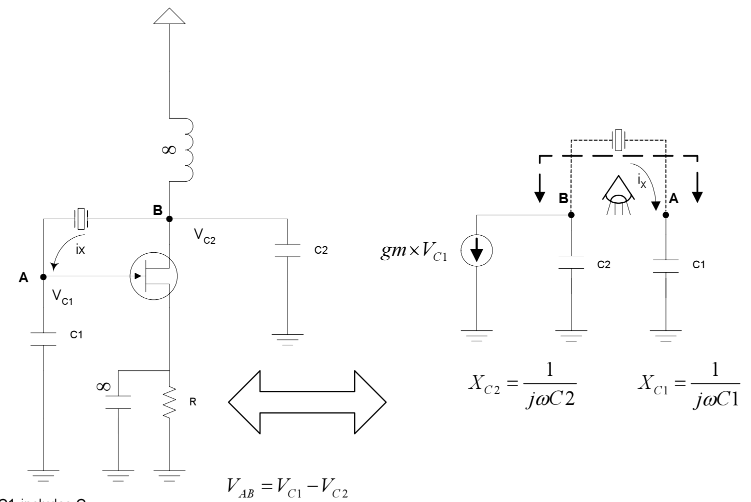

Assume C1 includes C_{GS}

Assume $X_{C2} << r_O$

Assume $I_G = 0$

$$V_{AB} = V_{C1} - V_{C2}$$

$$V_{C1} = i_X \times \frac{1}{j\omega C1} = i_X \times X_{C1}$$

$$V_{C2} = -(i_X + gmV_{C1}) \times \frac{1}{j\omega C_2}$$

$$V_{AB} = i_X \times \frac{1}{jwC1} + (i_X + gmV_{C1}) \times \frac{1}{j\omega C2}$$

$$V_{AB} = i_X \times \frac{1}{jwC1} + \left(i_X + gm\left(i_X \times \frac{1}{j\omega C1}\right)\right) \times \frac{1}{j\omega C2}$$

$$\frac{V}{I} = \frac{1}{j\omega C1} + \frac{1}{j\omega C2} - \frac{gm}{\omega^2 C1C2}$$

Imaginary — This Term is called *"negative resistance"* $= -gmX_{C1} \times X_{C2}$ **GAIN**

$$Imaginary = \frac{C1+C2}{j \times \omega \times C1 \times C2}$$

Figure 4 Negative Resistance Derivation

CL - Load capacitance for a specified parallel load resonant frequency. This is useful in determining the exact load required to make the crystal operate at the specified frequency. Example: A 13.5 MHz crystal is ordered in to a 14 pF load but due to the Frequency Calibration Tolerance 13.500000 MHz occurs at 13.76 pF. The crystal manufacturer specifies this in PPM Frequency Tolerance at 25°C.

The active branch that is typically employed is the three terminal transistor connected in a Pierce oscillator configuration. The important point to stress here is that unlike the tunnel diode the following active network is comprised of an active device and a passive network. This is necessary in creating a condition of negative resistance. This analysis is valid for the Pierce gate oscillator as well.

The following diagram and set of equations listed in Figure 4, will be presented to help describe the term negative resistance.

The familiar term, ($-R = -gm \cdot X_{C1} \cdot X_{C2}$), describes the negative resistance of the active network as a function of the gm or transconductance of the active device along with the reactance value of the two Pierce capacitors, C1 and C2. One can see that in order to raise the negative resistance from the active network you have to raise the gm or lower the capacitance of the two Pierce capacitors. The design limit being that in the case of C1 and C2 the crystal manufacturer will not generally specify the Crystal Load Capacitance, CL, below a value of 8

$$CL = \left[\frac{C1 \times C2}{C1 + C2}\right]$$

This sets the lower limit of C1 and C2 at 16 pF each since it is their series combination including strays that comprises the load seen by the crystal, CL. The design limit for the active device in the case of gm is its size.

Figure 5 illustrates the change in negative R with respect to C1 and C2.

At the frequency of 27 MHz the negative resistance is 600 Ω for C1 and C2 equal to 20 pF each. One can see that the negative resistance with C3 and C4 equal to 40 pF

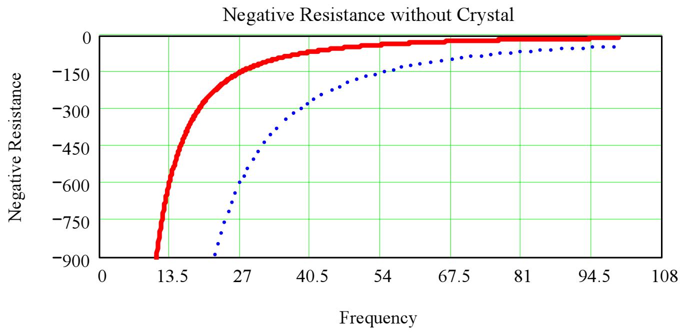

Figure 5 Negative Resistances versus C1&C2

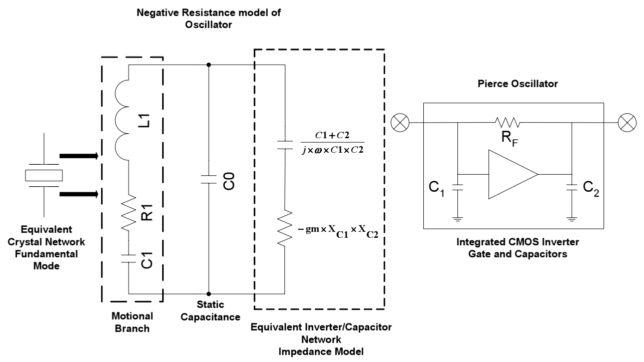

Figure 6 Negative Resistance Oscillator Model

each has now dropped at 27 MHz to 150 Ω. This is the point in the analysis where most people will stop and require the semiconductor manufacturer to supply an active network with a specific negative resistance based on an arbitrary design rule of thumb, never having specified the crystal! The addition of the crystal to the active network will drastically change the value of negative resistance that the active network can provide. The crystal as an equivalent network and the active network must now be analyzed as a whole. Figure 6 is a negative resistance model of an oscillator with the crystal connected as the motional branch.

Not only does the crystal supply a motional branch necessary in forming an oscillator circuit but along with it comes an additional capacitance C0, refer to Figure 3 for the crystal model and description. It is the shunt capacitance that dramatically alters the behavior of the active network and severely limits the amount of negative resistance that can be supplied. Figure 7 illustrates the effect on negative resistance when a crystal with a C0 equal to 7pF is added to a circuit with C1 and C2 both equal to 20pF. The negative resistance at 27 MHz has now dropped from 600Ω to approximately 150Ω. This equals the value of negative resistance when C3 and C4 were both equal 40 pF and no crystal was added. C0 is an intrinsic property of the crystal and it cannot be ignored. This is why the crystal vendor, customer, and the semiconductor manufacturer must communicate and agree on design goals and measurement methodology.

Due to the contribution of C0 an active network that delivered 600Ω at 27 MHz when the crystal was not connected will not achieve a negative resistance of 600Ω when combined with a crystal with a 60Ω resistance and a C0 of 7pF. This circuit now will not satisfy a negative resistance design rule of thumb of ten times the motional resistance.

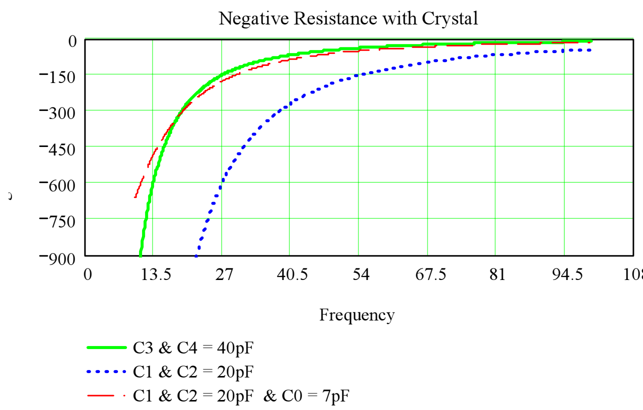

Figure 7 Negative Resistance with Crystal C0 versus no C0

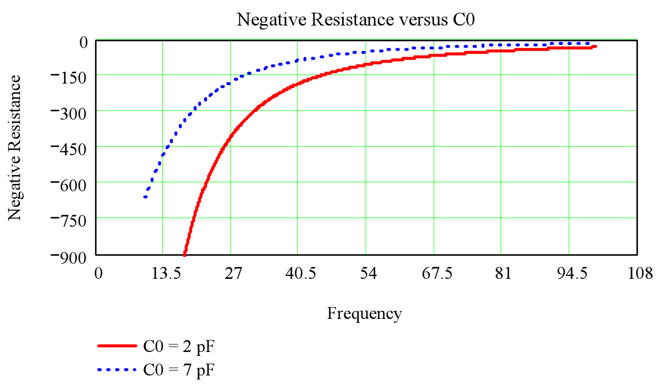

Figure 8 Negative Resistance versus Crystal C0

Figure 8 demonstrates the effect on negative resistance when the same active network is attached to two different crystals with varying C0s. C0 is proportional to the physical size of the crystal and electrode size. VCXOs generally require a larger C1 that translates into a larger electrode. A larger metal can crystal will have a larger C0 than a smaller SMD type crystal. That is why an engineer should not use a negative resistance rule of thumb in oscillator design.

We have now shown that the crystal and the active element should both be analyzed as a whole for any given oscillator application. Choice of negative R or the active element gain does not have to be left up to generic rules of thumb. There is a mathematical way to choose the optimum negative resistance and gm (transconductance) for any given active network and crystal pair. Eric Vittoz presented this in a paper presented at the IEEE Journal of Solid State circuits.

The first equation relates the maximum negative R obtainable with a crystal and Pierce oscillator circuit where C0 and C1 and C2 are known. This is the standard case for any given oscillator configuration. Equation 1 is an expression for the maximum obtainable negative resistance. This maximum negative R occurs at an optimum gm (transconductance), value and is given in equation 2.

Equation 1:

[1] $$R_{N(MAX)} = \frac{-1}{2\omega \cdot C0\left(1 + C0\frac{C1+C2}{C1C2}\right)}$$

Equation 2:

[1] $$gm_{OPT} = \omega\left(C1 + C2 + \frac{C1C2}{C0}\right)$$

The following diagram, figure 9, taken from Vittoz's paper illustrates the effect of varying gm. If the transconductance of the active device is increased beyond the optimal value then there is a decrease in negative resistance and a region is approached where no oscillation can occur. In applying an arbitrary rule of thumb the end user can now reach a point where instead of safeguarding and creating a gain margin in their design they have now created the same effect of having not enough negative resistance. Their oscillator circuit will not start.

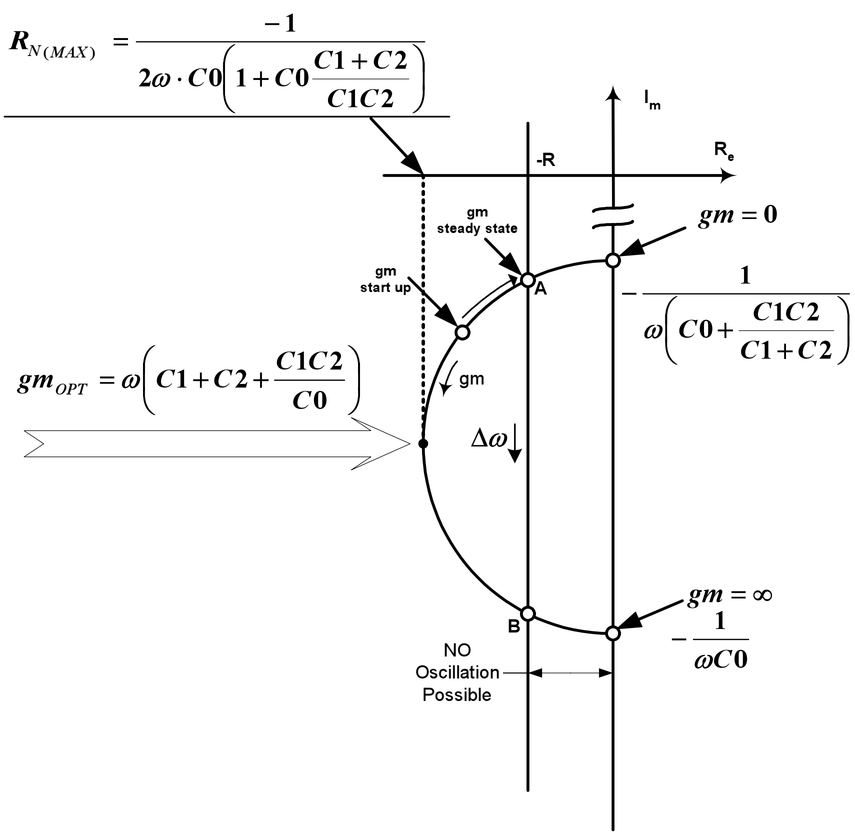

Figure 9: Complex plane representation of the lossless three-point oscillator (linear) [1].

As gm is increased past the optimal point the obtainable negative resistance actually decreases and enters a region where the oscillator will no longer start.

If the active device gain was set by an arbitrary rule of thumb to satisfy a specified negative resistance value and then later combined with a crystal that had a certain C0 the end result can be that the oscillator will never start. This can easily happen as devices are designed and sold to cover a broad range of markets and applications. Circuits can no longer be custom tailored to specific applications, as this is not an economically viable business strategy. A Set Top Box application may require a larger crystal based on cost alone where as a hand held application demands the use of a small SMD crystal. The active element must now be able to properly function with crystals of varying parameters.

In conclusion we now have the ability to take any given crystal oscillator requirement and design and compute the optimal negative resistance based on the proper application and manufacturing process constraints. This insures a robust oscillator design. Cypress offers a high degree of design flexibility with the use of programmable die and strong product support. Our programmable die allows us to choose the optimal gm and the correct negative resistance for any given configuration. Our technical expertise and programmable parts allow for an overall easy, flexible, and safe design.

References:

[1] E. Vittoz, "High-Performance Crystal Oscillator Circuits: Theory and Application" IEEE Journal of Solid State Circuits, vol. 23, No. 3, June 1988 pp. 774-783.
[2] Benjamin Parzen with Arthur Ballato, "Design of Crystal and Other Harmonic Oscillators" 1983, A Wiley-Interscience publication: division of John Wiley & Sons, Inc.

www.cypress.com

The Next BIG Thing Part 2

BIG Thing Technology

In Part 1 in the August issue, The Next BIG Thing was characterized as Whole-house Digital Media over AC Power Lines - instant digital media access from every, and any, location in the home. That includes whole-house access to the Internet, TV/IPTV/Video (both standard- and high-definition video).

By Mark E. Hazen, Senior Technical Writer, Intellon Corporation

Now, HomePlug AV technology is examined on the physical layer to see how a 200-Mbps bit rate (a.k.a. channel rate) is accomplished. The residential house wiring is a very harsh and electrically noisy medium over which to attempt high-data-rate digital communications. Even so, HomePlug powerline communication coexists on the household power wiring along with 120 or 240 volts AC, appliance-generated line noise and other signals, such as security and lighting control signals and induced EMI/RFI.

What's more, HomePlug AV is designed to provide robust high-speed powerline communications using very low transmit levels that satisfy regulations around the world. Despite the low transmit power in the presence of high voltage and intermittent noise and invading signals, HomePlug AV technology finds its own space to ride and work above and around would-be interference.

The AC Power Line

Figure 1 illustrates how the occupants of the AC power wiring coexist in the frequency domain. At the low end of the spectrum is the 50/60 Hz, 120/240 VAC followed by legacy security and control system signals such as X10. HomePlug AV spectrum ranges from approximately 2 to 30 MHz, above power and other carrier signals. Frequency separation allows the use of passive filtering to successfully isolate low-band signals from the HomePlug AV powerline communications spectrum. Figure 1 does not show the random wideband appliance-generated noise or any induced EMI or RFI that challenges powerline communications.

The HomePlug AV spectrum is easily separated from low-band signals using passive filtering. However, high-pass filtering does not prevent in-band broad-spectrum noise, as generated by home appliances, or EMI/RFI. Clever techniques must be employed to mitigate the challenge that in-band noise presents. The first step is to use a robust and flexible broadband modulation scheme known as Orthogonal Frequency Division Multiplexing (OFDM).

Windowed OFDM

OFDM is a physical medium transmission technique composed of a large number of evenly spaced carriers (frequency division), each of which can be orthogonally modulated using Phase Shift Keying (PSK) or Quadrature Amplitude Modulation (QAM). The robustness and bit efficiency of this technique is emphasized when one considers that it is also used in DSL phone line based systems (tone modulation) and in both Wi-Fi and WiMAX wireless technologies. Figure 2 illustrates how OFDM is employed for HomePlug AV powerline communications - 1155 individual carriers are spaced at approximately 24.4 kHz.

HomePlug AV technology utilizes 'windowed' OFDM, which means that selected carriers can be turned off (dropped) to remove interference to and from wireless services that occupy the same spectrum. Carriers, both used and not used, comprise what is known as the 'tone map', each carrier referred to as a tone. A firmware-enabled tone mask is used to mute carriers that would interfere with legacy services such as the Amateur Radio bands. In addition to masking, the HomePlug AV standard allows for individual tones (carriers) to be programmed over a range of amplitude, which allows for line equalization associated with various applications.

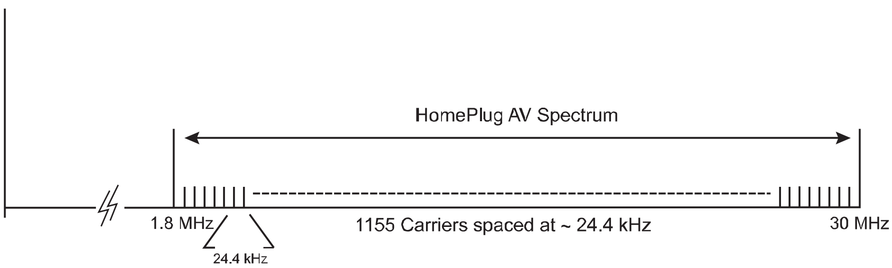

Figure 2: HomePlug AV OFDM Spectrum

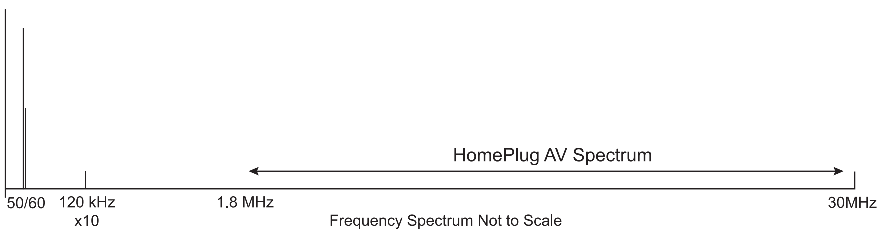

Figure 1: AC Line Spectrum – HomePlug AV Separated in Frequency

In practice, the HomePlug AV tone map consists of 917 active carriers comprising the channel. Channel efficiency is optimized using dynamic channel adaptation in which the channel is periodically analyzed for interference and other line conditions to establish an optimal tone map in which each carrier (tone) is intelligently loaded with data bits before data transfer begins.

Carrier Bit Loading
Each carrier is modulated (loaded) using either Binary Phase Shift Keying (BPSK), Quadrature Phase Shift Keying (QPSK), 8-Quadrature Amplitude Modulation (QAM), 16-QAM, 64-QAM, 256-QAM, or 1024-QAM modulation, depending on channel conditions. 1024-QAM provides the highest bit rate per carrier because each of the 1024 unique analog phase/amplitude symbols represents 10 digital bits.

With 917 carriers active in the HomePlug AV tone map and each modulated with 1024 QAM (10-bit symbol), the channel bit rate is 10 X 917 = 9170 bits per symbol period. The symbol period is the inverse of the carrier spacing (1/24400 Hz = ~41 µs) plus a small guard period of approximately 5.5 µs. Thus, the total symbol period during which 9170 bits are conveyed is 41 µs + 5.5 µs = 46.5 µs. Using the 46.5 µs period, the channel bit rate is 9170 bits/46.5 µs = ~197 Mbps. Thus, HomePlug AV offers a maximum physical layer channel rate of approximately 200 Mbps. If all 1155 carriers were used, there would be 11550 bits per symbol period and the maximum channel rate would be approximately 248 Mbps.

In practice, not all carriers can be loaded with the maximum number of bits (10). In a process called 'channel estimation', bit loading for each channel is established when the communications path between two HomePlug AV devices is initialized and is continuously refreshed to adapt to changing channel conditions to achieve the highest throughput rates. Each carrier is dynamically loaded with the maximum number of bits that prevailing line conditions allow.

The individual carrier bit loading capability enables interesting flexibility. Under the very worst of line conditions, all carriers could be modulated with the same data using a low-bit rate loading, BPSK for example. This would ensure that the information gets through on one or more carriers. At the other extreme, each carrier can contain different data, each with the highest bit loading. This would yield the highest possible channel bit rate and information flow.

AC Line Synchronization
While windowed OFDM allows channel frequency-domain adaptation and individual-carrier bit loading, AC line synchronization is also employed to adapt to time domain characteristics. AC cycle synchronization allows the system to identify and work around periodic and intermittent appliance-generated line noise in relation to the AC waveform. Synchronization to the AC cycles allows the system to optimize channel capacity by adjusting bit loading during periodic noise events of significant amplitude.

Line noise, in general, tends to fluctuate during a line cycle period. Impulse noise tends to be synchronous and occurs in limited periods of the line cycle. HomePlug AV line synchronization capability utilizes multiple time slots that are synchronized with the AC cycle and evaluated for noise during channel estimation periods. This allows HomePlug AV devices to minimize the effects of the noise by optimizing carrier bit loading according to noise conditions. The carrier bit loading is part of the tone map that is generated with each channel estimation period, allowing the communications to adapt to the line and impulse noise in any network path.

Powerful Forward Error Correction Technology
HomePlug AV technology employs powerful advanced coding technology to accomplish Forward Error Correction (FEC). This technology achieves exceptional performance and realizes greater throughputs in the presence of noise, allowing HomePlug AV home networks to operate at a lower SNR. This advanced FEC coding has power efficiencies approaching (within 1 dB of) the theoretical Shannon limit and is well proven, having been widely adopted in harsh communications environments such as cellular telecommunications (CDMA2000 and W-CDMA), satellite (DVB-RCS, CCSD), and broadband wireless (802.16, WiMAX).

Ready for 'Next BIG Thing' Rollout
HomePlug AV technology is now ready for primetime with service providers eager to rollout new systems, products and services. HomePlug AV technology is a key enabler of 'The Next BIG Thing', offering very high channel and data throughput bit rates because of advanced channel estimation, adaptive and flexible tone mapping, line synchronization and powerful FEC coding technology. HomePlug AV is making the home network truly ubiquitous and fully capable of delivering both service providers' and home owners' digital content throughout the home to every AC outlet – digital media over power – entertainment at every AC outlet.

www.intellon.com

www.homeplug.org

PWM Controller Simplifies High Power LED Designs

Dimming ratios of 3000:1

High brightness (HB) and super HB LEDs are found in LCD TFT backlighting in high-end TVs, industrial lighting, and projectors. One popular area is for instrument panel backlighting, interior lighting, and the brake lights of many cars and trucks.

By Tony Armstrong, Product Marketing Manager, Linear Technology Corporation

Luxury automobile manufacturers are increasingly taking advantage of the latest technologies in solid-state LED lighting to enhance the aesthetics of their 2007-2008 model vehicles by relying on these lighter, smaller, and more durable devices for interior and exterior illumination. LEDs promise lower long-term cost and longer life which are among many advantages over incandescent light bulbs for interior lighting, for example, and HID (high-intensity discharge) and halogen lamps for headlights

Driving LEDs at high current requires a DC/DC converter to accurately regulate the current to ensure uniform light intensity and color integrity as well as to protect the LEDs. Furthermore, a significant challenge is to power one or several strings of LEDs from a battery voltage that can be less than, equal to, or higher than its load voltage. Yet another concern is to efficiently dim the LEDs over a large dimming ratio while preserving their chromatic characteristics at both low and high brightness levels. Furthermore, efficient operation of the DC/DC driver is a crucial requirement, especially in driving HB (high brightness) LEDs, since all the power not emitted as light is dissipated as heat.

The new LTC3783 from Linear Technology is a current-mode multi-topology converter with constant-current PWM dimming for driving high-power LED strings and clusters. Proprietary techniques provide extremely fast, true PWM load switching with no transient undervoltage or overvoltage issues: dimming ratios of 3000:1 (at 100Hz) can be achieved digitally as True Color PWM dimming guarantees color integrity of white and RGB LEDs. The LTC3783 allows an additional 100:1 dimming ratio using analog control. This is an important criterion since the human eye is extremely sensitive to minor changes in ambient light. This versatile controller can be used as a boost, buck, buck-boost, SEPIC, or flyback converter, and as a constant-current/constant-voltage regulator. No RSENSE operation uses a

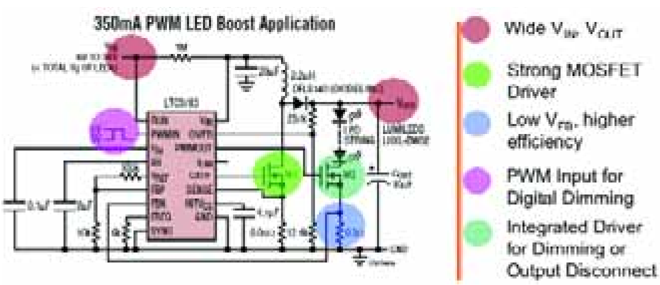

Figure 1 The LTC3783 integrates powerful MOSFET drivers to deliver high output power to a cluster of LEDs. (Please see electronic file for color version of this diagram).

MOSFET's on-resistance to eliminate the current-sense resistor and increase efficiency. Applications for the LTC3783 include high-voltage LED arrays and LED backlighting, as well as voltage regulators in telecom, automotive and industrial control systems.
Figure 1 details a typical LTC3783 circuit schematic in a boost configuration to drive a string of high power LEDs. Its key performance features are defined in areas one through five. >>

Features and Benefits of the LTC3783

High Current: To deliver high current (³1.5A), the LTC3783 drives an external N-channel MOSFET to power high brightness (HB) and Super HB LEDs.

High Voltage: The LTC3783's 3V to 36V input operation and an output voltage that is scalable depending on the choices of the external power components, easily drives strings (series) or clusters (series + parallel) of LEDs.

Protection: The IC incorporates accurate current and output voltage regulation necessary to protect HB LEDs. Additional protections include overvoltage, overcurrent, and soft start.

Dimming: With True Colorä PWM 3000:1 digital dimming the LED's constant color is preserved over a wide dimming ratio. Also, the LTC3783 is capable of additional analog 100:1 dimming.

Dimming has three uses in HB LED applications:
Adjust brightness of LED;Protect the LED by dimming it when LED becomes too hot Create multiple colors by separately dimming red, green and blue LEDs

Multi-Topology: The LTC3783 can be specified for many LED arrangements as buck, boost, buck-boost, or flyback. One IC can be qualified for a variety of system requirements independent of input-output voltage ratio.

Conclusion

To reliably drive a string or cluster of high brightness or super high brightness LEDs the driver controller must have accurate current and voltage regulation, protection circuitry and dimming capability. These LEDs are found in large LCD TFT backlighting in automobile, notebook, TV and monitors, industrial lighting, projectors as well as automotive interior and exterior lighting. These systems may require 16V at 5A. The LTC3783 has special circuitry that makes it ideal for driving LEDs in variety of topologies. One major advantage of the LTC3783 is its simplicity in the single-inductor buck-boost topology (see data sheet). Moreover, the LTC3783's digital PWM input can be used to digitally dim LEDs. The IC also has a PWM driver for driving a second MOSFET for dimming.

www.linear.com

30V-DirectFET for DC-DC buck

International Rectifier has introduced a new 30V-synchronous buck converter chipset consisting of the IRF6631 Control MOSFET and IRF6638 Synchronous MOSFET. The pair features IR's benchmark DirectFET packaging with double-sided cooling and the latest HEXFET MOSFET technology to reach higher levels of efficiency and thermal performance at the intermediate current levels (below 18 amps). Applications include telecom, datacom, advanced notebook and desktop computers and general purpose synchronous buck designs where small size, high efficiency, and improved thermal conduction result in increased power density.

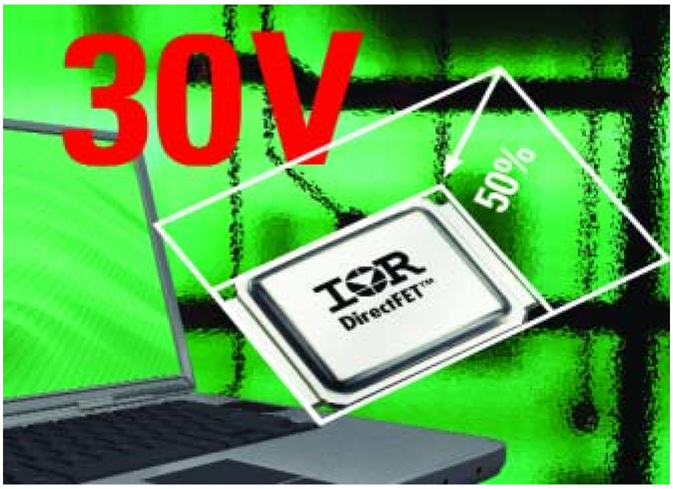

The new DirectFET chipset is an excellent choice for designers seeking very compact and efficient switching in mid-range, 15- to 18-amp power converter applications.

In addition to improving efficiency by over 1% in the five- to eight-amp range, the board space savings is almost 50% compared to the typical approaches using three SO-8 devices.

Each device is tailored to maximize performance in its role within synchronous DC-DC buck converter circuits. The IRF6631 DirectFET Control MOSFET reduces switching losses, while the IRF6638 DirectFET synchronous MOSFET lessens conduction losses and reverse-recovery charge.

The IRF6631 Control FET features a gate charge of 12nC and delivers a 16% reduction in figure of merit of on resistance-gate charge (99.6 mWnC) compared to previous offerings. The IRF6638 Synchronous FET delivers a typical on-state resistance of 3.0 mÙ at 4.5V, a 12% reduction over existing devices while maintaining the same gate charge.

www.irf.com

Complete Current-Shunt Monitor

Texas Instruments announced a complete comparison solution that combines a high-side current-sense amplifier, two comparators and a voltage reference in a small 14-pin package. The unique integration and functionality of the INA206 simplifies design of current comparison circuits and reduces application board space. Target applications include computer, power management and automotive systems.

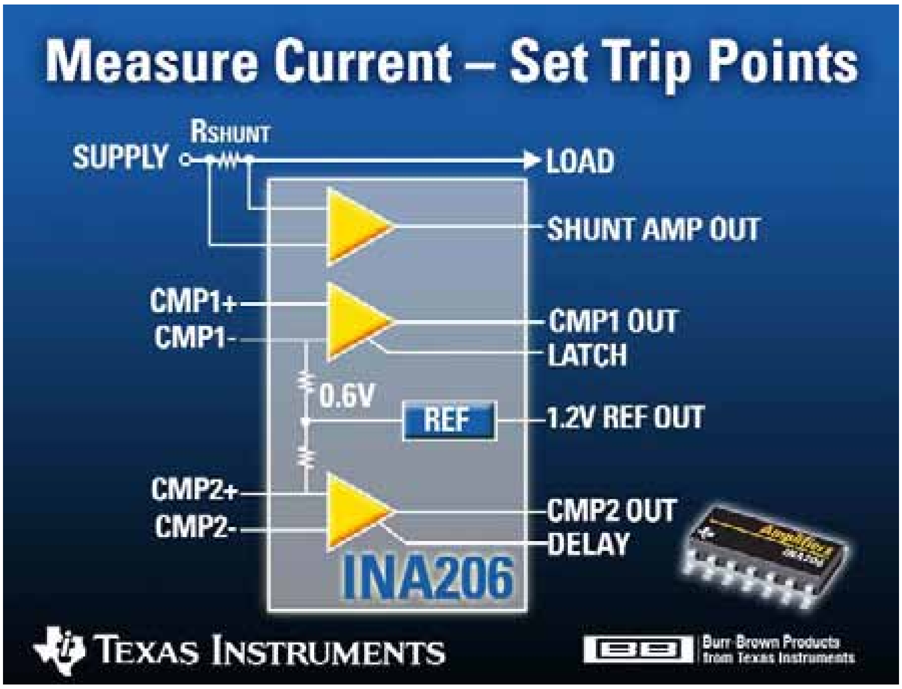

(See www.ti.com/sc06139.)

The two uncommitted comparators can be used to provide over/under current detection or power supply over/under voltage detection. This versatile design allows the two comparators to do the work of three since one offers a delay function that can be used for a low-level warning output while the other comparator has a programmable latch function for higher-level instantaneous critical outputs. Both comparators are open-drain output devices with internal 0.6V references that can be overridden.

The INA206 also features a wide common-mode voltage range of -16V to +80V, 500kHz bandwidth and a wide supply range of 2.7V to 18V. It is specified for +/-3.5 percent maximum output error over the -40C to +125C extended temperature range.

The device offers a gain setting of +20V/V. Two additional factory-trimmed gain setting versions will be available in Q4 2006: +50V/V (INA207) and +100V/V (INA208).

In power management applications, the INA206 is especially suited for use with the TPS2490 hot-swap controller.

www.ti.com

Power Supply Unit for Microprocessors

The NCP1526 dc-dc buck converter with integrated low noise LDO, is a single-device solution that supports multimedia functions such as mobile TVs on cellular phone

ON Semiconductor introduced the NCP1526. This high efficiency synchronous dc-dc buck (step-down) converter features an integrated low noise LDO. Offered in a unique 0.55 mm ultra-thin DFN package, it is ideal for portable applications. The device is designed to power an application microprocessor in multimedia portable devices such as portable media players (PMP), MP3 players and either DMB or DVB-H mobile TV chipsets in cellular phones.
This NCP1526 integrated buck converter accepts input voltage from 2.7 volts (V) to 5.2 V, and features a 3.0 megahertz (MHz) buck converter that supplies a fixed output voltage with current capability of 400 milliamp (mA). The NCP1526 delivers fast transient response, making the converter ideal to power the digital core of a portable microprocessor. The device's integrated LDO provides a 150 mA current capability and its low noise characteristic enables it to power radio frequency (RF) sensitive analog circuitry. The NCP1526 offers a fixed output of 1.2 V from the converter and 2.8 V from the LDO. Other output voltage options are available upon request. The device is offered in a Pb-free, 3 mm x 3 mm x 0.55 mm ultra-thin DFN-10 package. It is priced at $0.90 per unit in 3,000 unit quantities.

www.onsemi.com

Automotive Dual-Range, Non-Intrusive Current Sensors

LEM has introduced a series of dual-range, automotive-qualified sensors for accurate, wide-range current measurements in vehicle battery monitoring applications. The 25 models in the DHAB range are the first in the industry to offer non-intrusive, galvanically-isolated solutions in this application.
A DHAB Hall-effect sensor is fixed onto the battery cable of a car. Its two cores allow it to be used for two separate current ranges – one between ±20 and ±80A and the other between ±50 and ±600A. This enables full-range current measurements to be made in combination with highly-accurate measurements at lower currents.

The sealed housing of the DHAB sensors means that no potting is required. Panel and cable-mount versions are available to offer maximum mounting versatility. The sensors meet all relevant standards, including ISO-TS and RoHS.
The DHAB sensors benefit from the company's proven high-quality approach to manufacturing and are backed by a five-year guarantee. Principal applications are expected to be in the measurement of battery-pack current in electric and hybrid vehicles.

www.lem.com

Digital 3 Amp Power Management IC

Zilker Labs introduced the industry's only single-chip 3A power conversion solution that integrates full digital power management capabilities. The ZL2105 extends Zilker Labs' innovative Digital-DC technology into lower power applications and combines a synchronous step-down converter including synchronous power MOSFETs with key power management functionality in a tiny 6 x 6 mm package. A ZL2105 circuit with full digital power management capabilities requires less than two square centimeters of board space, representing size and component count reductions of up to 50 percent. Like all Digital-DC ICs, the ZL2105 is designed to be a digital building block that can be seamlessly combined with other Digital-DC devices to provide a comprehensive solution for board-mounted power management and conversion.
"The ZL2105 is a key addition to our Digital-DC product family and advances our goal of making advanced power design simple. The ZL2105 combines the digital power management capabilities, simple configurability and high efficiency of our existing ZL2005 into a part that is ideal for lower power applications," said Jim Templeton, Zilker Labs' vice president of marketing. "Customers can combine multiple Digital-DC devices on a given PCB and easily configure the parts to simplify a complicated power design. Ours are the only solutions to offer this 'plug and play' experience for board-level power."
An evaluation kit, the ZL2105EV1, is available.

www.zilkerlabs.com

Ultra-Thin Surface Mount Inductors

Design engineers looking for a miniature surface mount inductor that provides effective EMI protection for their applications will find the new DR365-1 and DR365-2 Inductors from Datatronic Distribution, Inc., offer superior performance and reliability. The inductors also meet the requirements for RoHS compliance. The ultra-thin DR365-1 and DR365-2 Inductors feature a seated height as low as 0.047 inches (1.2 mm) above the printed circuit board depending on the inductance value required by the design. These inductors are ideal for a wide range of portable, compact and miniature devices, such as PDAs, mobile phones, portable hard drives, medical appliances, bar code scanners—wherever high-density circuit board design is a requirement. In addition to their small size, the DR365-1 and DR365-2 feature a wide inductance range from 3.3 to 100 uH (at 100 kHz, 0.1V), with a DCR range from 0.11 to 2.8 ohms and a maximum rated current from 0.20 to 1.2 amps. They operate over a wide temperature range from -20 to +80ºC, making them suitable for use in many rugged environments.

The DR365-1 and DR365-2 Inductors are designed with materials that meet the requirements of UL94V-0 for flammability. Custom designed DR365-1 and DR365-2 Series Inductors are available upon request to meet unique circuit requirements.

www.datatronics.com

Thermistors for Power Line

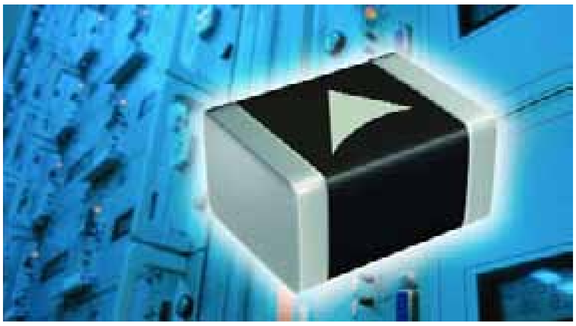

Epcos has extended the SMD PTC series for overcurrent protection and now offers a chip PTC for maximum voltages up to 265 V for the first time. With a 1210 package, this PTC can handle rated currents of up to 15 mA. This current represents its limiting point. Higher rated currents are achieved by parallel connection of several PTC thermistors. This product complements the highly successful series of the same type that was previously restricted to maximum voltages of 80 V.

With this product innovation, Epcos satisfies the requirement for an SMD solution that can handle power line voltages. This PTC is thus suited for primary-side applications. Another conceivable application is as secondary-side overcurrent protection in the event of accidental contact with the power line.

www.epcos.com

Mid-Voltage Bipolar Transistors

Zetex Semiconductors has introduced a range of mid-voltage bipolar transistors in the SOT23 package, capable of handling a power dissipation of up to 1.25W. With the 3mm x 2.5mm footprint, these seven NPN and six PNP devices help to significantly increase circuit power density by replacing the much larger DPAK, SOT89 and SOT223 packaged parts.

Spanning the collector emitter voltage range from 40 to 100V, the ZXTN and ZXTP bipolars create high efficiency switches for lamp, relay and solenoid driving in automotive, industrial and telecom applications.

Capable of blocking voltages up to 180V and handling a continuous collector current up to 5A, the transistor range will switch loads as high as 500W. In addition, pulsed current ratings up to 12A mean that higher capacitance MOSFETs and IGBTs in power supply circuits can be driven at higher speeds.

Lower heat dissipation and cooler running is achieved thanks to the transistors' very low saturation voltage – 40mV for the 50V rated ZXTN2031F, while their low equivalent on-resistance - down to 30m? for the 100V rated ZXTN2020F – is much lower than that of alternative MOSFETs in the same sized package.

Also characterised by very high gain – a minimum of 300 for the 40V rated ZXTP25040DFH, these latest high efficiency bipolar transistors from Zetex enable ICs to drive larger loads directly, without the need for additional buffering.

www.zetex.com

First Components market KEC MOSFETs

KEC, the largest manufacturer of discrete electronic components in Korea and Vishay Intertechnology have signed an agreement under which Vishay will license its Vishay Siliconix TrenchFET power MOSFET technology to KEC. In signing the agreement with Vishay, KEC will now be able to offer its customers power MOSFETs built on TrenchFET technology.

As the first manufacturer of Trench power MOSFETs in Korea, KEC will address a local market for power MOSFETs valued yearly at $266.7 million. Until now, demand for Trench power MOSFETs in Korea has been supplied entirely by imported devices.

KEC is represented by the German distributor First Components GmbH in Europe.

www.firstcomponents.de

Automotive MOSFET Pre-Driver ICs

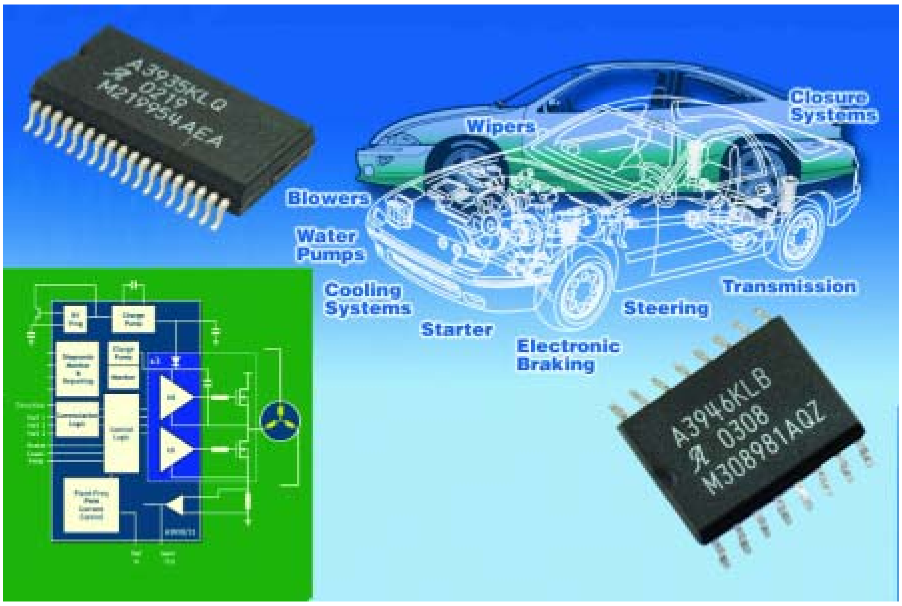

A range of automotive-grade MOSFET pre-driver ICs for in-vehicle motor control applications is now available from Allegro MicroSystems Europe.

The device family, which will operate over a junction temperature range from -40°C to +150°C, are designed for use in applications including wipers, blowers, water pumps, cooling systems, starter, electronic braking, steering, transmission and closure systems.

The range includes four devices:

The A3935 is designed specifically for automotive applications that require high-power motors. Each device provides six high-current gate drive outputs capable of driving a wide range of n-channel power MOSFETs.

The A3935 integrates a pulse-frequency modulated boost converter to create a constant

supply voltage for driving the external MOSFETs. Direct control of each gate output is possible via six TTL-compatible inputs. A differential amplifier is integrated to allow accurate measurement of the current in the three-phase bridge.

The A3940 is also designed for applications that require high-power motors. Each device provides four high-current gate drive outputs capable of driving n-channel power MOSFETs in a full-bridge configuration. Bootstrap capacitors are used to provide the above battery supply voltage required for n-channel FETs. An internal charge pump for the high side allows for DC (100% duty cycle) operation of the bridge.

The A3946 is designed for applications that require high power unidirectional DC motors, three-phase brushless DC motors, or other inductive loads. It provides two high-current gate drive outputs: a

high-side gate driver which switches an N-channel MOSFET to control current to the load, and a low-side gate driver that switches an N-channel MOSFET as a synchronous rectifier

The A3930/31 is a 3-phase brushless DC motor controller for use with n-channel external power MOSFETs, and incorporates much of the circuitry required to design a cost-effective 3-phase motor drive system, including integrated commutation logic based on Hall sensor inputs. A charge pump regulator provides adequate gate drive for battery voltages down to 7 V, and allows the device to operate with a reduced gate drive at battery voltages down to 5.5 V.

www.allegromicro.com

ADVERTISING INDEX

ABB Entrelec	43	Fairchild	C2	LEM	3
ABB Semiconductors	C3	Fischer electronik	39	Microsemi Power Products Group	47
Berquist	19	Fuji	9	Mitsubishi	29
Bodo´s Power	12	H2 Expo	51	Sharp	13
Correlec	insert	Infineon/eupec	15	SPS	49
CT Concept Technologie	5	International Rectifier	11/C4	Tyco	27
Danfoss Silicon Power	23	IXYS	17	Würth Elektronik	45
Electronica	35/37				